Nutrients Removal in Constructed Wetlands in a Cold Temperate Region

By

Shuntian Liang

A thesis submitted in partial fulfilment of the requirements for the degree of

Master of Science

In

Water Resources Engineering

Department of Civil and Environmental Engineering

University of Alberta

Abstract

Constructed stormwater wetlands have become an effective management practice to control urban stormwater, which contributes to eutrophication in urban aquatic ecosystems. This study examined the effectiveness on nutrient control of two created wetlands, the Rocky Ridge wetland (RR) and the Royal Oak wetland (RO), in Calgary, Alberta, Canada, in a cold temperate region. Field measurements were conducted from May to November 2018 and April to November 2019. The considered meteorology parameters and flow data were collected, and nutrient concentrations were measured from the inlets to the outlets. The water budget analysis was done to guarantee the reliability of flow data. The concentration reduction and load reduction of nutrients were analyzed to assess the performance of these two stormwater wetlands. The effect of weather characteristics and hydraulic parameters on removal efficiency was also examined.

The volumes of direct rainfall on the wetlands and evaporation were minor components of the event budgets, but evaporation had a certain important effect on the water budget in these two wetlands annually, especially in 2018 with less annual rainfall depths, reaching 63.9% in the Rocky Ridge wetland and 23.6% in the Royal Oak wetland of annual outflow volume, respectively.

The loading of total nitrogen (TN) into the RR wetland was retained at approximately 59.7% in 2018 and 70.1% in 2019. Nevertheless, the RO wetland trapped 48.6% of TN inflow loadings in 2018 and only trapped 10.9% in 2019. Both wetlands can effectively remove total phosphorus (TP) from stormwater, given the annual TP reductions were 47.0% in 2018 and 66.8% in 2019 by the RR wetland and 84.1% in 2018 and 83.1% in 2019 by the RO wetland, respectively. Both wetlands can have excellent annual reduction rate of TN and TP in wet year. The RR can have better nitrogen performance while the RO can have better performance on phosphorus.

Results of nutrient measurements also indicate that the event removal efficiency (RE) of TN ranged from -68.6% to 98.4% of the RR wetland and from -104.1% to 93.8% of the RO wetland. The median and mean RE-TN of these two wetlands were close, they were 41.6% and 34.1% of the RR wetland, 44.2% and 31.5% of the RO wetland, respectively. The RE-TP ranged from 29.9% to 97.2% of the RO wetland and from -160% to 80.3% of the RR wetland. The RO wetland had better phosphorus reductions than the RR wetland, comparing the median and mean RE of TP and total reactive phosphorus (TRP). Both wetlands' capability to remove nutrients exhibited better in the wet year 2019. The event REs of TN and TP only exhibited the same fluctuations as the dry year's hydraulic loading rate in both wetlands, while the event RE-TN positively correlated with the inflow concentrations in both wetlands.

Specifically, nutrient removal can be attributed to the suspended solid reductions in the RR wetland, which was influenced by air temperature, evaporation rate, hydraulic loading rate and retention time. The major processes of nutrient retention in this wetland should be vegetation uptake and accompanying sedimentation. In the RO wetland, rainfall characteristics and evaporation rate played important roles in nitrogen removal efficiency. The sedimentation forebay acted as a nitrate/nitrite internal source, while organic decomposition and nitrification were assumed to be the reasons for poor annual nitrogen removal. In comparison, the evaporation rate exhibited a contrary correlation with the event RE of TN and TP in these two wetlands. Additionally, small and clean rainfall events which have low flow rates can reduce the reliability of phosphorus removal assessment by the RR wetland. The interference from large rainfall events on the nitrogen removal by the RO wetland needs to be explored in the future.

Preface

This thesis is an original work by Shuntian Liang under the guidance of Dr. Zhu and Dr. Loewen. No part of this thesis has been previously published.

This thesis is part of a research project led by Dr. Zhu and Dr. Loewen at the University of Alberta. The data collection process during fieldwork has been a part of my responsibilities. I clean data related to wetlands and wet ponds' flow and water quality. Additionally, I am responsible for assessing the performance of wetlands and wet ponds, and for writing the manuscript. As supervisory authors, Dr. Zhu and Dr. Loewen are involved in concept formation and manuscript composition. Dr. Zhu and Dr. Loewen also guided me in the data analysis in chapters 4 and 5, as well as in the literature review in chapter 2.

Acknowledgements

The author would like to thank her supervisors, Dr. David Z. Zhu and Dr. Mark Loewen, for their assistance and guidance in all aspects of this project. All the time and effort they have put into helping her is very much appreciated.

Thanks to Dr. Wenming (William) Zhang, Dr. Tadros Ghobrial, Sherif Ahmed, Arlette Fernandez for field work operations and general discussions on the completion of this work. Thanks to Christine Zawadski, Tamara Quinteros, Kevin Zhu, Yangbo Tang, Zhao Zhou for their help on the field work.

This research was funded by the City of Calgary and the Natural Sciences and Engineering Research Council of Canada (NSERC), which are gratefully acknowledged. The funding for the author comes from China Scholarship Council (CSC), which is gratefully acknowledged.

A very special thank you to my families for their unending confidence and encouragement throughout my program.

Table of Contents

Abstract .... **ii**

Preface .... **iv**

Acknowledgements .... **v**

List of Tables .... **viii**

List of Figures .... **x**

List of Abbreviations .... **xv**

1 Introduction **1**

1.1 Research Background 1

1.2 Study Objectives 4

1.3 Thesis Structure 4

2 Literature Review **5**

2.1 Water Budget 6

2.2 Evaporation and Direct Rainfall 7

2.3 Water Environment Parameters 8

2.4 Removal Mechanisms and Factors for Nutrients 9

2.4.1 Nitrogen Removal Pathways 12

2.4.2 Phosphorus Removal Pathways 13

3 Methodology **15**

3.1 Site Description 15

3.2 Field Measurement Program 22

3.3 Definitions and Formulas 27

3.4 Statistical Analysis 28

4 Water Budget **29**

4.1 Annual Water Budget 29
4.2 Event Water Budget and Event Hydrograph 36
4.3 Discussions and Conclusions 47
5 Nutrient Analysis 49
5.1 Nutrient Concentrations from Inflow to Outflow 49
5.1.1 Spatial Comparation Among all Locations 49
5.1.2 Spatial and Temporal Variability of Nutrients 56
5.1.3 Event Comparation between Inflow and Outflow 67
5.2 Nutrient Removal 72
5.2.1 Event Removal Efficiency 72
5.2.2 Annual Reduction 74
5.3 Pond Environmental Conditions 76
5.4 Discussions 91
5.4.1 Factors on Event Performance 91
5.4.2 Comparisons Between Wetlands 97
5.5 Summary 99
6 Conclusions and Future Study 103
7 References 106

List of Tables

Table 3-1. Characteristics of the study wetlands and the associated catchments. NWL, normal water level. 15

Table 3-2. The flow meters installation information in these two wetlands 24

Table 3-3. Water quality constituents analyzed in the lab, their analytical methods, and detection limit. 26

Table 4-1. RMSE of simulated surface elevation and observed elevation in Royal Oak Wetland, the pipe inflow was computed using velocity area formula from 750-sensor data and was from 2150-module. 750AV and 750Man mean the pipe inflow is from 750-sensor with area velocity and Manning formula, respectively. 35

Table 4-2. Annual water budget summary of the Royal Oak Wetland. Unit: m^3 36

Table 4-3. Summary of the captured runoff events by the auto-samplers. 39

Table 4-4. Summary statistic of the fully monitoring stormwater events for the Rocky Ridge wetland; ADP: antecedent dry period; Rdu: rainfall duration; Rde: rainfall depth; MRI: maximum rainfall intensity; ARI: average rainfall intensity; T_{air}: air temperature; E_p: evaporation rate; HLR: hydraulic loading rate; HRT: hydraulic retention time. 40

Table 4-5. Summary statistic of the fully monitoring stormwater events for the Royal Oak wetland; ADP: antecedent dry period; Rdu: rainfall duration; Rde: rainfall depth; MRI: maximum rainfall intensity; ARI: average rainfall intensity; T_{air}: air temperature; E_p: evaporation rate; HLR: hydraulic loading rate; HRT: hydraulic retention time. 41

Table 4-6. Summary of the event water budget. Unit: m^3. dV was the pool storage change and was calculated by stage-curve; it states that the change in storage in the wetland results from the difference between inflows and outflows; Residual equal to the differences between IO and dV; IO equal to the differences between total inflow and total outflow. 42

Table 5-1. Summary of event removal efficiencies of nutrients, n is the observed stormwater events. 73

Table 5-2. Summary of annual reductions for nutrients, in/out means the stormwater events in the pipe inlet and the outlet. 76

Table 5-3. Correlation analysis results for nitrogen of the Rocky Ridge wetland in 2018. Red color is significant at the 0.01 level (2-tailed); blue color is significant at the 0.05 level (2-tailed); In, Mid, and Out are the in-pond sampling locations (inlet, middle, outlet). 81

Table 5-4. Correlation analysis results for nitrogen of the Rocky Ridge wetland in 2019. Red color is significant at the 0.01 level (2-tailed); blue color is significant at the 0.05 level (2-tailed); In, Mid, and Out are the in-pond sampling locations (inlet, middle, outlet). 82

Table 5-5. Correlation analysis results for phosphorous of the Rocky Ridge wetland in 2018. Red color is significant at the 0.01 level (2-tailed); blue color is significant at the 0.05 level (2-tailed); In, Mid, and Out are the in-pond sampling locations (inlet, middle, outlet). 83

Table 5-6. Correlation analysis results for phosphorous of the Rocky Ridge wetland in 2019. Red color is significant at the 0.01 level (2-tailed); blue color is significant at the 0.05 level (2-tailed); In, Mid, and Out are the in-pond sampling locations (inlet, middle, outlet). 83

Table 5-7. correlation analysis results for Nitrogen of the Royal Oak wetland in 2018. Red color is significant at the 0.01 level (2-tailed); blue color is significant at the 0.05 level (2-tailed); In, Mid, and Out are the in-pond sampling locations (inlet, middle, outlet); top and bot are the sampling top layer and bottom layer. 88

Table 5-8. correlation analysis results for Nitrogen of the Royal Oak wetland in 2019. Red color is significant at the 0.01 level (2-tailed); blue color is significant at the 0.05 level (2-tailed); In, Mid, and Out are the in-pond sampling locations (inlet, middle, outlet); top and bot are the sampling top layer and bottom layer. 89

Table 5-9. correlation analysis results for phosphorous of the Royal Oak wetland in 2018. Red color is significant at the 0.01 level (2-tailed); blue color is significant at the 0.05 level (2-tailed); In, Mid, and Out are the in-pond sampling locations (inlet, middle, outlet); top and bot are the sampling top layer and bottom layer. 90

Table 5-10. correlation analysis results for phosphorous of the Royal Oak wetland in 2019. Red color is significant at the 0.01 level (2-tailed); blue color is significant at the 0.05 level (2-tailed); In, Mid, and Out are the in-pond sampling locations (inlet, middle, outlet); top and bot are the sampling top layer and bottom layer. 91

List of Figures

Figure 2-1. Schematic of a stormwater wetland (free water surface), the blue dotted lines indicate components of the water budget. 6

Figure 2-2. Simplified major nitrogen transformation pathways in stormwater wetlands. Adapted from Troitsky et al. (2019). DNRA is dissimilatory nitrate reduction.. 11

Figure 2-3. Simplified major phosphorus transformation pathways in stormwater wetlands. Adapted from Collins et al. (2010). 11

Figure 3-1. Aerial view of the studied wetlands' catchments. The catchment area is shown by the red line; the pond area is shown by the yellow line. 16

Figure 3-2. Aerial view of studied wetlands. The main flow path direction is indicated by the yellow arrows and white dotted line; the sampling and moored locations are shown by stars. ... 16

Figure 3-3. The rectangular concrete sediment vault for first flush treatment in the inlet of the Rocky Ridge wetland. 17

Figure 3-4. Side view of the outlet structure of the Rocky Ridge wetland. 18

Figure 3-5. Stage outlet discharge curve for the Rocky Ridge wetland where Q is the discharge and H is the head on the weir or orifice. Note that zero head corresponds to the NWL. 19

Figure 3-6. Stage-area curve for the Rocky Ridge wetland. 19

Figure 3-7. Side View-Control Structure of the Royal Oak wetland. 21

Figure 3-8. Stage discharge curve for Royal Oak wetland outlet structure. 21

Figure 3-9. Stage-area curve for the Royal Oak wetland. 22

Figure 3-10. A rain gauge (a, Onset Computer Corp., U.S) and the portable auto-samplers Teledyne-ISCO-6712 were equipped with 750/2150 area velocity flow modules (b, Teledyne Isco Inc, U.S). 24

Figure 3-11. (a) ISCO-Teledyne Model 6712 automated sampler located at the outlet of Royal Oak wetland; it was used to collect stormwater samples and store hydrologic data at the sampling point (blue rectangle) in the outlet pipe. Influent and effluent monitoring for wetland: (b) V-notch weir in Royal Oak outlet, (c) outlet pipe, AVM (red circle) inside outlet pipe. 25

Figure 4-1. The top surface elevation of observed vs. simulated of the Rocky Ridge wetland. The in750AV and in750Man mean the inflow is from 750-sensor with area velocity and Manning formula, respectively. 32

Figure 4-2. Hydrographs at the inlet and outlet of the Rocky Ridge wetland. 33

Figure 4-3. The top surface elevation of observed vs. simulated of the Royal Oak wetland. The in750AV and in2150 mean the inflow is from 750-sensor with area velocity formula and 2150-module, respectively. 34

Figure 4-4. The daily snow in Calgary, data downloaded from https://climate.weather.gc.ca/ ... 34

Figure 4-5. Hydrographs at the inlet and outlet of the Royal Oak wetland. 35

Figure 4-6. Event comparisons among rainfall intensity parameters, evaporation, and HLR for the Rocky Ridge wetland (a) – (b) and the Royal Oak wetland (c) – (d). 43

Figure 4-7. Hydrographs representing event behaviour: (a) (b) are the event-7, event-8 in the Rocky Ridge wetland; (c) (d) are the event-8, event-9 in the Royal Oak wetland. 43

Figure 4-8. The dynamic TN concentrations of events with discrete samples in the Rocky Ridge wetland. 44

Figure 4-9. The dynamic TP concentrations of events with discrete samples in the Rocky Ridge wetland. 45

Figure 4-10. The dynamic TN concentrations of events with discrete samples in the Royal Oak wetland. 46

Figure 4-11. The dynamic TP concentrations of events with discrete samples in the Royal Oak wetland. 47

Figure 5-1. Boxplots of nitrogen observed from the inflow, in-pond, and outflow of the Rocky Ridge wetland for 2018; In, Mid, and Out are the in-pond sampling locations (inlet, middle, outlet); top and bot are the sampling top layer and bottom layer; the numbers in the parentheses are sample sizes. 51

Figure 5-2. Boxplots of nitrogen observed from the inflow, in-pond, and outflow of the Rocky Ridge wetland for 2019; In, Mid, and Out are the in-pond sampling locations (inlet, middle, outlet);

top and bot are the sampling top layer and bottom layer; the numbers in the parentheses are sample sizes. 52

Figure 5-3. Boxplots of nitrogen observed from the inflow, in-pond, and outflow of the Royal Oak wetland for 2018; In, Mid, and Out are the in-pond sampling locations (inlet, middle, outlet); top and bot are the sampling top layer and bottom layer; the numbers in the parentheses are sample sizes. 53

Figure 5-4. Boxplots of nitrogen observed from the inflow, in-pond, and outflow of the Royal Oak wetland for 2019; In, Mid, and Out are the in-pond sampling locations (inlet, middle, outlet); top and bot are the sampling top layer and bottom layer; the numbers in the parentheses are sample sizes. 54

Figure 5-5. Boxplots of phosphorus observed from the inflow, in-pond, and outflow of the Rocky Ridge wetland: (a) and (b) are for 2018 and (c) and (d) are for 2019; In, Mid, and Out are the in-pond sampling locations (inlet, middle, outlet); top and bot are the sampling top layer and bottom layer; the numbers in the parentheses are sample sizes. 55

Figure 5-6. Boxplots of phosphorus observed from the inflow, in-pond, and outflow of the Royal Oak wetland: (a) and (b) are for 2018 and (c) and (d) are for 2019; In, Mid, and Out are the in-pond sampling locations (inlet, middle, outlet); top and bot are the sampling top layer and bottom layer; the numbers in the parentheses are sample sizes. 56

Figure 5-7. The observed nitrogen (NH_4-N, NO_x-N, TON) concentrations in the pond of the Rocky Ridge wetland; In, Mid, and Out are the in-pond sampling locations (inlet, middle, outlet); top and bot are the sampling top layer and bottom layer. 58

Figure 5-8. The observed nitrogen (TDN and PN) concentrations in the pond of the Rocky Ridge wetland; In, Mid, and Out are the in-pond sampling locations (inlet, middle, outlet); top and bot are the sampling top layer and bottom layer. 58

Figure 5-9. The observed phosphorus (TRP and URP) concentrations in the pond of the Rocky Ridge wetland; In, Mid, and Out are the in-pond sampling locations (inlet, middle, outlet); top and bot are the sampling top layer and bottom layer. 60

Figure 5-10. The observed phosphorus (TDP and PP) concentrations in the pond of the Rocky Ridge wetland; In, Mid, and Out are the in-pond sampling locations (inlet, middle, outlet); top and bot are the sampling top layer and bottom layer. 60

Figure 5-11. The observed nitrogen (NH_4-N, NO_x-N, TON) concentrations in the pond of the Royal Oak wetland; In, Mid, Out are the in-pond sampling locations (inlet, middle, outlet); top, bot is the sampling top layer and bottom layer. 62

Figure 5-12. The observed nitrogen (TDN and PN) concentrations in the pond of the Royal Oak wetland; In, Mid, Out are the in-pond sampling locations (inlet, middle, outlet); top, bot is the sampling top layer and bottom layer. 63

Figure 5-13. The observed phosphorus (TRP and URP) concentrations in the pond of the Royal Oak wetland; In, Mid, Out are the in-pond sampling locations (inlet, middle, outlet); top, bot is the sampling top layer and bottom layer. 64

Figure 5-14. The observed phosphorus (TDP and PP) concentrations in the pond of the Royal Oak wetland; In, Mid, Out are the in-pond sampling locations (inlet, middle, outlet); top, bot is the sampling top layer and bottom layer. 65

Figure 5-15. The concentrations of total nitrogen and total phosphorus in the pond and the EMCs of total nitrogen and total phosphorus in the outflows for the Rocky Ridge wetland. Pond-Out is the outlet top layer sampling location in the pond. 66

Figure 5-16. The concentrations of total nitrogen and total phosphorus in the pond and the EMCs of total nitrogen and total phosphorus in the outflows for the Royal Oak wetland. Pond-Out is the outlet bottom layer sampling location in the pond. 67

Figure 5-17. Bar charts showing EMCs of nutrients in the inflows and the outflows, and the flow volumes of the Rocky Ridge wetland for 24 storm events. Event-# is the fully captured events; the red line represents the protective threshold values. 70

Figure 5-18. Bar charts showing EMCs of nutrients in the inflows and the outflows, and the flow volumes of the Royal Oak wetland for 21 storm events. Event-# is the fully captured events; the red line represents the protective threshold values. 71

Figure 5-19. Event REs of TN, TP and the relevant HRT, HLR and rainfall depth for the Rocky Ridge wetland (a) and (b) and the Royal Oak wetland (c) and (d). 74

Figure 5-20. The environmental parameters in the pond of the Rocky Ridge wetland for Secchi depth and Chl-a; In, Mid, and Out are the in-pond sampling locations (inlet, middle, outlet); top and bot are the sampling top layer and bottom layer. Z_{secchi} is Secchi depth and Z_{mix} is water column depth. 78

Figure 5-21. The environmental parameters in the pond of the Rocky Ridge wetland for DO, pH, and T; In, Mid, and Out are the in-pond sampling locations (inlet, middle, outlet); top and bot are the sampling top layer and bottom layer. 79

Figure 5-22. The environmental parameters in the pond of the Royal Oak wetland for Secchi depth and Chl-a;In, Mid, Out are the in-pond sampling locations (inlet, middle, outlet); top, bot is the sampling top layer and bottom layer. Z_{secchi} is Secchi depth and Z_{mix} is water column depth. 85

Figure 5-23.The environmental parameters in the pond of the Royal Oak wetland for DO, pH, and T; In, Mid, Out are the in-pond sampling locations (inlet, middle, outlet); top, bot is the sampling top layer and bottom layer. 86

Figure 5-24. Scatter plots showing the event REs vs. inflow EMCs of TN and TP for the Rocky Ridge wetland (a) – (c) and the Royal Oak wetland (d) – (f). 93

Figure 5-25. Biplot representation of Principal Component Analysis for event REs and factors for the Rocky Ridge wetland and the Royal Oak wetland; the red dots mean observed data, and black lines and blue dots mean the vectors of parameters. PC (%) represents the percent variance explained for data. 95

Figure 5-26. Scatter plots showing the REs vs. E_p for the Rocky Ridge wetland (a) – (c) and the Royal Oak wetland (d) – (f). 96

Figure 5-27. Scatter plots showing the event REs vs. factors for the Rocky Ridge wetland (a) – (b) and the Royal Oak wetland (d) – (f), with high R^2. RE-TP vs. RE-TSS for the Rocky Ridge wetland (c). 97

List of Abbreviations

A	Top surface area relative to an arbitrary datum
ADP	Antecedent dry period
ARI	Average rainfall intensity
AV	Area & velocity
BMPs	Stormwater Best Management Practices
Chl-a	Chlorophyll-a
COD	Chemical oxygen demand
De	Top water surface elevation
DNRA	Dissimilatory nitrate reduction
DO	Dissolved oxygen
DOC	Dissolved organic carbon
e	Actual vapor pressure of air
ê	Saturation vapor pressure of air
EMC	Event mean concentration
E_p	Evaporation rate from the pool top surface
ET	Evapotranspiration
HLR	Hydraulic loading rate
HRT	Hydraulic retention time
M	Mass load
MDL	Method Detection Limits
MRI	Maximum rainfall intensity
NH_3	Ammonia gas

NH_4-N	Ammonium nitrogen
NO_x-N	Nitrate+Nitrite
NWL	Normal water level
P	Direct rainfall to the pool top surface
PN	Particle nitrogen
PCA	Principal component analysis
Rde	Rainfall depths
Rdu	Rainfall duration
RE	Removal efficiency
RH	Relative humidity
RMSE	Root mean square error
RO	Royal Oak wetland
RPD	Relative percent difference
RR	Rocky Ridge wetland
RSD	Relative standard deviation
S.d	Standard Deviation
T_{air}	Mean air temperature
TDP	Total dissolved phosphorus
TKN	Total Kjeldahl nitrogen
TN	Total nitrogen
TP	Total phosphorus
TRP	Total reactive phosphorus
TSS	Total suspended solids

V	Volume of water stored in a wetland relative to an arbitrary datum
Z_{mix}	Water column depth
Z_{secchi}	Secchi depth

1 Introduction

1.1 Research Background

The growth of the urban population and the increase of urban impervious land covers make stormwater runoff peakier, have larger volume, and contain higher concentrations of nutrients, sediments, and other pollutants (Barbosa et al., 2012). Thus, eutrophication has been a common issue in urban aquatic ecosystems (Xu et al., 2014), especially during the last few decades. Eutrophication can cause various adverse impacts on water quality, e.g., it changes watercolor, emits odors, reduces its transparency, and ultimately reduces biodiversity in the water (Dunalska et al., 2015; Luo and Li, 2018). Just 10 – 20% of the total impervious area in an urban basin could lead to significant aquatic degradation without proper management (Carey et al., 2013). Therefore, urban stormwater management is critical to protecting urban aquatic environments, and many municipalities are working to balance ecosystem health and flood protection (Li et al., 2017). Various best management practices (BMPs) have been implemented. In many countries, constructed stormwater ponds and wetlands have become a promising option for stormwater management (Ahilan et al., 2019). They can provide a range of benefits including peak flow attenuation, high pollutant removal efficiencies, feature easy operation and maintenance, and cost-effectiveness (Kadlec and Wallace, 2008; Zhang et al., 2009; Li et al., 2017; Ahilan et al., 2019). Additionally, they can provide wildlife habitat, increase biodiversity, and serve as entertainment and an aesthetic feature for communities (Cui and Jiang, 2013; Zhang et al., 2014).

The mechanisms for water quality improvement involve complex physical, chemical, and biological processes in stormwater ponds or wetlands (Vymazal, 2005). The pollutant removal can be influenced by various factors such as the stochastic nature of the hydrology, characteristics of a drainage system and region, land use, nature and frequency of storms, and catchment area (Stein and Hook, 2005; Wu and Xu, 2011; Li et al., 2017). It also depends on the pond configuration variables such as pond age, shape, depth, vegetation, and baffling (Zhao et al., 2011). Therefore, the performance of ponds and wetlands can vary significantly. Studies have shown that vegetated ponds and wetlands tend to remove nutrients more efficiently than non-vegetated systems and the removal efficiency is related to the types of plants (Wang and Sample, 2014; Borne, 2014; Ge et al., 2016; Olguín et al., 2017). Aquatic plants can absorb nutrients for growth and transport oxygen to anaerobic layers in bottom sediments; they can also provide a large surface area for microbial growth (Kadlec and Wallace, 2008). However, the nutrient removal efficiencies of wetlands are limited during extended periods of high-water levels (Bavor et al., 2001). There still exist two opposing thoughts on macrophytes relationships with nutrients: either they can uptake and assimilate nutrients into organic forms acting as net nutrient sinks, or they can contribute to the transport of nutrients from the sediment to the water.

The ability of stormwater wetlands and ponds to remove pollutants from runoff should be considered as a function of influent concentration and hydraulic loading rate (HLR, or hydraulic retention time, HRT), which are in turn functions of rainfall parameters, runoff volume, and pond design, like surface area, and pool volume (Kadlec and Knight, 1996; Carleton et al., 2001). Even though hydraulic conditions and inflow patterns appear to be more important in terms of biological responses (Jiang and Chui, 2022), it is unclear how nutrient removal is affected by the coupled effect of climate conditions and stormwater management design or what kinds of design modifications could minimize the detrimental effect of climate on nutrient removal (Valenca et al., 2021; Jiang and Chui, 2022).

A number of previous studies have focused on pollutant removal from variously designed wetlands where HRT and HLR play a vital role (Nayeb et al., 2021; Jiang and Chui, 2022). For example, Zhang et al. (2012a) found that nutrients could increase with longer HRT and lower HLR, because the interaction between water, plants, and soil is enhanced. However, Sultana et al. (2016) found a minimal effect on pollutant removal efficiency from an increase in HRT. Although increased HRT in wetlands is mentioned in some papers, most of them do not provide the exact values because of the short duration, high fluctuation, and difficulty in monitoring (Jiang and Chui, 2022). HRT and HLR in stormwater wetlands depend on individual pool design and influent flow rates, primarily driven by local rainfall and catchment characters. The importance of proper sizing of pond area and volume was recognized in early design guidelines and recommended area ratio ranges were 1.0 – 6.5% of watershed, and the treatment volume should be large enough to capture 90% of all storm events (Kadlec and Wallace, 2008).

Additionally, local climate condition is another important factor for nutrient removal, mainly because the biotic processes in the pond are governed by fluctuations in pH, dissolved oxygen, and water temperature determined by the local climate (Valenca et al., 2021). In summer wet seasons, increased water and material flux into the wetlands, greater irradiance, and higher temperatures all promote primary production and decomposition (Hagerthey et al., 2010), therefore, nutrient uptake by water column primary production was greatest during the wet season (Griffiths et al., 2021). The removal of nitrogen and phosphorus by stormwater wetlands could be affected by local climate differently, for instance, nitrogen removal rates were observed to decrease during periods of high seasonal precipitation (Drake et al., 2018), while the lowest phosphorus reductions were observed during dry seasons (Dunne et al., 2005). The nitrate removal in hot-summer Mediterranean climates is higher than the removal in a humid subtropical climate, partially because of the longer antecedent dry period between rainfall events (Valenca et al., 2021). However, after significant dry periods, subsequent rewetting can cause a noticeable release of detrital phosphorus into the water column (Pant and Reddy, 2001).

It is still needed to examine how nutrient removal is affected by the coupled effect of climate conditions and stormwater management design or to study what kinds of design modifications could minimize the detrimental effect of climate on nutrient removal (Valenca et al., 2021; Jiang and Chui, 2022). This study selected five rainfall characteristic parameters and evaporation rate and air temperature, as well as defined four hydraulic parameters to be considered. The considered rainfall characteristics include rainfall depths, rainfall duration, rainfall intensity (maximum and average), and antecedent dry periods.

In Alberta, the Elbow River, the Bow River, and the North Saskatchewan River have experienced serious water quality deterioration because of increased loadings of nutrients and suspended solids, mainly from Calgary and Edmonton stormwater runoff (Sosiak and Dixon, 2006; Neufeld, 2010; Morales-marín et al., 2017; Laceby et al., 2019; City of Edmonton, 2021; City of Calgary, 2021). Alberta government made guidelines for nutrient loading to receiving waters and considered removing sedimentations with particle sizes larger than 75 µm (Environment, Alberta. 2001; Troitsky et al., 2019). In Alberta, many stormwater ponds and wetlands have been designed in new communities to control flow and remove nutrients and suspended solids. This study focused on the treatment performance analysis of two existing wetlands in Calgary. We investigated the pond physiochemical conditions under the influence of various factors to understand the key factors affecting the nutrients removal in the studied wetlands to explore their design optimization.

1.2 Study Objectives

This study examines the effectiveness of two constructed stormwater wetlands, the Royal Oak and the Rocky Ridge wetlands, controlling urban stormwater in Calgary, Alberta, a cold temperate region during ice-free seasons in 2018 – 2019. Both concentration and load reduction were considered to assess the performance of stormwater wetlands. This study aims to (1) Monitor the efficiency of two wetlands for removing nutrients by storm events; (2) Evaluate the annual variability of the treatment efficacy with a focus on the differences between the dry year and wet year; (3) Examine the effect of rainfall characteristics, evaporation, air temperature, hydraulic parameters on the removal efficiency; (4) Determine if the current hydraulic design parameters are suitable for effective nutrient removal for these two stormwater wetlands in current weather conditions.

1.3 Thesis Structure

This research consists of three components: field observation, water budget analysis, and nutrient removal assessment. This thesis is divided into six chapters. A brief description of each chapter is summarized below:

- Chapter 2 reviews literature on field observation uncertainty and nutrient removal mechanisms and statements of the study problems.
- Chapter 3 describes the field observation and the data analysis.
- Chapter 4 presents the results of the water budget.
- Chapter 5 discusses the nutrient removal performance.
- Chapter 6 presents conclusions and future research needs.

2 Literature Review

The International Stormwater Best Management Practices (BMPs) Database Annual Report (Clary et al., 2020) shows that, as of 2020, over 7090 lakes and streams in the USA have been identified as impaired, of which over 6600 are due to organic enrichment and oxygen depletion that is often associated with nutrient loading. Nitrogen and phosphorus are the main nutrients for aquatic plants; in excess, they can be considered contaminants relevant to eutrophication in water bodies (Collins et al., 2010). Stormwater runoff with high nutrient concentration is a hydrologic manifestation of many changes that result from urbanization. It can elevate nutrient and contaminant concentrations of receiving water bodies and degrade the integrity of urban aquatic ecosystems (Jefferson et al., 2017). Different solutions have been applied to urban stormwater management, treating storm water as a pollution source or recycled water resources. Constructed stormwater ponds and constructed stormwater wetlands have been designed and built to remove pollutants that flush off from landscapes, and they are widely utilized in managing stormwater flow, sediment, and nutrient loads into receiving waters (Bavor et al., 2001). Stormwater wetlands usually differ from ponds in that they support substantively submerged and emergent vegetation communities (Vogel and Moore, 2016). Stormwater wetlands and ponds are one of the least expensive treatment systems to operate and maintain, because they have natural environmental energies at work and need minimal fossil fuel energy and chemicals to meet treatment objectives (Kadlec and Scott, 2008). As the stormwater flows through the wetland, it is treated by the processes of sedimentation, filtration, oxidation, reduction, adsorption, and precipitation (Kadlec and Scott, 2008). The components in a typical stormwater wetland are shown in Figure 2-1. These stormwater treatment systems contain areas of open water, floating microbes, and submerged and emergent plants, either by design or as an unavoidable consequence of the design configuration (Kadlec and Scott, 2008).

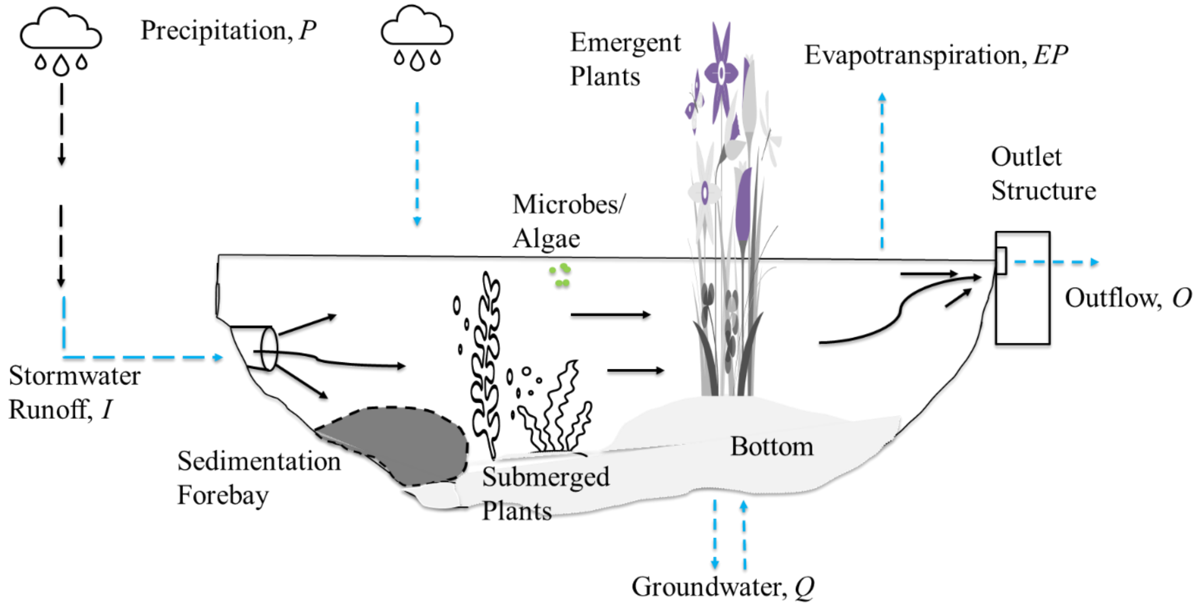

Figure 2-1. Schematic of a stormwater wetland (free water surface), the blue dotted lines indicate components of the water budget.

2.1 Water Budget

Stormwater enters wetlands via pipe runoff, surrounded land runoff, groundwater discharge, and precipitation (Figure 2-1), and leaves via drainage outflow, evapotranspiration (ET), and groundwater recharge (Kadlec and Wallace, 2008). However, most wetlands would normally be isolated from groundwater (Kadlec and Wallace, 2008). Thus, water storage in the pool is determined by the inflow and outflow together with the characteristics of the wetland basin. In response to the high variability in the inflows and outflows, large variations in storage are therefore possible (Kadlec and Wallace, 2008).

Thin-plate weirs and orifices installed in hydraulic structures are normally used for outflow regulation in constructed stormwater wetlands and wet ponds (Hamid et al., 2017). The calculation formulas of such devices rely upon some empirical coefficients. Many lab experiments have been conducted to achieve different weir calibrations and discharge coefficients (Johnson and Green, 1977; Chanson and Wang, 2013; Hamid et al., 2017). The steady stage-discharge relationships are used in unsteady flow conditions since the performance of water measurement structures and devices in unsteady flow conditions has rarely been studied (Ghasemzadeh et al., 2020). In terms of field flow observation, an inevitable error of flow monitoring is that poor channel conditions may cause incorrect or erratic readings by flow meters (ISCO, 2016), like outfalls or channel intersections, flow streams at very low levels with high flow rates, turbulence, depths that consistently run below 1 inch. Heiner et al. (2011) justified that any field monitoring devices or operations are subjected to errors and uncertainties. The inaccuracy of flow measurement is still a challenge for effective water management (Heiner et al., 2011).

The nutrient mass budget is related closely to the water budget, since the inputs and outputs of nutrients are primarily through hydrologic pathways (i.e. inflows and outflows). To guarantee the reliability of flow data, the water budget analysis must be done. This also allows a very good quantification of flow, rainfall, and evaporation. For water budget, in theory, any one term may be calculated if all the other terms are known using the equation 2 – 1 (Kadlec and Scott, 2008). But in practice, none of the measurements is very precise, and large errors may result from such a calculation (Winter, 1981). The computation of the volume of water stored in a wetland requires the stage-storage curve for the wetland, and the derivative of this function is the water surface area (Kadlec and Wallace, 2008). The general equation describing the hydrologic balance of a wetland is as follows:

$$\mathrm{dV} = \mathrm{I} - \mathrm{O} \tag{2 - 1}$$

where, V is the volume of water stored in the pool relative to an arbitrary datum and dV is volume change rate; I is the total inflow which includes inlet inflows, surface runoff, and rainfall; O is the total outflow which includes outlet discharges and evaporation.

2.2 Evaporation and Direct Rainfall

Precipitation and evaporation are mainly determined by the climate type and change seasonally, they are important in the treatment of wetlands in tropical regions (Baskar and Thattai, 2014; Zhang et al., 2012b). As aforementioned, stormwater enters wetlands can via precipitation dropping into the top surface, and they leave can via evaporation from the top surface (Kadlec and Wallace, 2008). Jiang and Chui (2022) reviewed that precipitation and evaporation water sources normally account for below 10% of wetland’s volume, mainly because most of the treatment wetlands are typically constructed to optimize hydraulic control to improve pollutant treatment efficiency (Dong et al., 2012). In mild temperate climates, annual rainfall typically slightly exceeds annual evapotranspiration (ET), and there is little effect on atmospheric gains and losses over a year (Kadlec and Wallace, 2008). However, for long-term operation and analysis of treatment wetlands which are under various hydrological scenarios, precipitation and evaporation should be examined.

ET acts to concentrate contaminants remaining in the water (Kadlec and Wallace, 2008), and the impacts of evaporation on the water quality performance should be explored. For instance, Platzer and Netter (1994) report that the wetland accomplished 88% ammonia removal on a mass basis. When coupled with the 70% water loss, the ammonia concentration reduction could be almost 60% (Kadlec and Wallace, 2008). The implications for water quality from rainfall are not inconsequential, as internal mixing patterns can blur the effects of the rain on water quality (Kadlec and Wallace, 2008).

2.3 Water Environment Parameters

In water bodies, nitrogen and phosphorus processes are dominated by some environmental parameters, including temperature, pH, bacteria community, and dissolved oxygen (Kadlec and Knight, 1996). Some comparative studies between vegetated and unvegetated wastewater treatment systems have elucidated the critical role of oxygen on nitrogen removal (Ouellet-Plamondon et al., 2006; Maltais-Landry et al., 2007; Chazarenc et al., 2009; Maltais-Landry et al., 2009; Zhang et al., 2010). Specifically, a lack of oxygen in wastewater treatment systems often inhibits nitrification (Haberl et al., 1995; Ramirez et al., 2005; Cerezo et al., 2001). However, predominant anoxic conditions can promote denitrification in these systems with a suitable carbon source (Haberl et al., 1995; Rousseau et al., 2008).

pH, is another crucial environmental parameter that can control nutrient removal and can influence many biological transformations. Many treatment bacteria are not able to exist outside the range $4.0 < pH < 9.5$ (Metcalf and Eddy, 1991). For example, denitrifiers operate best in the range $6.5 < pH < 7.5$, and nitrifiers prefer pH = 7.2 and higher (Kadlec and Wallace, 2008). The protonation of phosphorus changes with pH, and the hydroxide and oxyhydroxide precipitates of iron and aluminium are pH sensitive (Kadlec and Wallace, 2008). Aluminium phosphate precipitates best at a theoretical pH of 6.3, and iron phosphate precipitates best at a theoretical pH of 5.3 (Kadlec and Knight, 1996).

In terms of water temperature, literature reviews illustrate that water temperature decrease can have a negative impact on nutrient removal (Ruan et al., 2006; Akratos and Tsihrintzis, 2007; Zhang et al., 2011). The favourable temperature for nitrification range between 16.5 and 32 ℃ in constructed wetlands (Demin and Dudeney, 2003; Katayon et al., 2008). Very little nitrification is observed when the water temperature is below 5 – 6 °C or over 40 °C (Knight, 1994; Werker et al., 2002; Xie et al., 2003). Denitrification was found slowly at a low temperature of 5 °C (Knight 1994; García et al., 2010), and it can increase exponentially with increasing temperature and reaches a plateau between 20 and 25°C (U.S. EPA, 1975; Saeed and Sun, 2012).

Algae can affect phosphorus/nitrogen cycling either directly uptake/release or indirectly through photosynthesis/respiration-induced pH and DO changes in water and soil/water interface (Vymazal, 1995). Almost all the distributions of all parameters from environmental, metals, and nutrients could be affected by algae blooms. Here, Chlorophyll-a, a biological pigment, can be used to assess the occurrence of harmful algae blooms (Bulgakov and Levich, 1999; Brient et al., 2008; Hushchyna and Nguyen-Quang, 2017; Nguyen-Quang et al., 2018).

2.4 Removal Mechanisms and Factors for Nutrients

Nitrogen is transported in surface runoff in both particulate and dissolved phases. The common forms of nitrogen include organic nitrogen, inorganic ions (ammonium, nitrite, and nitrate), and inorganic molecules (ammonia, nitrous) in natural water. Nitrite tends to be more mobile and persistent, as a short-lived intermediate in a series of biologically catalyzed reactions of the nitrogen cycle (Kadlec and Knight, 1996). Nitrate is readily available for biological uptake when the phosphorus is sufficient, which can cause eutrophication (WERF, 2005). The major nitrogen biological and chemical processes are consumption and assimilation, denitrification, nitrification, ammonification, fixation, and dissimilatory reduction of nitrogen to ammonium. Nitrogen is mainly removed by assimilation, denitrification, and sedimentation (Troitsky et al., 2019). Key factors influencing nitrogen processes include temperature, pH, bacteria community, and dissolved oxygen (Kadlec and Knight, 1996). The microbial mediated processes such as nitrification, denitrification, and ammonification are found to be temperature and pH-dependent, and they also rely on bacteria mediation (Kadlec and Wallace, 2008). Dissolved oxygen is an important environmental factor, involving the respiratory oxidation process but inhibiting the denitrification process (Kadlec and Knight, 1996). Organic carbon must be a food source for relevant bacterial communities (Kadlec and Knight, 1996). The major nitrogen transformations in stormwater wetlands are shown in Figure 2-2.

In natural water, phosphorus is primarily transported with eroded sediments because it tends to sorb to soil particles and organic matter. Total phosphorus primarily has inorganic phosphate and organophosphate components, and they are mainly derived from soil, plant, and animal materials (Clary et al., 2020). The dissolved parts of total phosphorus are typically divided into soluble reactive phosphorus and soluble unreactive phosphorus. Soluble reactive phosphorus, which is mainly composed of inorganic orthophosphates, is actively involved in plants, algae, and microorganisms' growth. Various organic compounds and polyphosphates compose soluble unreactive phosphorus primarily. For the particulate total phosphorus, the principal constituent comes from zooplankton, algae, detritus, bacteria, and some silt and clay inorganic particulates. Some bacteria can convert organic particulate phosphorus into orthophosphates eventually (Tchobanoglous and Schroeder, 1985; Clary et al., 2020).

The phosphorus processes are not fully understood since the categorization of phosphorus forms is complex, but the direct transformations of phosphorus include uptake and assimilation, desorption and dissolution, adsorption, and mineralization (Clary et al., 2020). The major phosphorus transformations in stormwater wetlands are shown in Figure 2-3. The main removal mechanisms of phosphorus are sedimentation and burial (Troitsky et al., 2019). Key factors influencing phosphorus processes are temperature, pH, cation exchange capacity, and oxidation-reduction potential (Holford and Patrick, 1979; WERF, 2005; Clary et al., 2020). WERF (2005) stated that the solubility of phosphorus species in stormwater ranges from over 80% at a pH of 6 to less than 1% at a pH of 8. Phosphorus and metals tend to adsorb onto particles at appropriately high pH (Holford and Patrick, 1979). The relationship between pH and sorption capacity of particles which depends on cation exchange capacity and the amount of phosphorus already present is complex and non-monotonic (Clary et al., 2020). The temperature has a substantial impact on microbial and plant activities, as well as the water viscosity and settling velocity for sedimentation related to phosphorus.

Both nitrogen and phosphorus can be taken up through the growth of plants, algae, and microorganisms. Apart from these removal processes, phosphorus can readily undergo surface complexation reactions, to be adsorbed with sticky soils or precipitated with metals like iron, aluminium, and calcium. The transformation and removal of nitrogen in stormwater BMPs is very complex. Studies show that the sedimentation and denitrification of the nitrogenous solids of nitrate are probably the most important treatment processes for nitrogen removal in the stormwater system (Clary et al., 2020). The final product from denitrification is N_2 gas, which can be released into the atmosphere. However, the particulate-bound nitrogen and phosphorus can be reversible and is the major concern for long-term removal (WERF, 2005). Nitrogen/phosphorus via sedimentation and biotic assimilation may only produce temporary reductions in concentrations unless captured solids are removed and vegetation is harvested regularly.

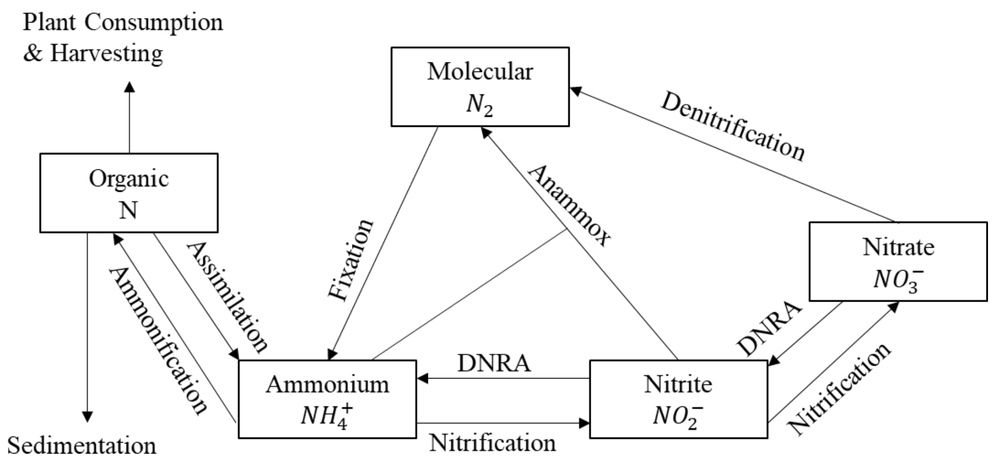

Figure 2-2. Simplified major nitrogen transformation pathways in stormwater wetlands. Adapted from Troitsky et al. (2019). DNRA is dissimilatory nitrate reduction.

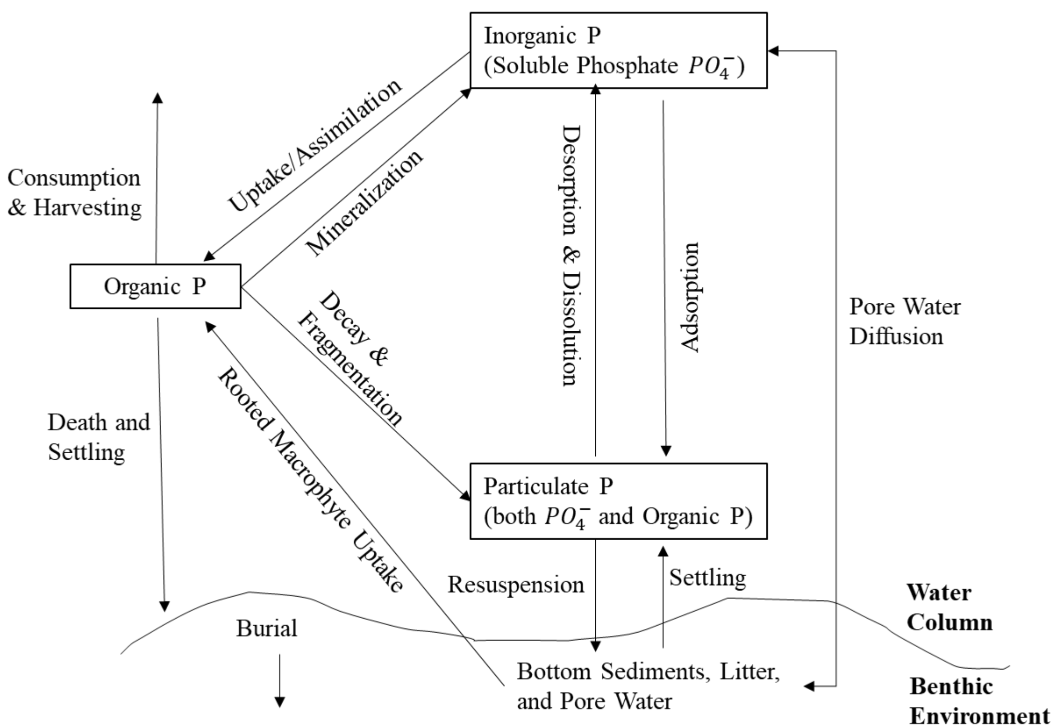

Figure 2-3. Simplified major phosphorus transformation pathways in stormwater wetlands. Adapted from Collins et al. (2010).

2.4.1 Nitrogen Removal Pathways

In a constructed wetland rich with organic nitrogen, ammonification initiates the first step of N transformation. The ammonification process decreases with depth, indicating that ammonification is faster in the upper zone where the condition is aerobic and slower in the lower zone where the environment switches from facultative anaerobic to obligate anaerobic conditions (Reddy and Patrick, 1984). The ideal pH range for ammonification is 6.5 – 8.5 (Patrick and Wyatt, 1964; Vymazal, 1995). Ammonification proceeds faster at a higher temperature, the rate doubles with a temperature increase of 10 °C (Kadlec and Knight, 1996). Nitrification is the second step of N transformation and is a two-step process, where ammonia (NH_4-N) in presence of oxygen, is first converted to nitrite N (NO_2-N) by strictly chemo lithotrophic Nitrosomonas, Nitrosococcus, and Nitrosospira bacteria, and then to nitrate N (NO_3-N) by facultative chemo lithotrophic bacteria Nitrospira, and Nitrobacter. Nitrification can consume alkalinity and result in a substantial drop in pH in water (Kadlec and Knight, 1996). Denitrification, a bacterial process (Vymazal, 1995) has been observed in a suspended and attached bacteria growth environment with lower dissolved oxygen content (should be maintained at < 0.3 – 0.5 mg/L to accomplish NO_3-N reduction) and anoxic zones (Kadlec and Knight, 1996; Cerezo et al., 2001; Lee et al., 2009; Bertino, 2010). Some studies indicate that the optimum pH for the denitrification process is observed at a pH range of 6.5 – 7.5, and it can be hampered at pH < 6.0 and pH > 8.0 (Kadlec and Knight, 1996). Dissimilatory nitrate reduction (DNRA), which transfers NO_x-N to NH_4-N, is generally observed in carbon-rich environments and nitrate-limited conditions (Kadlec and Wallace, 2008; Laanbroek, 1990).

Macrophytes can not only provide surfaces and oxygen for nitrification (Bayley et al., 2003; Kaseva, 2004; Langergraber, 2005; Cui et al., 2010) but can also provide carbon for denitrification (Brix, 1997; Masi, 2008; Białowiec et al., 2011; Caselles-osorio et al., 2011; Wang et al., 2012). Different comparative studies between unplanted and planted wetlands show that higher N removal occurs in planted systems, indicating the necessity of macrophytes for improving N removal performances (Drizo et al., 2000; Huett et al., 2005; Maltais-landry et al., 2009; Cui et al., 2010; Zhao et al., 2010; Leverenz et al., 2010; Hoang et al., 2011; Herouvim et al., 2011). Nitrogen uptake by plants differs according to the pond configurations, inflow loadings, and environmental conditions (Drizo et al., 1997; Eylon et al., 1998; Healy & Cawley, 2002; Meers et al., 2008;

Kantawanichkul et al., 2009; Białowiec et al., 2011). Decaying plant materials can increase effluent nutrient concentration (Brodrick et al. 1988).

In alkaline water bodies (like pH > 9.3), NH_4-N ions can be converted to NH_3 gas followed by the release of the gas from the water surface to the atmosphere (Cooper, 1996; Białowiec et al., 2011). However, this physical removal process is generally negligible, when the pH value is below 7.5 – 8.0 in water bodies (Reddy and Patrick, 1984). Nitrogen adsorption usually occurs through cation exchange between specific media components and NH_4-N ions in water (Bayley et al., 2003), the adsorbed NH_4-N can be nitrified due to predominant aerobic conditions inside the media (Connolly et al., 2004; Vymazal, 2007). However, the matrix-oriented ammonium adsorption process is not frequently observed in wetland systems since the adsorption capacity of wetland media is usually low (Keffala and Ghrabi, 2005).

2.4.2 Phosphorus Removal Pathways

Adsorption and storage of phosphorus in biomass are saturable processes that cannot contribute to long-term sustainable removal (Dunne and Reddy, 2005). While Marshall (1986) found that peat/soil accretion controls long-term phosphorus sequestration in wetlands, it could be effective only in treatment wetlands with high biomass production and water overlying the sediment. In natural wetlands, the sediment-litter compartment is the major phosphorus pool (Verhoeven, 1986). Adsorption refers to the movement of soluble inorganic phosphorus from soil porewater to soil mineral surfaces (Rhue and Harris, 1999). In organic soils, anaerobic soils can show stronger adsorption/desorption processes than aerobic soils due to the change brought about in ferric oxyhydroxide by soil reduction conditions (Patrick and Khalid, 1974). Some melic parameters, like Al, Fe, Ca, and Mn, have been related to phosphorus adsorption/desorption and precipitation/dissolution (Patrick et al., 1973; Richardson, 1985; Reddy and D'Angelo, 1994). These precipitation processes typically occur at high concentrations of either phosphate or the metalloid cations, under some circumstances but may re-dissolve under altered conditions (Rhue and Harris, 1999; Kadlec and Knight, 1996).

Plant uptake and storage of phosphorus should not be considered as part of the long-term phosphorus removal capacity of wetlands and ponds, because aquatic plants grow and decay on an annual cycle (Boyd, 1969; Vymazal, 1995; Kadlec and Knight, 1996). Microbiota (bacteria, fungi, algae etc.) uptake is rapid, but the amount stored is low. However, Vymazal (1995) pointed out that algae can significantly influence nutrient cycling in areas with open water, but its role is mostly neglected. Algae can affect phosphorus/nitrogen cycling either directly uptake/release or indirectly through photosynthesis/respiration-induced pH and dissolved oxygen (DO) changes in water and soil/water interface (Vymazal, 1995).

3 Methodology

3.1 Site Description

Calgary is a semi-arid city in Alberta, Canada, with a long winter season. The ice-free season usually runs from April to October. In this study, the Royal Oak wetland (RO, built-in 2000) and Rocky Ridge wetland (RR, built-in 1995) were selected for study in consultation with the City of Calgary Water Resources staff, considering they are not slated for rehabilitation during the study period. The wetlands are located 250 m apart in residential areas in the northwest region of the city with a road separating their respective catchments (Figure 3-1). Both are constructed wetlands with outlet structures that regulate the water level and pond outflow discharges. The distance along the flow path is approximately 130 m for Royal Oak and 90 m for Rocky Ridge, Figure 3-2. The summarized characteristics of these two wetlands can be seen in Table 3-1.

Table 3-1. Characteristics of the study wetlands and the associated catchments. NWL, normal water level.

/	Unit	Rocky Ridge Wetland	Royal Oak Wetland
Catchment Type	–	Residential	Residential
Catchment Area	ha	15.90	15.20
Imperviousness Ratio	%	60.00	51.00
Slope of Catchment	%	6.77	8.22
Slope of Inlet Pipe	%	0.17	6.71
Diameter of Inlet Pipe	m	0.75	0.90
Sedimentation Features	–	Sediment Vault	Sediment Forebay
Surface Area at NWL	m^2	5389.40	4375.00
Wet Pool Volume at NWL	m^3	5743.80	2497.90
Average Normal Depth	m	1.07	0.57
Length to Width Ratio	–	1.25:1	2:1
Vegetation Type	–	Submerged Plant	Emergent Macrophytes

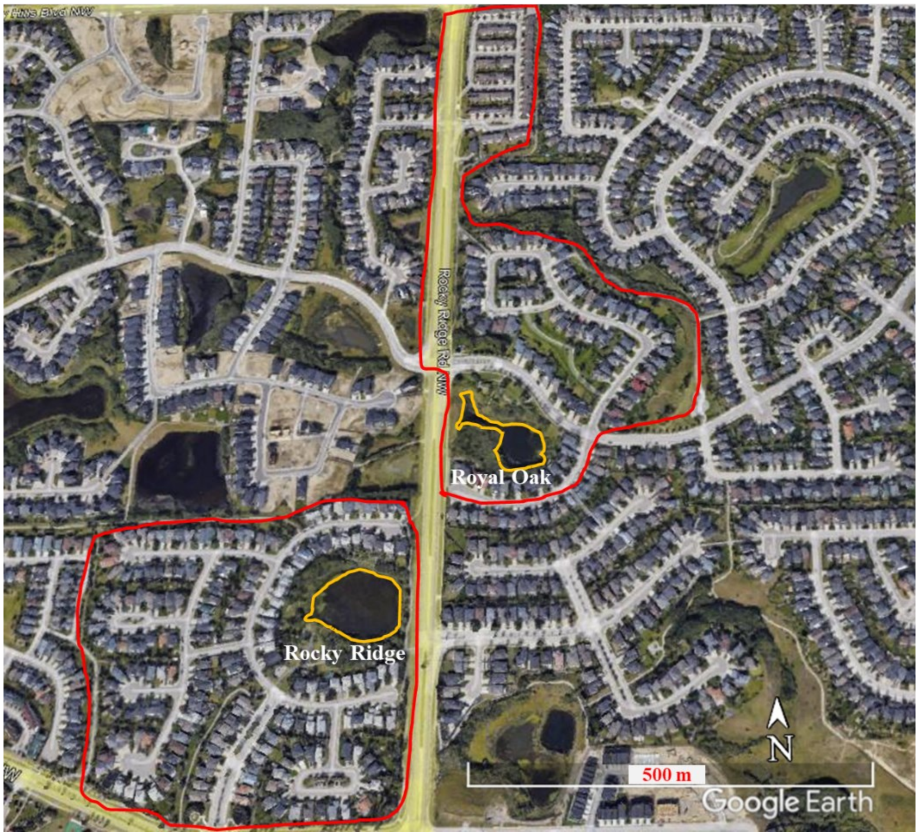

Figure 3-1. Aerial view of the studied wetlands' catchments. The catchment area is shown by the red line; the pond area is shown by the yellow line.

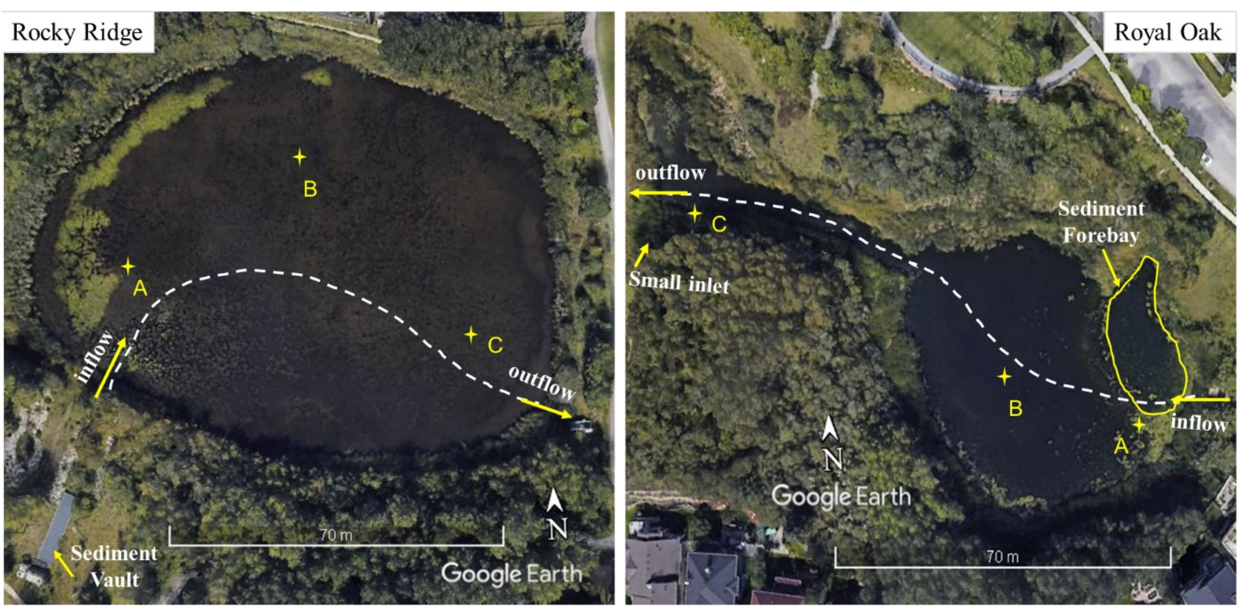

Figure 3-2. Aerial view of studied wetlands. The main flow path direction is indicated by the yellow arrows and white dotted line; the sampling and moored locations are shown by stars.

Figure 3-3. The rectangular concrete sediment vault for first flush treatment in the inlet of the Rocky Ridge wetland.

The Rocky Ridge catchment includes a ~15.9 ha drainage area, which primarily consists of single-family residential units. The pond has a single inlet pipe that is a 750 mm diameter concrete pipe that normally carries flow into a rectangular concrete sediment vault for first flush treatment, Figure 3-3. There is also a 750 mm diameter concrete bypass for extreme storm events. The outlet structure consists of a circular orifice for normal discharge control and a rectangular weir for events with return periods of 100 years or greater, Figure 3-4. The outlet discharge is controlled via two methods depending on the water level. The weir regulates the discharge from the normal water level (NWL = 1259.010 m) up to a surface elevation of 1259.042 m, at which point, the flow rate over the weir is equal to that through the orifice and the weir is drowned out (i.e., it becomes irrelevant). At higher water levels the downstream orifice regulates the discharge. The two stage-discharge equations (Martínez et al., 2005; Chyan et al., 2006; LMNO, 2014; Lindell et al., 2017) are as follows:

1. Weir controlling flow:

$$Q = \frac{2}{3} \times C_{rd} \times L \times \sqrt{2 \times g} \times H^{1.5} \tag{3-1}$$

2. Orifice controlling flow:

$$Q = C_d \times A_o \times \sqrt{2 \times g \times (H + 0.1075)} \tag{3-2}$$

where, C_{rd} is the discharge coefficient of the weir, 0.633; L is the weir width in the stop-log, 0.9 m; C_d is the discharge coefficient of orifice, 0.61; A_o is the area of the orifice, 0.0097 m^2; H(m) is the water depth from the bottom of the weir; g is the gravitational constant, 9.81. These two equations are shown plotted in Figure 3-5. The stage area curve of the pond is shown in Figure 3-6.

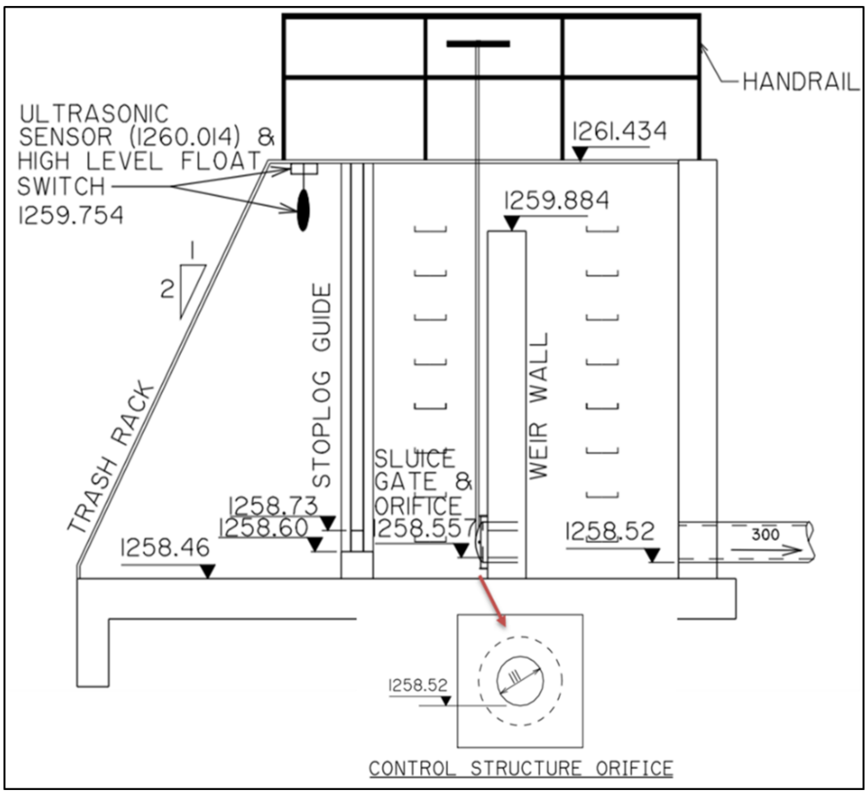

Figure 3-4. Side view of the outlet structure of the Rocky Ridge wetland.

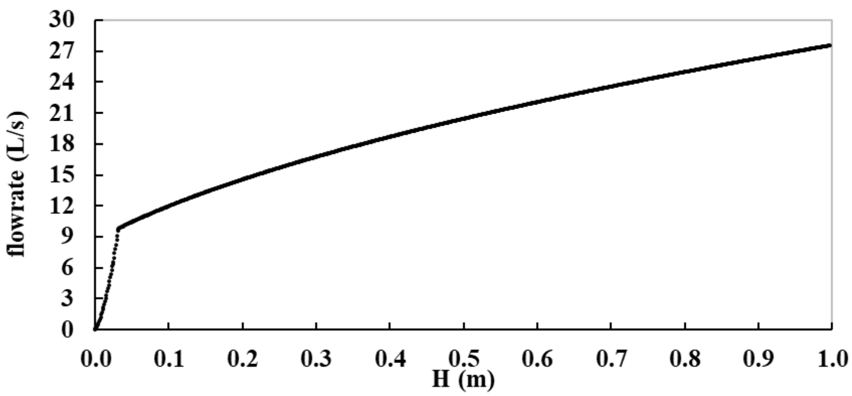

Figure 3-5. Stage outlet discharge curve for the Rocky Ridge wetland where Q is the discharge and H is the head on the weir or orifice. Note that zero head corresponds to the NWL.

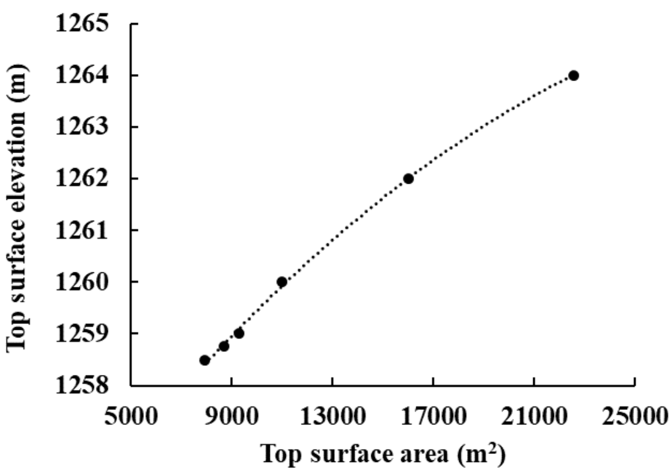

Figure 3-6. Stage-area curve for the Rocky Ridge wetland.

Royal Oak has a ~15.2 ha drainage area which primarily consists of single- and multi-family housing. This wetland has two inlets and a single outlet as shown in Figure 3-2. The main inlet conveys stormwater runoff from ~14 ha of the drainage area into a sediment forebay in the wetland through a 900 mm diameter concrete pipe. The runoff from the rest of the drainage area flows into the wetland through a minor inlet near the outlet. The outlet structure is composed of a plate V-notch weir that was bolted to the existing rectangular concrete weir and a circular orifice, Figure 3-7. Water flows through the outlet structure in three regimes. In the first regime, the V-notch weir controls the flow from zero up to a surface elevation of 0.220 m. In the second regime (0.220 – 0.237 m), the flow is overtopping the weir, giving a compound v-notch and rectangular flow area. However, since the water becomes level (i.e., both sides of the shaft reach the same total water depth) roughly 0.017 m above the top of the weir, an assumption that the flow will act the same as before (i.e., the weir continues to govern the flowrate) will be made. Therefore, the same equations will be used from the point of overtopping to the point where the water levels become around 0.237 m. In the last regime, once the water level has become constant within the shaft, the orifice will control the structure's flow and a new equation will be needed. It should be noted that the assumptions would affect the accuracy of the rating curve in the section when water surface elevation is around 0.220 – 0.237 m. The three stage-discharge equations (Martínez et al., 2005; Azim et al., 2015; Lindell et al., 2017) are as follows:

1. Weir controlling the flow

$$Q = \frac{8}{15} C_{TD} \sqrt{2g} \tan\left(\frac{\theta}{2}\right) (h + k)^{5/2} \tag{3 - 3}$$

2. Flow of the approximation area

0~0.237 m over the weir crest (still weir governs flow)

3. Orifice controlling the flow

$$Q = C_d Ao \sqrt{2g(h + offset)} \tag{3 - 4}$$

Where, C_{TD}: discharge coefficient of the v-notch weir, 0.61; θ: angle, 1.04719755 (60˚); h (m): water depth over weir notch; k: correctional factor, considering the surface tension and viscosity, 0.00112816; C_d: discharge coefficient of the circular orifice, 0.61; g: gravitational constant, 9.81. Ao: orifice area, 8.754×10^{-3} m^3; offset (m): the depth from orifice centerline to water surface, 0.502. These two equations are shown plotted in Figure 3-8. Figure 3-9 shows the stage-area curve for the pond.

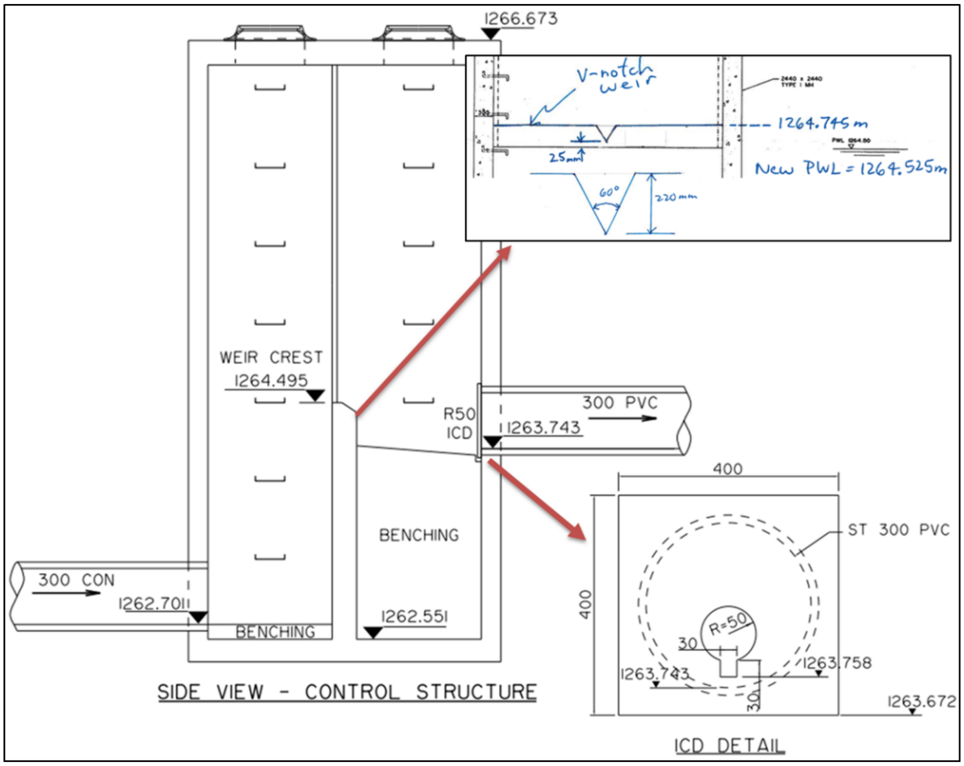

Figure 3-7. Side View-Control Structure of the Royal Oak wetland.

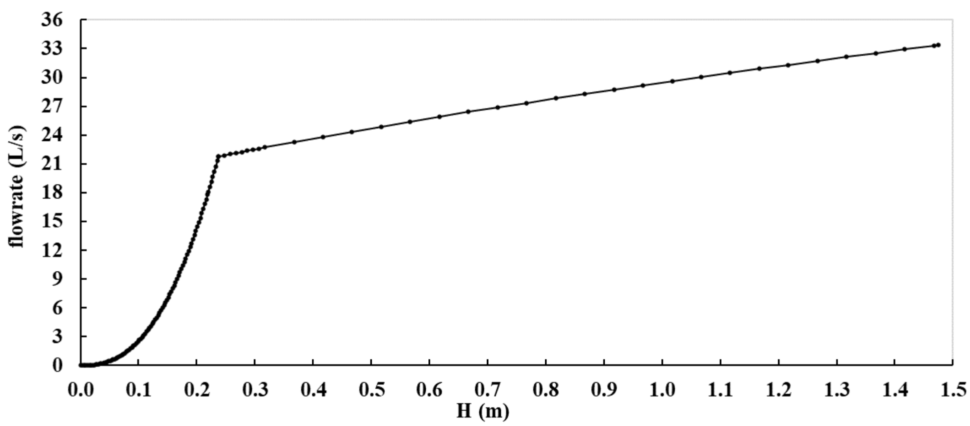

Figure 3-8. Stage discharge curve for Royal Oak wetland outlet structure.

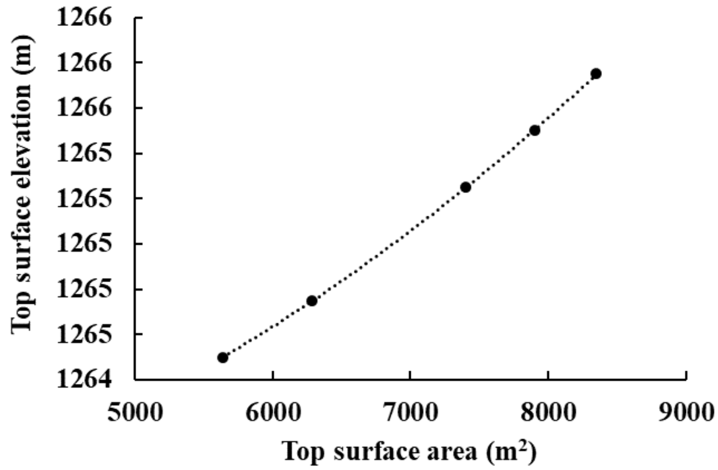

Figure 3-9. Stage-area curve for the Royal Oak wetland.

3.2 Field Measurement Program

Field measurements were conducted from May to November in 2018 and April to November in 2019. One weather station was placed on the bank of every study site to record meteorology parameters every five minutes interval: rain intensity, air temperature, atmospheric pressure, relative humidity, solar radiation, and wind speed and direction (Figure 3-10a). The weather station consists of a HOBO RG3-M Data Logging Rain Gauge and a HOBO RX300 Remote Monitoring Station (Onset Computer Corp., U.S). The Data Logging Rain Gauge consists of two major components: a tipping-bucket rainfall collector, and a HOBO ® event/temperature data logger. Precipitation data from weather stations mounted adjacent to each wetland was used to estimate the volume of precipitation falling directly on the pool surface.

In the inlets/outlets, portable auto-samplers Teledyne-ISCO-6712 equipped with 750/2150 area velocity flow modules were used to measure flow velocities, flow depths, and flow rates with a 5-min interval, and were used to collect stormwater samples (Figure 3-10b, Figure 3-11; Teledyne Isco Inc, U.S). Teledyne-ISCO-6712 auto-samplers collected water samples with a maximum collection capability of 24×1 L bottles, triggered by the set and adjusted water level at the AV sensor location. There were several reasons why samples were not successfully collected: No liquid detected failures; ISCO not triggered by small rain event, or point was set too high; power failure of the unit due to drained battery; or samples were discarded because the sample bottles had not been properly cleaned after earlier rain events or the samples contained runoff from previous rain events. Pollutant concentrations in stormwater runoff can be temporally dynamic and change as the runoff progress, for this reason, aliquots are commonly collected at times or inflow-weighted interval, thus, the event mean concentration (EMC) is usually used to characterize a storm event (Al-Rubaei et al., 2016). Here, the pollutant concentrations of the composite samples represent the EMC of the rain events; the EMC of discrete samples is the sum of the interval loads divided by the interval runoff volume.

A detailed summary of flow meter installation can be seen in Table 3-2. In the inlets, one 750-area velocity flow module was used in the Rocky Ridge wetland, measuring flow velocities and flow depths. One 750-area velocity flow module was used in the downstream inlet pipe for flow velocities depths and two 2150-flow modules were in the upstream pipes for flowrate in the Royal Oak wetland. For the pipe inflow, there were 750AV and 750Manning for the RR wetland and 750AV and 2150 for the RO wetland, respectively. In the outlets, in the RR wetland, one 750-flow sensor was put in the downstream outlet pipe and monitored the flow data in 2018. One 750-flow sensor was placed at the bottom of the orifice weir for water depth in 2019. A 750-flow meter sensor was placed at the bottom of the V-notch weir and a 2150-flow meter sensor was at the bottom of the orifice weir in the Royal Oak wetland, monitoring the effective heads from zero for two years. There are some different types of errors in flow data, like missing points, negative velocity and flow rate. There are also some periods when no data has been read by the flow meters. Time gaps within 30 minutes were interpolated linearly, and negative data along with long-time gaps were set to zero, to ensure the integrity of the data. The preliminary results of the water budget, calculated from the observed pipe inflow and weir/orifice outflow data, show that either we overestimated the outflow or underestimated the inflow for both wetlands in both years. The inflow validation and outflow prediction were conducted through the water budget in chapter 4.

Table 3-2. The flow meters installation information in these two wetlands

Rocky Ridge Wetland	**2018**	**2019**
	1 × 6712 Auto Sampler	1 × 6712 Auto Sampler
Inlet	1 × 750 Flow Sensor	1 × 750 Flow Sensor
	1 × 6712 Auto Sampler	1 × 6712 Auto Sampler
Outlet	1 × 750 Flow Sensor	1 × 750 Flow Sensor
Royal Oak Wetland	**2018**	**2019**
	1 × 6712 Auto Sampler	1 × 6712 Auto Sampler
	2 × 2150 Flow Sensor (upstream pipe)	2 × 2150 Flow Sensor (upstream pipe)
Inlet	1 × 750 Flow Sensor (downstream pipe)	1 × 750 Flow Sensor (downstream pipe)
	1 × 6712 Auto Sampler	1 × 6712 Auto Sampler
	1 × 750 Flow Sensor	1 × 750 Flow Sensor
Outlet	1 × 2150 Flow Sensor (No value)	

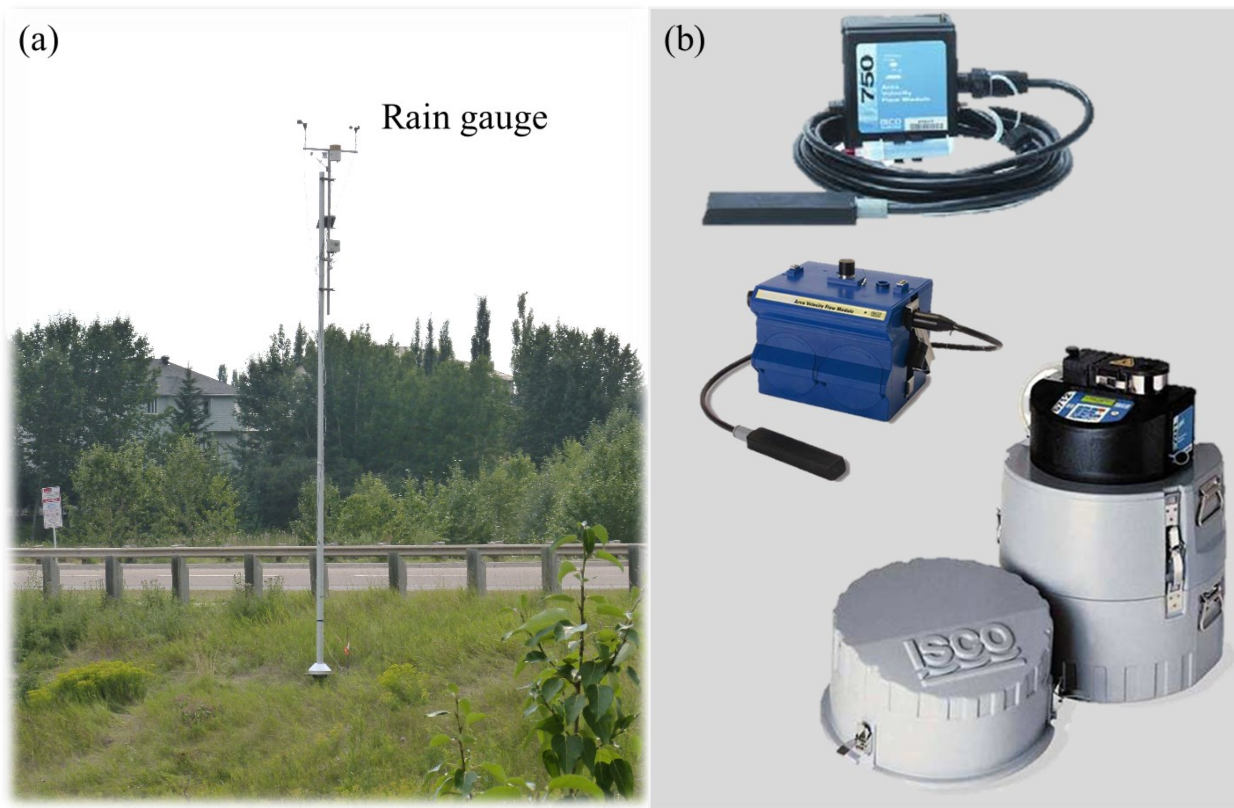

Figure 3-10. A rain gauge (a, Onset Computer Corp., U.S) and the portable auto-samplers Teledyne-ISCO-6712 were equipped with 750/2150 area velocity flow modules (b, Teledyne Isco Inc, U.S).

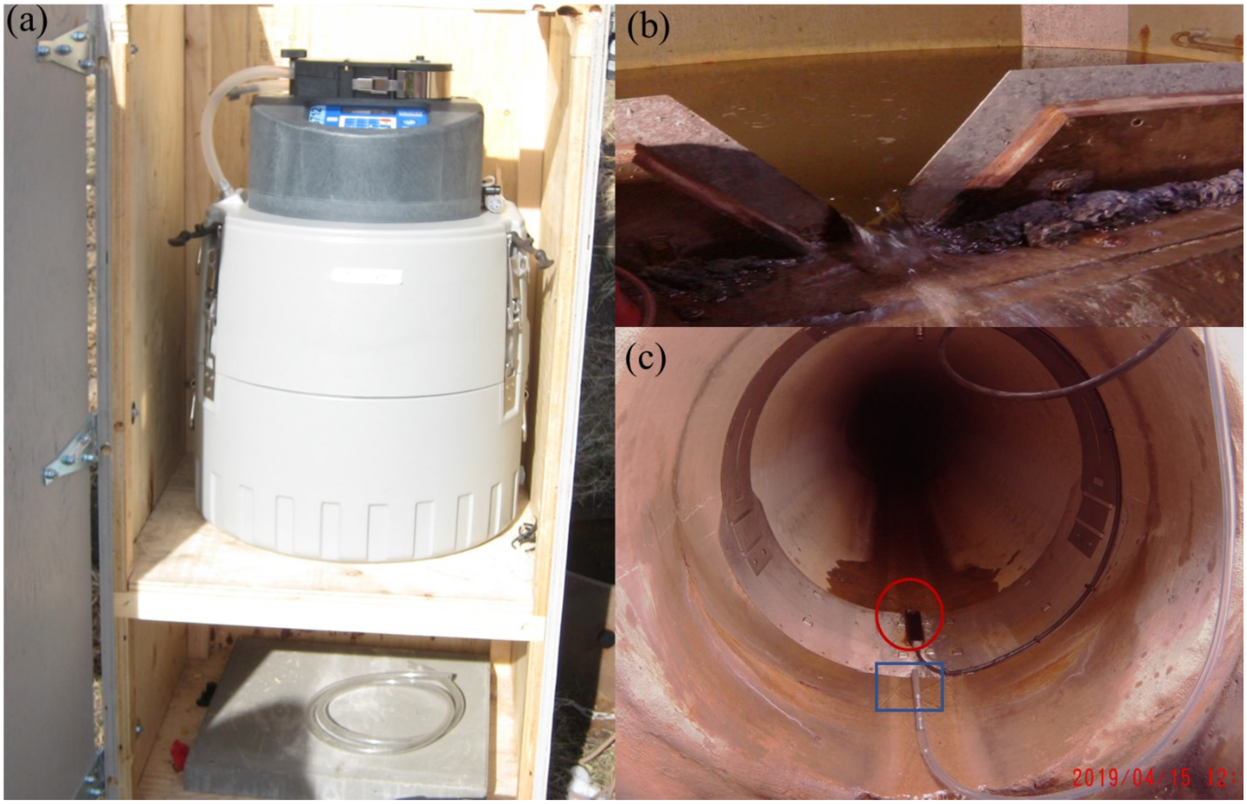

Figure 3-11. (a) ISCO-Teledyne Model 6712 automated sampler located at the outlet of Royal Oak wetland; it was used to collect stormwater samples and store hydrologic data at the sampling point (blue rectangle) in the outlet pipe. Influent and effluent monitoring for wetland: (b) V-notch weir in Royal Oak outlet, (c) outlet pipe, AVM (red circle) inside outlet pipe.

There were three locations (inlet, middle, and outlet, Figure 3-2) used for bi-weekly water sampling (top layer, bottom layer) as well as vertical profiling using an EXO3 for temperature (T), depth, Chlorophyll-a (Chl-a), pH, and DO in the wetlands. When the water depth was shallow, less than 0.6 m, a single sample was collected from sampling locations. A Secchi disk was used to measure the Secchi depth (Z_{Secchi}), water transparency, and the water column depth (Z_{mix}). The sampling and measuring depth work were performed not to stir up the bottom sediments.

Collected water samples from the inlets/outlets during rainstorms were analyzed for water quality parameters, including total suspended solids (TSS), ammonia (NH_4-N), total Kjeldahl nitrogen (TKN), nitrate/nitrite (NO_x-N), total nitrogen (TN), total dissolved phosphorus (TDP, only in 2019), total reactive phosphorus (TRP), total phosphorus (TP), dissolved organic carbon (DOC), chemical oxygen demand (COD), in a commercial laboratory in Calgary. In addition to the water quality parameters for the inlet/outlet water samples, a few additional parameters were measured: dissolved Kjeldahl nitrogen (DKN), dissolved nitrogen (DN), dissolved inorganic carbon (DIC), dissolved carbon (TDC), total organic carbon (TOC), total calcium (Ca), total iron (Fe), total manganese (Mn), total silicon (Si). After collection, samples were chilled, stored, and transported with pack ices and tested within holding hours in the lab, according to Standard Methods (Table 3-3). Duplicate and triplicate samples were collected every field trip and used for quality control and assessment. The sub-standard duplicated or triplicated samples were discarded when the relative percent difference (RPD) for duplicates was greater than 25% and the relative standard deviation (RSD) for triplicates over 18% (Patricia Mitchell Environmental Consulting, 2006). When concentrations were below the Method Detection Limits (MDL), the concentrations were equal to the MDL value (Li and Migliaccio, 2010; Borne et al., 2013).

Table 3-3. Water quality constituents analyzed in the lab, their analytical methods, and detection limit.

Parameters	Detection Method Reference	Lowest Detection Limit (mg/L)
NH_4-N	J. ENVIRON. MONIT., 2005, 7, 37-42, RSC	0.005
NO_x-N	CALCULATION	0.005
NO_2-N	EPA 300.1 (mod)	0.001
NO_3-N	EPA 300.1 (mod)	0.005
TON	CALCULATION	-
TKN	APHA Method 4500-Norg D	0.05
TN	APHA 4500 N-Calculated	0.05
DKN	APHA 4500-NORG D	0.05
TDN	APHA 4500 N-CALCULATED	0.05
TDP	APHA 4500-P PHOSPHORUS	0.002
TRP	APHA 4500-P PHOSPHORUS	0.001
TP	APHA 4500-P PHOSPHORUS	0.002
DIC	APHA 5310 B-WP	0.5
DOC	APHA 5310 B-Instrumental	0.5
DC	CALCULATED	1.2
TOC	APHA 5310	0.5
C_a	EPA 200.2/6020A (mod)	0.05
F_e	EPA 200.2/6020A (mod)	0.01
M_n	EPA 200.2/6020A (mod)	0.0001
S_i	EPA 200.2/6020A (mod)	0.05
COD	APHA 5220 D Colorimetry	10
Chl-a	EPA 445.0 ACET	0.1 µg/L
TSS	APHA 2540 D-Gravimetric	1.0

3.3 Definitions and Formulas

The performance effectiveness of stormwater wetlands can be expressed both as removal rates ($kg \cdot ha^{-1} \cdot yr^{-1}$) and removal efficiency (RE, %; Land et al., 2016), and removal efficiency can be analyzed by quantifying the pollutant concentration reduction or pollutant load reduction from inlet to outlet (Clary et al., 2020). However, the water quality improvement evaluation from the concentration assessment does not adequately reflect the effect of flow volume reductions in pollution control. In this study, the event pollutant mass load (M) and relevant event removal efficiency, as well as annual removal rate can be calculated as follows (Land et al., 2016):

$$\mathrm{M} = \int \mathrm{C(t)Q(t)dt} \tag{3-5}$$

$$\mathrm{RE\ (\%)} = \frac{\mathrm{M_{inflow}} - \mathrm{M_{outflow}}}{\mathrm{M_{inflow}}} \tag{3-6}$$

$$\text{Annual Load} = \sum_{1}^{n} \mathrm{M} \tag{3-7}$$

$$\text{Annual Removal Rates} = \frac{\text{Annual Load\_in} - \text{Annual Load\_out}}{\text{Pool Top Surface Area}} \tag{3-8}$$

where C(t) is the pollutant concentration as a function of time and Q(t) is the stormwater discharge as a function of time, n is the observed stormwater events in the inlet and the outlet. For the flow calculations, like average flow rate and flow volume, the stop threshold value is 2 L/s for inflows and 1 - 2 L/s for outflows, as the maximum outflow rate ranged from 1.6 L/s to 21.6 L/s for the RR wetland and from 1.1 L/s to 27.6 L/s for the RO wetland.

HRT is an important variable in designing and evaluating the treatment efficiency of wetland treatment systems (Hammer and Kadlec, 1983). The inverse of HRT is known as the turnover rate or renewal rate (t^{-1}, Guardo, 1999). The turnover rate, frequently used in limnological studies, indicates how rapidly the water in the system is replaced (Mitsch and Gossilink, 1986). Thus, it is considered as the average time that water remains in the wetlands, involving average inflow rate and pool volumes (Kadlec and Knight, 1996). In some instances, nominal HRT is not necessarily indicative of the actual HRT, because of the assumption that the entire volume of water in the wetland is involved in the flow (Kadlec and Knight, 1996). This assumption can generate considerable errors in HRT estimations in wetlands, especially when a relatively large volume of water remains in stagnant zones without taking part in the flow movement (Guardo, 1999). Here, we define the HRT considering the inflow. The volume ratio (Vol_R), a ratio of stormwater runoff volume to pool storage volume, was also considered in this study. HLR is defined as the rainfall equivalent of considered variable stormwater flow, but it does not imply uniform physical distribution of stormwater over the pond surface (Kadlec and Scott, 2008). The calculations are as follows (Ellis et al., 2003; Nayeb et al, 2021):

$$\mathrm{HRT} = \frac{\text{Pool Normal Volume}}{\text{Average Inflow Rate}} \tag{3-9}$$

$$\mathrm{Vol\_R} = \frac{\text{Event Ruoff Volume}}{\text{Pool Storage Volume}} \tag{3-10}$$

$$\mathrm{HLR} = \frac{\text{Average Inflow Rate}}{\text{Pool Top Surface Area}} \tag{3-11}$$

3.4 Statistical Analysis

The water budget analysis and flow validation had been done in MATLAB R2021b, and all statistical analyses were performed in IBM SPSS Statistic 27.

The non-parametric Mann-Whitney test was used to assess the differences of EMC from the inlets to the outlets for the two wetlands, also the differences between the pond concentrations and outlet EMCs (Selbig, 2016; Ivanovsky et al., 2018). Suppose the p-value is less than the indicated significance level of $\alpha = 0.05$, the null hypothesis (the two series are from the same population) is statistically insignificant and thus can be rejected. The used EMCs were from all the captured samples in the whole monitoring durations (2018 – 2019). The Kendall's tau (τ) analysis, a nonparametric correlation coefficient, was run to preliminarily estimate the correlation between nutrient concentrations and environmental parameters in the pond (Chrétien et al., 2016). The statistical significance of trends is defined using a significance level of $\alpha = 0.05$.

The principal component analysis (PCA) has been used to seek the underlying explanations that simple regressions cannot provide (Braskerud et al., 2005), and was applied for assessing relationships between the event REs objects and factor variables (Härdle and Simar, 2013; Al-Rubaei et al., 2017; Diamantini et al., 2018). Regression analysis between the event RE of specific nitrogen/phosphorus forms and factors was used as supplement tools (Carleton et al., 2001; Lv et al., 2011; Schober and Schwarte, 2018). The considered factors include influent concentrations, antecedent dry period (ADP), rainfall characters, air temperature (T_{air}), HRT, and HLR. The rainfall parameters include rainfall duration, rainfall depths, and rainfall intensity.

4 Water Budget

The general equation (USDA-SCS, 1989; Fenton, 1992) describing the hydrologic balance of a wetland is as follows:

$$\frac{dV}{dt} = I + P - E_p - O \quad (4 - 1)$$

$$dV = \frac{(A_i + A_{i+1}) \times \Delta D_e}{2} \quad (4 - 2)$$

Where, V is the volume of water stored in a wetland, m^3; I is the total inflow rate from the inlets and the surrounding lands, m^3/s; P is the direct rainfall to the pool water surface, m^3/s; E_p is the evaporation rate, m^3/s; O is the outflow rate, m^3/s; A is the wetland surface area, m^2; D_e is the wetland top water surface elevation, m; i is the time step point. The change in storage (dV) in a wetland can be easily predicted using the stage-storage curve, see the following sections.

The empirical Dalton's law (Wang, 2006) was applied to calculate the wetland evaporation rate (E_p) as follows:

$$E_p = 0.22 \times \sqrt{1 + 0.32 \times \text{wind}^2} \times (\hat{e} - e) \quad (4 - 3)$$

$$\hat{e} = 6.11 \times e^{\frac{17.27 \times T}{T + 273.15}} \quad (4 - 4)$$

$$e = \hat{e} \times RH \quad (4 - 5)$$

where, ê and e is the saturation vapour pressure of air and the actual vapour pressure of air, hPa; wind is the wind speed, m/s; T is the air temperature, °C; RH is the relative humidity (percentage, %).

The root mean square error (RMSE) was used for error analysis of the simulated pond elevation and the observed pond elevation, and the simulated elevation was used for predicting the outlet discharge.

4.1 Annual Water Budget

The observed vs. simulated elevations and RMSE results are shown in Figure 4-1 and Table 4-1 for the RR wetland. The pipe inflow of 750AV (in750AV) can get better simulated elevation than 750Manning (in750Man) from June to August 2018 (Figure 4-1a), while the simulated elevation from the pipe inflow of 750Manning can match better with the observed elevation in the three highest peaks in 2019 (Figure 4-1b). The RMSE values of both pipe inflows are below 5 cm, which is acceptable, compared with the normal surface elevation (~1259.0 m), see Table 4-1. Nevertheless, the maximum absolute differences between simulated and observed elevation are approximate 5 cm of in750AV and 6 cm of in750Man in 2018 and 23 cm of in750AV and 14 cm of in750Man in 2019, respectively. There is no estimation of potential groundwater, the unmatched parts that happen in some durations can be reasonable. Besides, flow meters cannot capture accurate data at extremely high flow conditions (ISCO, 2016), which could result in inaccurate flow peaks. Both in750AV and in750Man can be the appropriate choice for the Rocky Ridge wetland in both years; the in750AV is used for the analysis including water budget and calculation of nutrient removal. The final observed long-term hydrographs at the inlets and outlets are shown in Figure 4-2 for the RR wetland.

The observed vs. simulated elevations and RMSE results are shown in Figure 4-3 and Table 4-1 for the RO wetland. Using the pipe inflow from the 2150-flow module (in2150) can get a better simulated elevation than the 750-flow module (in750AV) in both 2018 and 2019 (Figure 4-3). Especially, the simulated elevations from in2150 have the same fluctuations as the observed elevations during the snow season in October 2018. Figure 4-4 shows the downloaded snow data in October 2018 from the Calgary government website. All the RMSE values are within the acceptable range of 1.604 – 3.412 cm (Table 4-1), compared with the normal water elevation (~ 1264.5 m). The in2150 has lower values of both the maximum of absolute differences and the RMSE values than in750AV. Similarly, the unmatched parts that happen in some durations can be reasonable since there is no estimation of potential groundwater either. Finally, the pipe inflow from 2150 flow module data is the best choice for Royal Oak of 2018 – 2019, and Figure 4-5 shows the long-term hydrograph in the inlet and the outlet for the RO wetland.

The results of the annual water budget are shown in Table 4-2. The total stormwater volume flowing into the RR wetland through the inlet pipe was about 2432 m^3 in 2018 and 16740 m^3 in 2019, respectively. The water flowing away from this wetland by weir/orifice was 37.0% in 2018 and 86.8% in 2019 of the total flowing stormwaters, with 1556 m^3 in 2018 and 18927 m^3 in 2019, respectively. Rainfall volume was almost 56.5% of the total pipe inflow volume while evaporation volume was almost 176.9% of the total weir/orifice outflow volume in 2018. However, the evaporation volume and rainfall volume were much smaller than both the weir/orifice outflow and pipe inflow volume in 2019, accounting for 15.5% of outflow and 21.0% of pipe inflow, respectively. The residual water budget was -97.3 m^3 in 2018 and -46.1 m^3 in 2019, these were about 2.3% and 0.2% of the stormwater flow through this wetland, respectively. These residual values are acceptable, compared with other study cases (Mierau and Trimble, 1988; Guardo, 1999; Kadlec and Scott, 2008), which recommended that balance closure with great care could still be held to the ± 5 – 10% range.

The total stormwater volume flowing into the RO wetland through the inlet pipe was about 5213 m^3 in 2018 and 18214 m^3 in 2019. The water flowing away from this wetland by weir/orifice was 5497 m^3 in 2018 and 23361 m^3 in 2019, accounting for 76.8% in 2018 and 90.7% in 2019 of the total flowing water. Unlike in the RR wetland, the evaporation volume and rainfall volume were much smaller than both the weir/orifice outflow volume and the pipe inflow volume in the RO wetland in both years. Rainfall volume was almost 17.6% in 2018 and 13.3% in 2019 of the total pipe inflow volume, while evaporation volume was almost 30.8% in 2018 and 10.6% in 2019 of the total weir/orifice outflow volume. The errors in the water budget in this wetland are mainly associated with the volume of flows entering and leaving the wetland through the inlet pipe and weir/orifice. The residuals of flow balance were -35.8 m^3 in 2018 and -78.2 m^3 in 2019, these were about 0.5% and 0.3% of total water flow through this wetland, respectively.

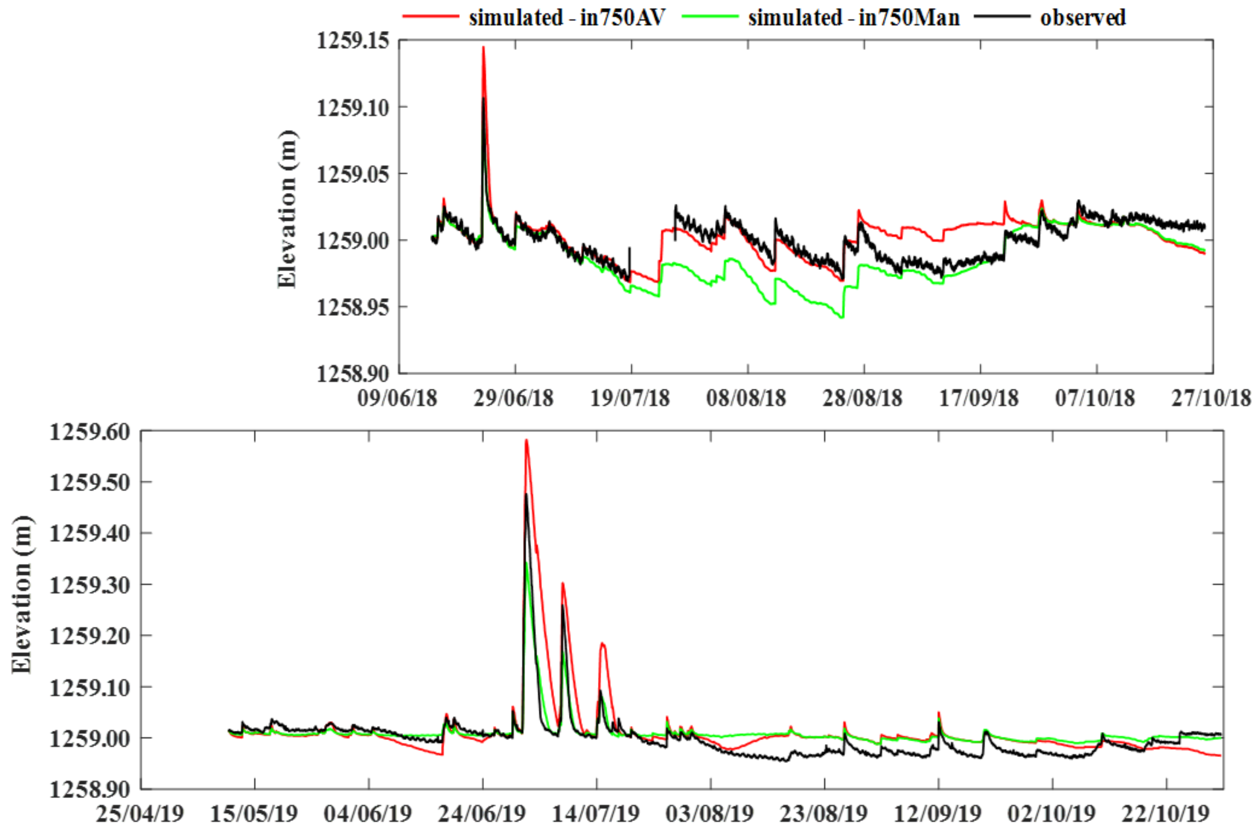

Figure 4-1. The top surface elevation of observed vs. simulated of the Rocky Ridge wetland. The in750AV and in750Man mean the inflow is from 750-sensor with area velocity and Manning formula, respectively.

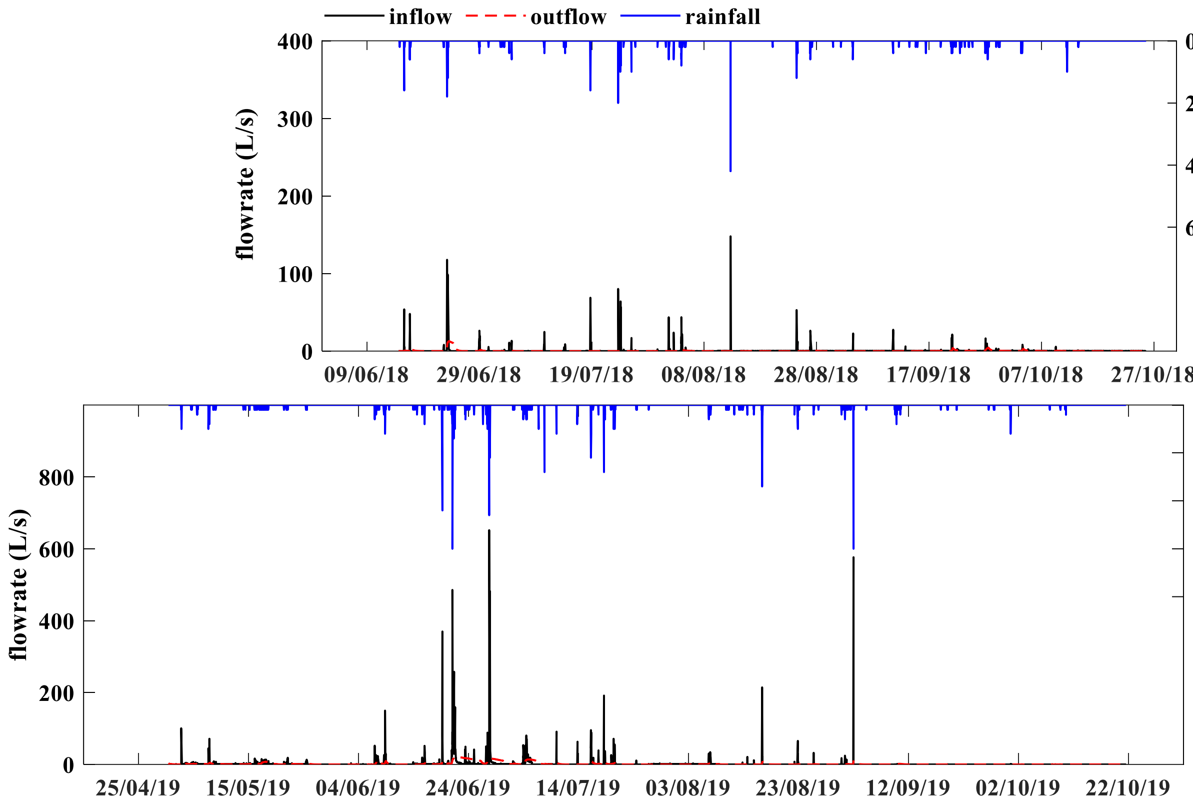

Figure 4-2. Hydrographs at the inlet and outlet of the Rocky Ridge wetland.

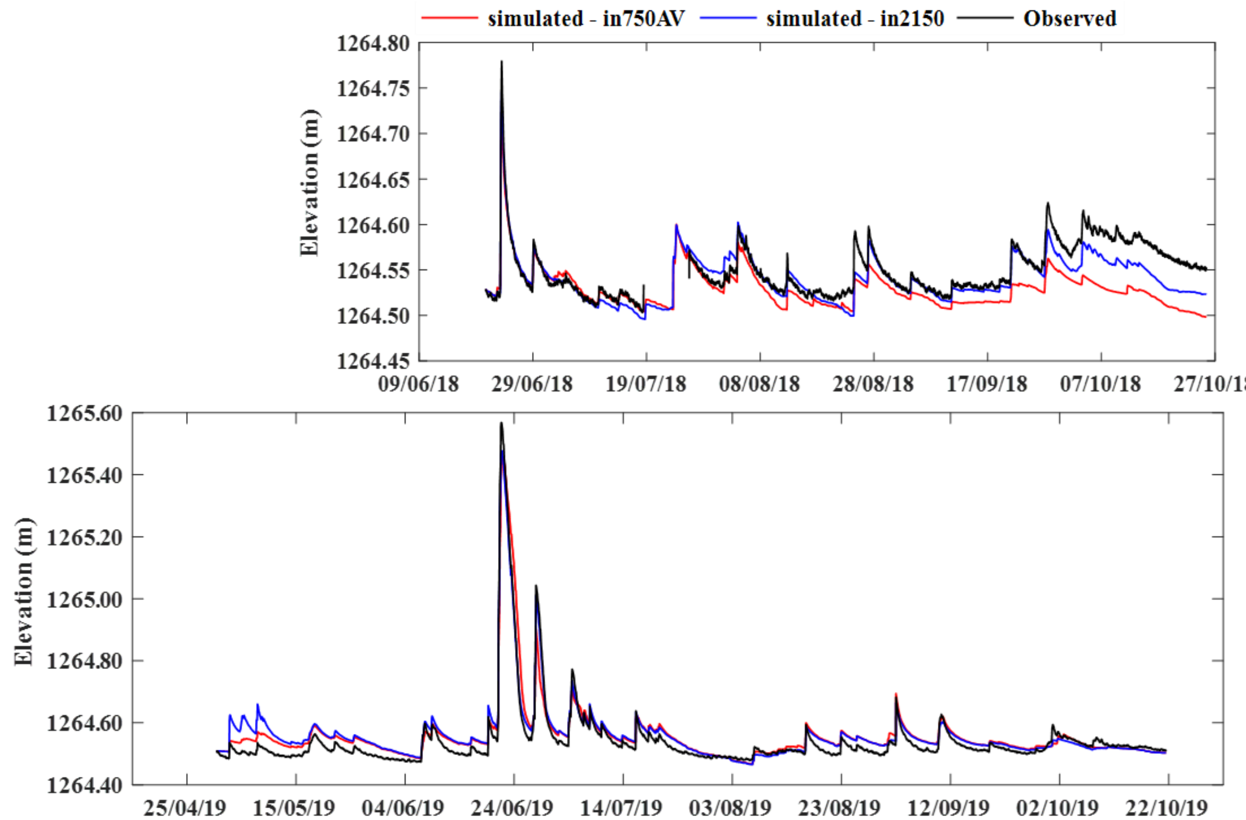

Figure 4-3. The top surface elevation of observed vs. simulated of the Royal Oak wetland. The in750AV and in2150 mean the inflow is from 750-sensor with area velocity formula and 2150-module, respectively.

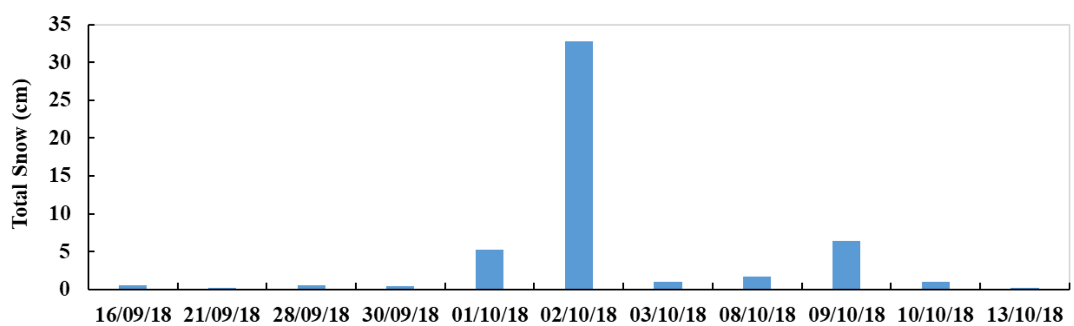

Figure 4-4. The daily snow in Calgary, data downloaded from https://climate.weather.gc.ca/

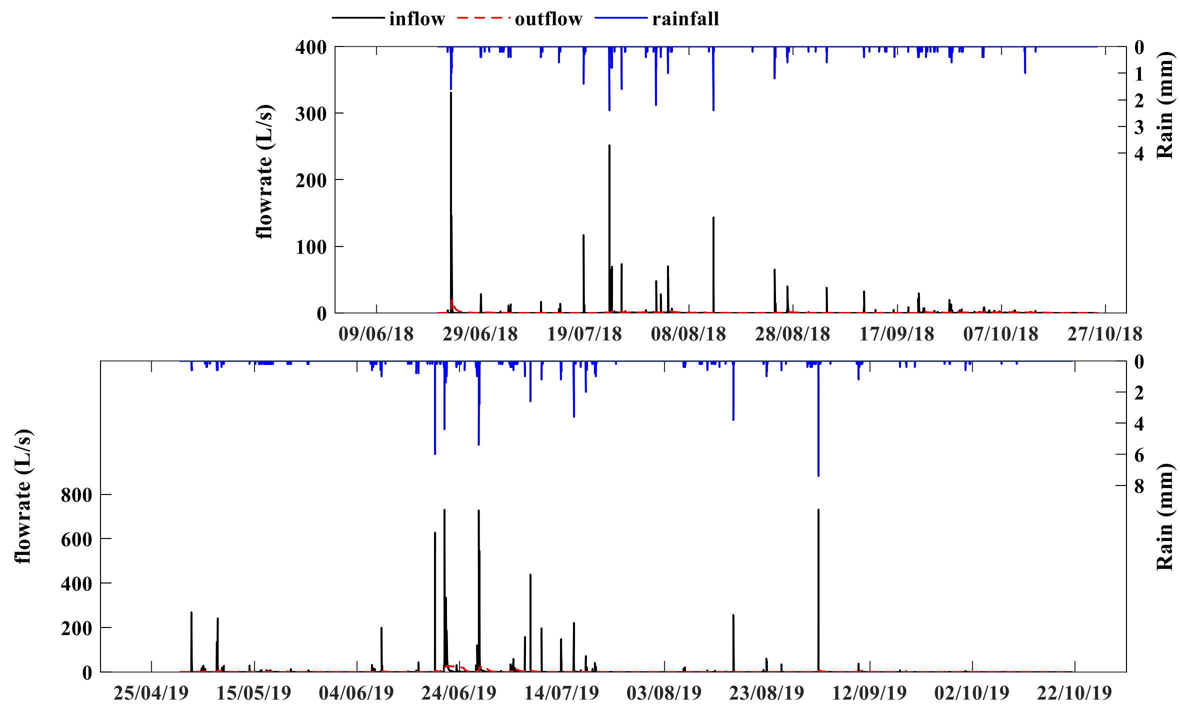

Figure 4-5. Hydrographs at the inlet and outlet of the Royal Oak wetland.

Table 4-1. RMSE of simulated surface elevation and observed elevation in Royal Oak Wetland, the pipe inflow was computed using velocity area formula from 750-sensor data and was from 2150-module. 750AV and 750Man mean the pipe inflow is from 750-sensor with area velocity and Manning formula, respectively.

Rocky Ridge Wetland		**2018**	**2019**
750AV	RMSE (cm)	1.45	3.52
	Max of absolute differences (cm)	4.76	22.58
	Mean of absolute differences (cm)	1.29	2.21
	Mean of simulated elevation (m)	1258.99	1259.01
750Man	RMSE (cm)	2.58	2.39
	Max of absolute differences (cm)	5.53	14.39
	Mean of absolute differences (cm)	2.16	1.80
	Mean of simulated elevation (m)	1258.98	1259.01
Mean of observed elevation (m)		1259.00	
Royal Oak Wetland		**2018**	**2019**
750AV	RMSE(cm)	2.94	3.41
	Max of absolute differences (cm)	7.33	20.44
	Mean of absolute differences (cm)	2.19	2.49
	Mean of simulated elevation (m)	1264.53	1264.56
2150	RMSE(cm)	1.60	3.14
	Max of absolute differences (cm)	4.81	12.54
	Mean of absolute differences (cm)	1.17	2.50
	Mean of simulated elevation (m)	1264.54	1264.56
Mean of observed elevation (m)		1264.55	

Table 4-2. Annual water budget summary of the Royal Oak Wetland. Unit: m^3

/	Duration	Pipe Inflow	Extra Pipe Inflow	Surrounded Land Inflow	Rainfall	Evaporation	Weir/Orifice Outflow	Residual of flow balance
Rocky Ridge	06/14/2018 - 10/25/2018	2431.9	/	404.3	1373.8	2751.6	1555.7	-97.3
Wetland	04/30/2019 - 10/21/2019	16740.0	/	1555.2	3520.1	2934.8	18926.5	-46.1
Royal Oak	06/20/2018 - 10/25/2018	5213.4	742.4	284.3	916.3	1695.3	5496.9	-35.8
Wetland	04/30/2019 - 10/21/2019	18213.8	4029.4	1091.4	2428.5	2480.1	23361.2	-78.2

4.2 Event Water Budget and Event Hydrograph

Storm events are discretized using a 12 – hour inter-event time with a minimum depth of 2.5 mm, that is, successive rainfall events are broken into sub-events when the interval of rainfall events is greater than 12 hours; the rainfall depths of considered events are over 2.5 mm. In total, 10 rainfall events were captured during 2018 and 15 rainfall events during 2019. A summary of the runoff events captured by the autosamplers during 2018 - 2019 is provided in Table 4-3. Cells labelled with " √ " means a composite sample was successfully collected, cells labelled with " √ D" means discrete sample was collected, and the percentage inside each cell is the sample representativeness based on storm volume, otherwise, the cells labelled with "X" means that the sample is not successfully collected for that specific rainstorm event. The percentage stormwater volume represents all composited and discrete samples containing stormwater. The long-term annual removal efficiencies were from all captured events with concentrations from the inlets and outlets in the monitoring years. To examine the most outstanding influences on wetlands' performance, we selected the fully captured events to analyze removal efficiency. For an event to be considered fully captured at each wetland, samples for nutrient concentration analysis have to be concurrently collected at both the inlet and the outlet.

A summary of the conditions during the fully captured events is presented in Table 4-4 and Table 4-5. The data show that conditions varied over a wide range during the events with the varying antecedent dry period (ADP) varying from <1 to 12.3 days, rainfall depths (Rde) from 2.6 - 87.8 mm, maximum rainfall intensity (MRI) from 4.8 to 88.8 mm/hr, average rainfall intensity (ARI) from 0.1 to 6.4 mm/hr, rainfall duration (Rdu) from 1.2 to 38.5 hrs, mean air temperature (T_{air}) from 2.1 to 12.3 °C, and mean evaporation rate (E_p) from 0.02 to 0.37 cm/d. The fully captured events in the two wetlands were very similar (Table 4-4 and Table 4-5). The total measured rainfall was 204.6 mm in 2018 and 402.8 mm in 2019 at RR, and at RO it was 221.8 mm in 2018 and 414.4 mm in 2019.

Hydrological processes can be described in terms of water budget (Ellis et al., 2003; Lee et al., 2016), as water budget can summarize the different stages of the hydrological processes located at their dominant locations, for example, precipitation and evaporation (atmosphere), and subsurface flow. A water budget is conducted for each fully captured event, the results are summarized in Table 4-6. The pipe inflow and weir/orifice outflow were often the dominant terms in the water budgets for these two wetlands, with the least percentage of 56% of inflow and 90% of outflow. The event errors in the closure of the event water budget for the RR wetland ranged from -37.2% to 13.6%, and for the RO wetland ranged from -8.8% to 46.8%. These acceptable percentages were based upon the combined water inflow. A similar lack of closure has been reported by Kadlec and Wallace (2008), where all mass balance terms are measured independently, and the annual percentage residuals could be around ± 50%. The conclusion is that these apparent water losses are due to faulty inflow/outflow measurements or ignored exchange with groundwater (Kadlec and Wallace, 2008).

Evaporation volume accounted for only 0.4 – 10% of the total outflow volume in the RR wetland and 0.5 – 17.8% in the RO wetland, and it was negligible when compared to the outlet outflow volume. Rainfall played an important role in the RR wetland, accounting for 10.1 – 33.4% of the total inflow volume. For small rainfall volume events (<15 mm, Mangangka et al., 2015), such as the 29th June, 27th August, and 27th September events in 2018, 16th and 31st August in 2019, the rainfall volume was almost half of the pipe inflow volume, Table 4-6. But rainfall volume only constituted 4.4 – 19.6% of the total inflow for all fully captured events in the RO wetland.

In terms of event hydraulic parameters, in Table 4-4 and Table 4-5, for storm events with short ADP, the HLR increased to a level higher than that of the storm events with long ADP. These two wetlands had almost the same catchment areas, but they had different imperviousness ratios or slopes of catchment and inlet pipe (Table 3-1), the final inflow would be different even under the same rainfall event. The average inflow rates were almost the same but the maximum rates of both inflow and outflow were different in these two wetlands (Figure 4-8, 4-10). Combined with the differently designed pool volume and top surface area (Table 3-1), the magnitudes of HRT and HLR of these two wetlands were different (Table 4-4 and Table 4-5). They ranged from 1.0 to 18.4 days of HRT and 5.8 to 104.5 cm/d of HLR in the RR wetland and 0.2 to 3.0 days of HRT and 19.3 to 293.9 cm/d of HLR in the RO wetland, respectively, depending on the storm magnitudes.

Figure 4-6 compares the rainfall intensity parameters (MRI and ARI) with the evaporation rate (E_p) and the hydraulic loading rate (HLR) for the fully captured events, as these parameters have the same unit. Besides, the hydraulic loading rate is defined as the rainfall equivalent of whatever flow is under consideration. It does not imply uniform physical distribution of water over the wetland surface (Kadlec and Wallace, 2008). At the RR wetland, MRI was approximately the same as HLR in 2018 but significantly higher for some events in 2019 in the RR wetland. While MRI had almost the same values as HLR in seven storm events in the RO wetland, without any specific patterns of other climate parameters in these events. ARI was significantly higher than evaporation in both wetlands in both years, but both were lower than HLR. Because some rain events are extremely localized (Kadlec and Wallace, 2008), the observed MRI and ARI were different in these two wetlands in the same rainfall events.

For all fully captured events which were used for the analysis of removal efficiency, the average inflow rate ranged from 3.6 L/s to 65.2 L/s for the RR wetland and from 9.8 L/s to 148.8 L/s for the RO wetland, respectively. Figure 4-7 shows the hydrographs of two example stormwater events of these two wetlands, the outflow peaks from the two wetlands were significantly lower than the inflow peaks. Pollutant Concentrations in stormwater runoff can be temporally dynamic and change as the runoff progress (Al-Rubaei et al., 2016), for this reason, discrete samples were usually used to characterize a storm event. Figure 4-8 and 4-9, 4-10 and 4-11 show the observed TN/TP concentrations in certain stormwater events. The exported dynamic concentrations of TN and TP observed in the outlets can be stable, with narrow ranges, especially in the RR wetlands (Figure 4-8 and 4-9). For instance, the TN concentrations in the outflow of the RR wetland were 0.72 – 0.84 mg/L with standard deviation (S.d) = 0.04 mg/L in event-8, 0.70 – 0.75 mg/L with S.d = 0.02 mg/L in event-9, 0.77 – 0.96 mg/L with S.d = 0.06 mg/L in event-11, 0.75 – 0.91 mg/L with S.d = 0.07 mg/L in event-12, respectively. The TP concentrations in the outlet of the RR wetland were 0.06 – 0.10 mg/L with S.d = 0.02 mg/L in event-8, 0.03 – 0.05 mg/L with S.d = 0.004 mg/L in event-9 and 0.04 – 0.05 mg/L with S.d = 0.006 mg/L in event-11, respectively. For the RO wetland, the TP concentrations in the outlet were 0.06 – 0.09 mg/L with S.d = 0.008 mg/L in event-9, 0.03 – 0.06 mg/L with S.d = 0.009 mg/L in event-11, 0.04 – 0.06 mg/L with S.d = 0.006 mg/L in event-13, respectively, Figure 4-11.

Table 4-3. Summary of the captured runoff events by the auto-samplers.

Storm #	**Storm Event**	**Rocky Ridge**		**Royal Oak**	
		inlet	**outlet**	**inlet**	**outlet**
1	22-Jun-18	√ (99%)	√ (100%)	X	√ (96%)
2	29-Jun-18	√ (96%)	√ (53%)	√ (100%)	√ (95%)
3	10-Jul-18	√ (82%)	X	X	√ (33%)
4	19-Jul-18	√ (98%)	√ (71%)	√ (100%)	√ (97%)
5	24-Aug-18	√ (76%)	√ (80%)	√ (96%)	√ (88%)
6	28-Aug-18	√ (79%)		√ (72%)	
7	10-Sep-18	√ (57%)	X	X	X
8	21-Sep-18	√ (58%)	X	X	X
9	27-Sep-18	√ (87%)	X	√ (71%)	X
10	02-Oct-18	√ (91%)	X	X	√ (96%)
storm captured		**10**	**4**	**5**	**6**
Captured at inlet and outlet		**4**		**3**	
1	30-Apr-19	X	X	√ (78%)	X
2	02-May-19	√D (95%)	X	√D (79%)	√ (33%)
3	21-May-19	X	√D (62%)	X	√ (55%)
4	10-Jun-19	√ (86%)	√ (63%)	√ (29%)	X
5	20-Jun-19	√ (73%)	X	√ (81%)	√ (94%)
6	25-Jun-19	√ (95%)	√ (13%)	√ (8%)	
7	27-Jun-19	√D (61%)	√D (22%)	√D (16%)	√D (26%)
8	02-Jul-19	X	√ (30%)	√ (78%)	√ (45%)
9	16-Jul-19	√D (73%)	√D (75%)	√D (67%)	√D (82%)
10	08-Aug-19	√(100%)	X	√ (72%)	X
11	16-Aug-19	√ (40%)	√ (50%)	√ (60%)	√ (63%)
12	22-Aug-19	X	√ (22%)	√D (58%)	√D (41%)
13	01-Sep-19	√D (85%)	√D (36%)	√ (44%)	√ (67%)
14	11-Sep-19	√D (58%)	√D (31%)	X	√D (64%)
15	20-Sep-19	X	X	X	X
Storm captured		**10**	**10**	**12**	**11**
Composite sample event		**5**	**5**	**8**	**7**
Discrete sample event		**5**	**5**	**4**	**4**
captured at inlet and outlet		**7**		**9**	

Table 4-4. Summary statistic of the fully monitoring stormwater events for the Rocky Ridge wetland; ADP: antecedent dry period; Rdu: rainfall duration; Rde: rainfall depth; MRI: maximum rainfall intensity; ARI: average rainfall intensity; T_{air}: air temperature; E_p: evaporation rate; HLR: hydraulic loading rate; HRT: hydraulic retention time.

Event date	**Event no.**	**ADP (day)**	**Rdu (hr)**	**Rde (mm)**	**MRI (mm/hr)**	**ARI (mm/hr)**	**T_{air} (°C)**	**Ep (cm/d)**	**HLR (cm/d)**	**HRT (day)**
22-Jun-18	RR-1	<1	7.2	33.2	21.6	4.6	12.3	0.31	62.6	1.7
29-Jun-18	***RR-2***	5.4	3.7	7.2	4.8	1.9	9.1	0.17	18.2	5.9
23-Jul-18	-	-	-	-	-	-	-	-	-	-
25-Jul-18	-	-	-	-	-	-	-	-	-	-
24-Aug-18	-	-	-	-	-	-	-	-	-	-
27-Aug-18	***RR-3***	2.2	9.1	8.4	7.2	0.9	6.5	0.14	12.1	8.8
27-Sep-18	RR-4	2.2	15.4	11.6	7.2	0.8	2.1	0.02	5.8	18.4
02-May-19	-	-	-	-	-	-	-	-	-	-
07-Jun-19	RR-5	12.3	20.2	17.4	7.2	0.9	3.7	0.04	22.3	4.8
09-Jun-19	RR-6	<1	8.2	7.4	14.4	0.9	4.8	0.16	29.6	3.6
19-Jun-19	-	-	-	-	-	-	-	-	-	-
20-Jun-19	***RR-7***	<1	33.2	87.2	72.0	2.6	7.2	0.16	104.5	1.0
27-Jun-19	***RR-8***	2.2	17.8	42.0	55.2	2.4	10.6	0.20	72.2	1.5
03-Jul-19	-	-	-	-	-	-	-	-	-	-
16-Jul-19	***RR-9***	2.5	10.8	10.4	26.4	1.0	10.6	0.20	67.8	1.6
16-Aug-19	***RR-10***	1.3	5.5	10.2	40.8	1.9	8.8	0.13	59.9	1.8
22-Aug-19	-	-	-	-	-	-	-	-	-	-
31-Aug-19	RR-11	4.2	40.6	7.6	7.2	0.2	11.7	0.04	19.5	5.5
01-Sep-19	***RR-12***	<1	3.0	9.4	72.0	3.1	10.9	0.09	51.6	2.1
Max		12.3	40.6	87.2	72.0	4.6	12.3	0.31	104.5	18.4
Min		<1	3.0	7.2	4.8	0.2	2.1	0.02	5.8	1.0
Median		2.2	10.0	10.3	18.0	1.4	9.0	0.14	40.6	2.8
Mean		2.9	14.6	21.0	28.0	1.8	8.2	0.15	43.8	4.7

Table 4-5. Summary statistic of the fully monitoring stormwater events for the Royal Oak wetland; ADP: antecedent dry period; Rdu: rainfall duration; Rde: rainfall depth; MRI: maximum rainfall intensity; ARI: average rainfall intensity; T_{air}: air temperature; E_p: evaporation rate; HLR: hydraulic loading rate; HRT: hydraulic retention time.

Event date	**Event no.**	**ADP (day)**	**Rdu (hr)**	**Rde (mm)**	**MRI (mm/hr)**	**ARI (mm/hr)**	**T_{air} (°C)**	**Ep (cm/d)**	**HLR (cm/d)**	**HRT (day)**
22-Jun-18	-	-	-	-	-	-	-	-	-	-
29-Jun-18	***RO-1***	5.4	4.6	8.0	4.8	1.7	8.9	0.21	22.4	2.6
23-Jul-18	RO-2	4.6	24.3	15.8	28.8	0.6	10.9	0.09	38.8	1.5
25-Jul-18	RO-3	1.3	2.7	2.0	19.2	0.8	11.3	0.25	26.1	2.2
24-Aug-18	RO-4	4.2	5.2	9.8	14.4	1.9	8.1	0.11	36.0	1.6
27-Aug-18	***RO-5***	2.2	9.1	8.4	7.2	0.9	6.5	0.16	19.3	3.0
27-Sep-18	-	-	-	-	-	-	-	-	-	-
02-May-19	RO-6	4.3	2.4	5.6	7.2	2.3	4.2	0.11	94.2	0.6
07-Jun-19	-	-	-	-	-	-	-	-	-	-
09-Jun-19	-	-	-	-	-	-	-	-	-	-
19-Jun-19	RO-7	<1	10.2	12.8	72.0	1.2	7.1	0.26	239.3	0.2
20-Jun-19	***RO-8***	<1	33.2	87.8	52.8	2.6	7.6	0.20	120.1	0.5
27-Jun-19	***RO-9***	2.2	18.2	41.6	64.8	2.3	9.8	0.29	94.4	0.6
03-Jul-19	RO-10	1.4	38.5	37.4	7.2	1.0	8.2	0.08	23.9	2.4
16-Jul-19	***RO-11***	2.4	11.1	13.0	43.2	1.2	10.6	0.37	112.6	0.5
16-Aug-19	***RO-12***	1.3	6.2	11.0	45.6	1.8	8.5	0.25	82.6	0.7
22-Aug-19	RO-13	<1	5.5	7.0	12.0	1.3	10.7	0.26	40.6	1.4
31-Aug-19	-	-	-	-	-	-	-	-	-	-
01-Sep-19	***RO-14***	<1	9.9	10.2	88.8	1.0	10.3	0.26	293.9	0.2
Max		5.4	38.5	87.8	88.8	2.6	11.3	0.37	293.9	3.0
Min		<1	2.4	2.0	4.8	0.6	4.2	0.08	19.3	0.2
Median		1.8	9.5	10.6	24.0	1.3	8.7	0.21	61.6	1.0
Mean		2.2	12.9	19.3	33.4	1.5	8.8	0.23	88.9	1.3

Table 4-6. Summary of the event water budget. Unit: m^3. dV was the pool storage change and was calculated by stage-curve; it states that the change in storage in the wetland results from the difference between inflows and outflows; Residual equal to the differences between IO and dV; IO equal to the differences between total inflow and total outflow.

Event no.	Event Date	Pipe Inflow	Surrounded Land Inflow	Rainfall	Evaporation	Weir/Orifice Outflow	IO	dV	Residual of Flow Balance
RR-1	22-Jun-18	1237.1	109.9	316.5	39.3	1400.5	223.7	217.0	6.8
RR-2	***29-Jun-18***	172.0	18.9	63.5	6.2	55.5	192.6	162.7	29.9
RR-3	***27-Aug-18***	141.4	22.8	76.0	9.8	100.0	130.5	97.8	32.7
RR-4	27-Sep-18	193.8	36.3	105.2	1.0	248.9	85.6	181.9	-96.4
RR-5	07-Jun-19	847.7	54.2	158.1	3.3	660.8	395.9	264.4	131.5
RR-6	09-Jun-19	322.1	18.8	66.5	8.0	333.8	65.6	67.5	-1.9
RR-7*	***20-Jun-19***	6157.8	736.4	878.6	67.1	7700.8	4.9	-55.4	60.3
RR-8*	***27-Jun-19***	3290.1	166.3	386.5	92.5	3746.8	3.6	20.4	-16.8
RR-9	***16-Jul-19***	424.1	33.2	115.0	15.4	416.6	140.2	199.6	-59.4
RR-10	***16-Aug-19***	183.0	29.1	73.1	4.9	209.0	71.4	141.0	-69.5
RR-11	31-Aug-19	92.7	15.0	54.1	2.3	62.5	97.0	113.8	-16.8
RR-12	***01-Sep-19***	328.2	31.4	84.9	4.8	372.0	67.7	232.9	-165.3

Event no.	Event Date	Pipe Inflow	Extra Pipe Inflow	Surrounded Land Inflow	Rainfall	Evaporation	Weir/Orifice Outflow	IO	dV	Residual of Flow Balance
RO-1	***29-Jun-18***	158.0	32.0	14.4	42.8	15.1	84.3	147.7	146.7	1.1
RO-2	23-Jul-18	481.2	73.5	32.9	69.1	9.4	295.6	351.8	355.0	-3.2
RO-3	25-Jul-18	89.6	2.6	1.7	12.2	9.7	92.6	3.9	3.9	0.0
RO-4	24-Aug-18	154.8	45.8	20.0	53.9	6.8	38.7	229.0	184.3	44.7
RO-5	***27-Aug-18***	201.1	34.0	15.8	48.9	10.0	108.5	181.3	127.5	53.7
RO-6	02-May-19	642.9	43.8	10.3	32.0	4.7	243.0	481.2	140.3	340.9
RO-7	19-Jun-19	565.1	107.8	26.8	72.7	10.9	365.5	396.0	272.2	123.8
RO-8*	***20-Jun-19***	6256.7	1330.9	547.4	634.7	76.1	8749.6	-56.1	-12.6	-43.5
RO-9*	***27-Jun-19***	3414.0	299.0	71.7	258.2	84.5	3927.2	31.3	29.3	1.9
RO-10	03-Jul-19	1451.8	381.5	82.9	217.8	9.4	1943.8	180.9	367.9	-187.0
RO-11	***16-Jul-19***	498.2	138.7	33.2	105.7	41.2	484.4	250.2	272.2	-21.9
RO-12	***16-Aug-19***	294.8	94.8	22.8	63.1	21.1	174.5	280.0	175.6	104.3
RO-13	22-Aug-19	161.3	61.5	13.6	45.6	19.6	90.3	172.1	191.5	-19.4
RO-14	***01-Sep-19***	593.3	94.9	22.6	58.9	19.5	476.5	273.7	73.8	199.9

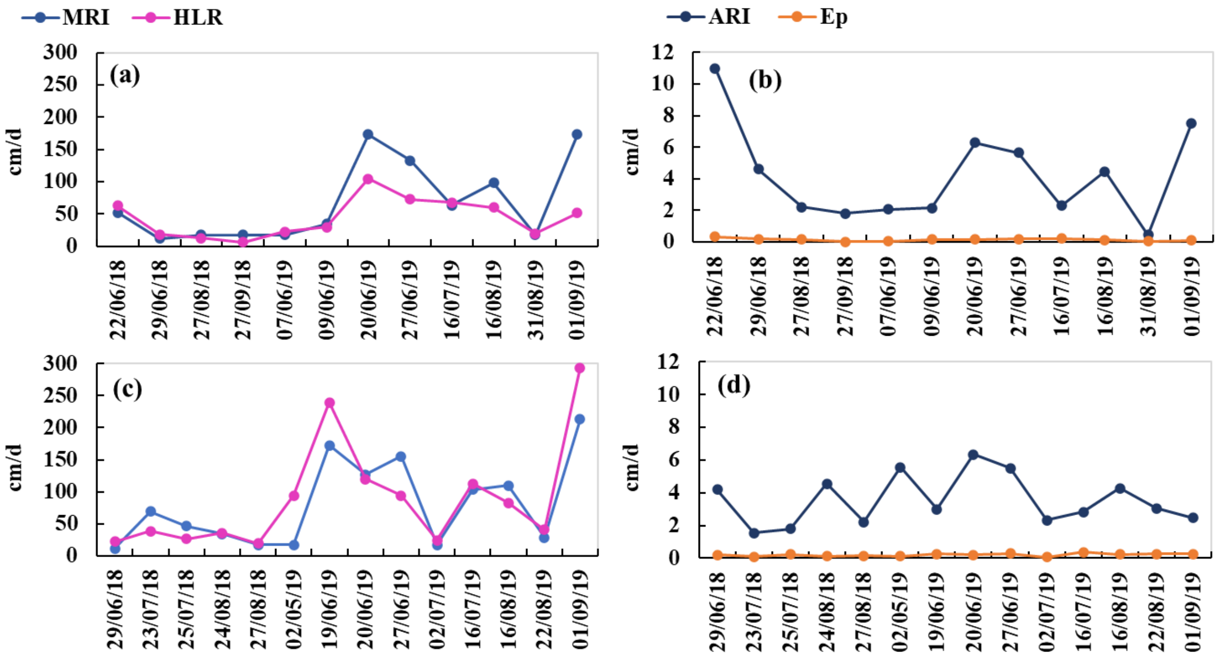

Figure 4-6. Event comparisons among rainfall intensity parameters, evaporation, and HLR for the Rocky Ridge wetland (a) – (b) and the Royal Oak wetland (c) – (d).

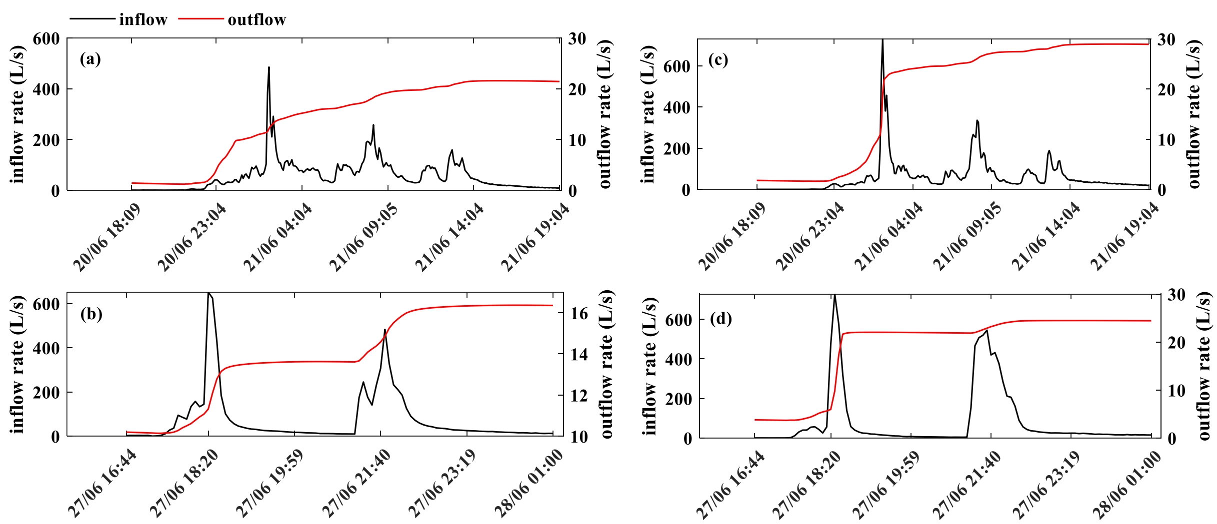

Figure 4-7. Hydrographs representing event behaviour: (a) (b) are the event-7, event-8 in the Rocky Ridge wetland; (c) (d) are the event-8, event-9 in the Royal Oak wetland.

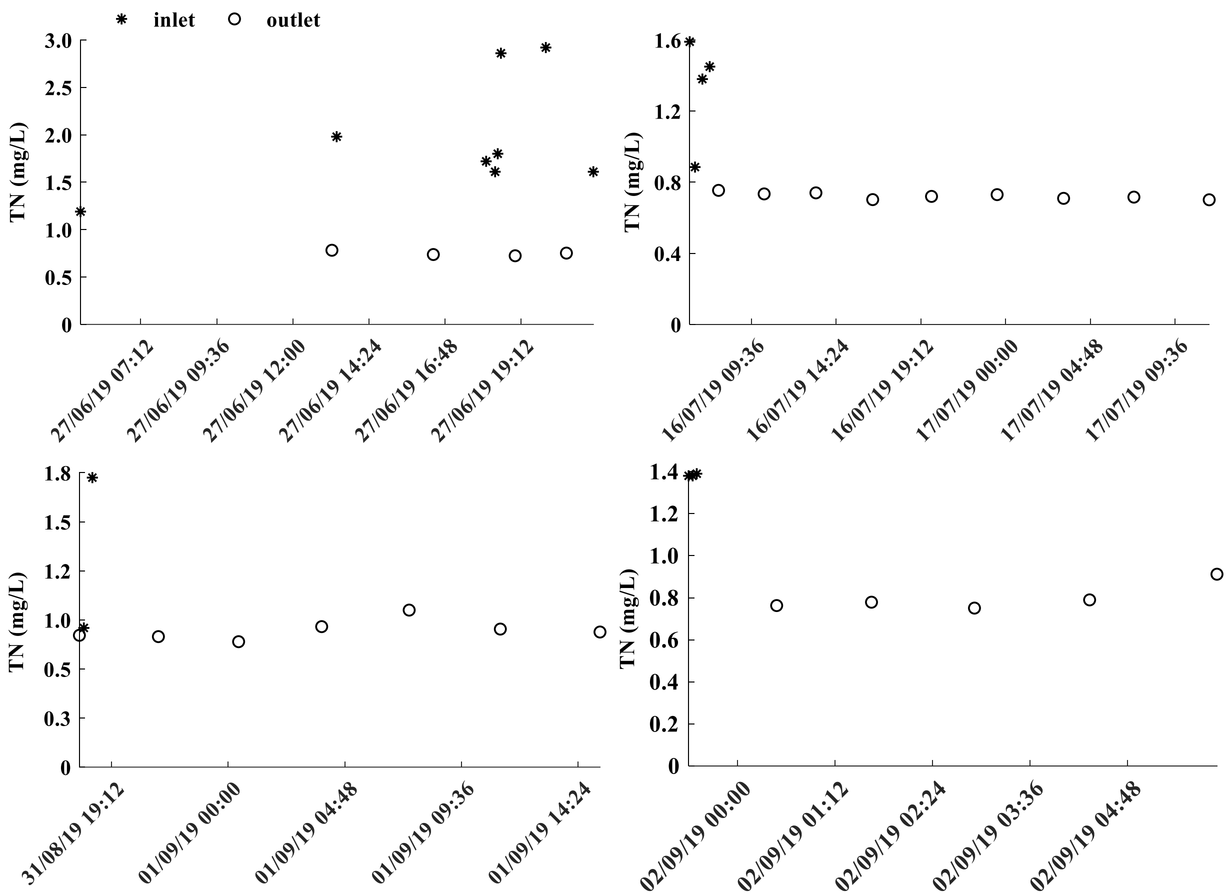

Figure 4-8. The dynamic TN concentrations of events with discrete samples in the Rocky Ridge wetland.

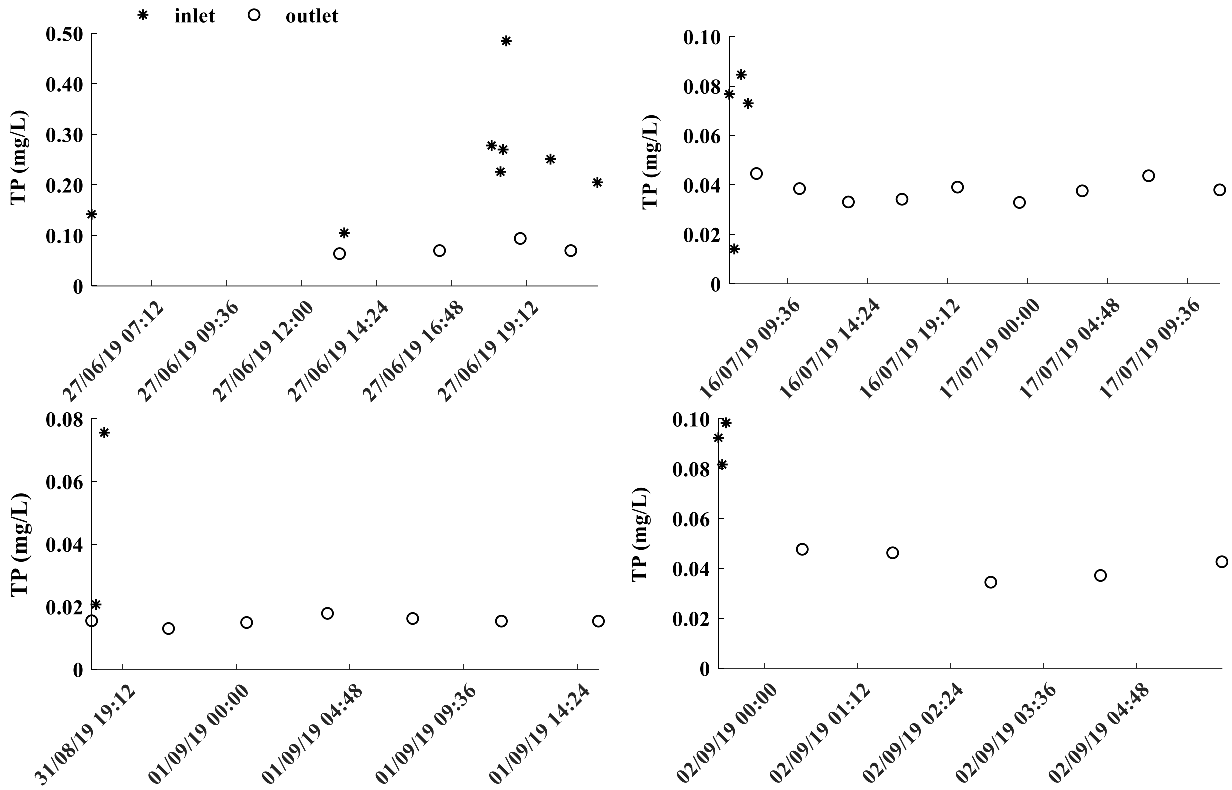

Figure 4-9. The dynamic TP concentrations of events with discrete samples in the Rocky Ridge wetland.

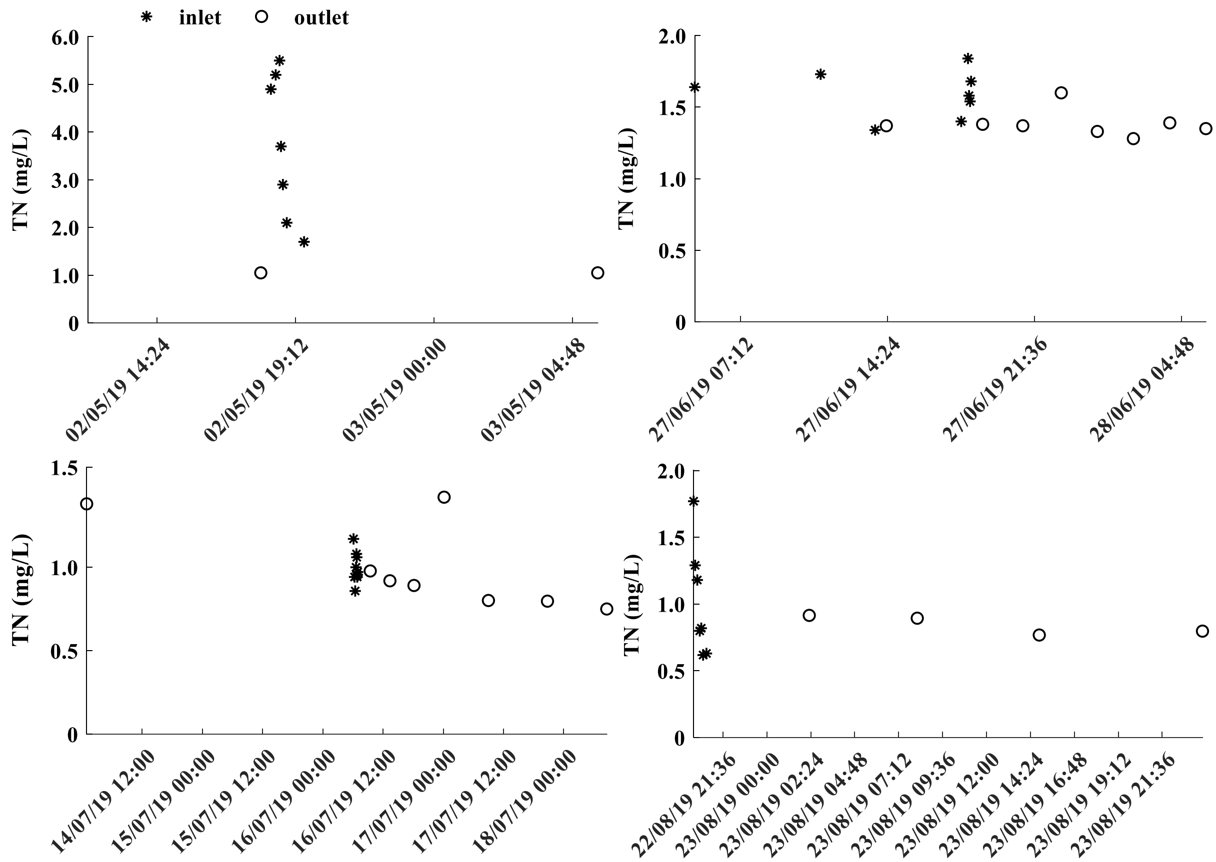

Figure 4-10. The dynamic TN concentrations of events with discrete samples in the Royal Oak wetland.

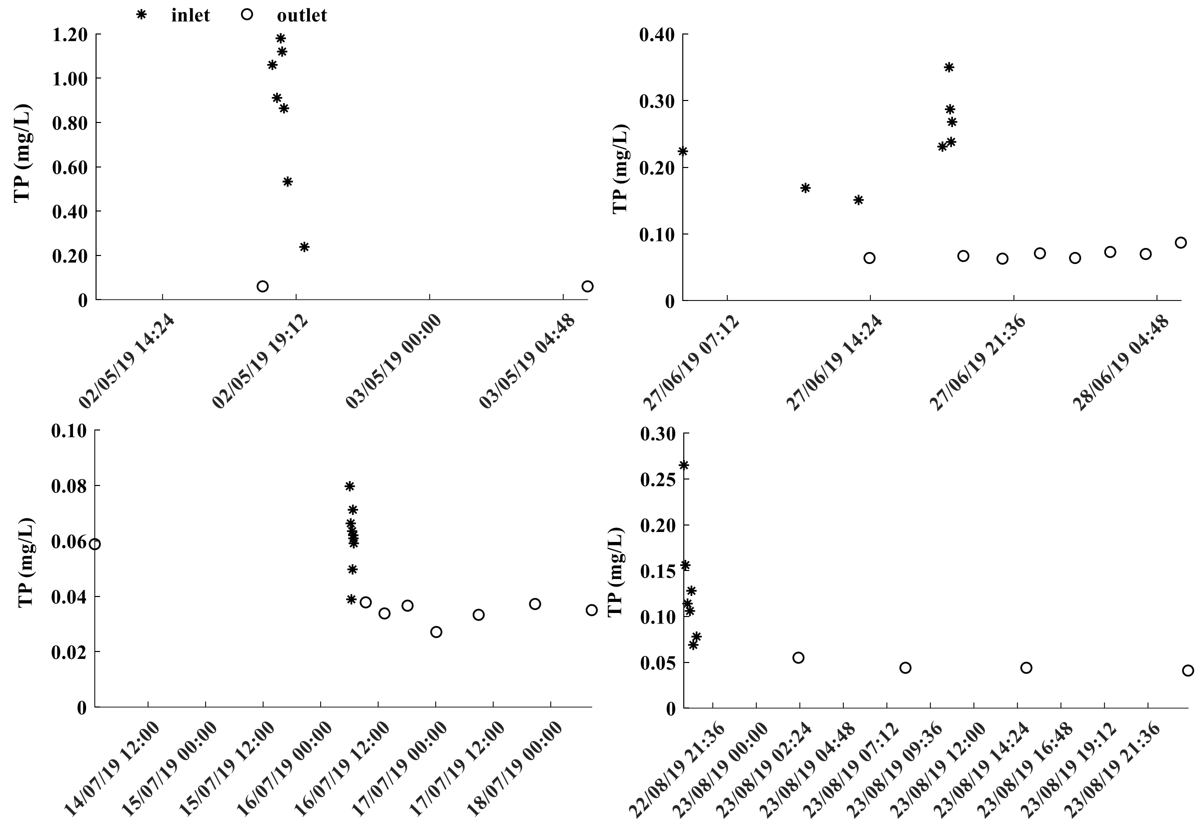

Figure 4-11. The dynamic TP concentrations of events with discrete samples in the Royal Oak wetland.

4.3 Discussions and Conclusions

Some studies had recommended wetland designers or operators that care must be taken in water flow measurements and that water budget differencing is apt to provide estimates with large uncertainty (Mierau and Trimble, 1988; Guardo, 1999; Kadlec and Wallace, 2008). According to the flow balance and simulated elevation results, the best choices from different inlet flow sensors for the Rocky Ridge wetland and the Royal Oak wetland are 750 AV/Manning data and 2150 flow data in two years, respectively. The final observed long-term hydrographs at the inlets and outlets are shown in Figure 4-2 for the RR wetland and in Figure 4-5 for the RO wetland. The peak discharges from the two wetlands were significantly lower than the inflow peaks. These wetlands are draining water very slowly, even though there is a heavy stormwater (Figure 4-7), the nature of artificial pond peak elimination complements with hydraulic retention time, which contributes to some nutrient processes in ponds.

The water budget states that the changes in storage in these wetlands result from the differences between inflows and outflows. The different components of the overall water budget are illustrated in Table 4-2 and Table 4-6, except that the potential role of groundwater was not discussed, as aforementioned. It is indicated that annual flow into these studied wetlands was mainly through the inlet pipes and flowed out over evaporation and weir/orifice control in RR wetland but mainly over weir/orifice control in RO wetland, respectively (Table 4-2). Inflow and outflow through the RO wetland were much larger than the components of the water budget associated with rainfall and evaporation (Table 4-2 and Table 4-6). The residuals of the annual water budget were reasonably within 3% in the RR wetland and 1% in the RO wetland in both years. These residual values are acceptable, compared with other study cases (Mierau and Trimble, 1988; Guardo, 1999; Kadlec and Scott, 2008), which recommended that balance closure with great care could still be held to the ± 5 – 10% range.

The impacts of evaporation and rainfall on the water budget were explored, evaporation had certain important effects on the water budget in these two wetlands annually, especially in 2018 with less total rainfall depths, Table 4-2 and Table 4-6. However, rainfall and evaporation were minor components of the event budgets, Table 4-6. Seepage to groundwater, assumed to be part of the residual component of the budgets, was also minimal if taken as the residuals (Table 4-2, Table 4-6), these findings are consistent with the study by (Nairn and Mitsch, 2000). As for some storm events, rainfall can play an important role in the budgets in the RR wetland, Table 4-6. The evaporation volume can be negligible in the event budgets and the evaporation rates were lower than rainfall intensity and HLR in both wetlands. The event error in the closure of the event water budget for the RR wetland ranged from -37.2% to 13.6%, and for the RO wetland ranged from -8.8% to 46.8%, respectively. These acceptable percentages are based upon the combined water inflow. A similar lack of closure has been reported by (Kadlec and Wallace, 2008), where all mass balance terms are measured independently, and the annual percentage residuals can be around ± 50%. These apparent water losses are due to faulty inflow/outflow measurements or ignored exchange with groundwater (Kadlec and Wallace, 2008).

5 Nutrient Analysis

5.1 Nutrient Concentrations from Inflow to Outflow

5.1.1 Spatial Comparation Among all Locations

There were several reasons that samples were not successfully collected from inflows and outflows, as discussed in section 3.2. Over the entire study period in 2018-19, there were 21 events with inflow concentrations and 15 events with outflow concentrations and 12 fully captured events for the RR wetland. There were 17 events with inflow concentrations and 18 events with outflow concentrations and 14 fully captured events for the RO wetland. The concentrations of nitrogen and phosphorus in the pond were observed regularly and the inflows and outflows were observed randomly because of rainfall events. Side-by-side boxplots of nitrogen concentrations from the influent to the pond to the effluent in these two wetlands were made and shown in Figure 5-1 to Figure 5-6.

Nitrogen

For the RR wetland, it is evident that the variabilities, mean and median values of concentrations in the outflow and the pond sampling sites tended to be less than the inflow concentrations for TN, NO_x-N, and NH_4-N during the monitoring season; this was not the case for TON, Figure 5-1 and Figure 5-2. Among nitrogen fractions, the concentrations of NO_x-N (Figure 5-1c) and NH_4-N (Figure 5-1d) were greater in the outflow than in the sampling sites of the pond in 2018, but their concentrations were almost the same in the outflow and these sites in 2019 (Figure 5-2c and Figure 5-2d). It is also evident that the range, mean and median values of concentrations were not notably different among sampling sites in the pond for NO_x-N (Figure 5-1c and Figure 5-2c) and NH_4-N (Figure 5-1d and Figure 5-2d) in both years.

For the RO wetland, Figure 5-3 and Figure 5-4 show that the variabilities of the inflow concentrations tended to be higher than that of the outflow and pond sampling sites for TN and TON in 2018. The mean and median values of NO_x-N concentrations in the middle bottom water layer were higher than the other sampling sites and flow concentrations (Figure 5-3c and Figure 5-4c). There were no concentration differences between the top and bottom layers in the middle sampling site for TN, NO_x-N, and NH_4-N during the entire monitoring season, while the concentrations of TN, NO_x-N, and NH_4-N in the outflow tended to be higher than the concentrations in the outlet sampling sites, Figure 5-3 and Figure 5-4.

By contrast, the range of NH_4-N and NO_x-N were almost the same in all sampling locations of the RR wetland in both years, being lower than the inflows. The range of TON and TN were different in all sampling locations of the RR wetland in both years. The range of TN, NH_4-N and NO_x-N were different in all sampling locations of the RO wetland in both years, and the range of TON were almost the same in all sampling locations. According to the Mann-Whitney test results, the concentrations decreased from the inflow to the inlet sampling sites for NH_4-N, NO_x-N, and TN in the RR wetland ($p < 0.001$), but the concentrations of NO_x-N increased from the inflow to the inlet in the RO wetland ($p < 0.001$). There were no differences in the concentrations between the inflow and the inlet for TON in the RR wetland and NH_4-N, TON, or TN for the RO wetland. Even though the exported concentration variabilities come from the pond conditions (Kadlec and Knight, 1996; Clary et al., 2020), significant increases had been tested from the pond outlet sampling site to the outflow for the concentration of NO_x-N and NH_4-N for both wetlands ($p < 0.001$). There were no significant differences in concentration between in-pond outlet water and effluent for TN or TON for both wetlands ($p > 0.05$).

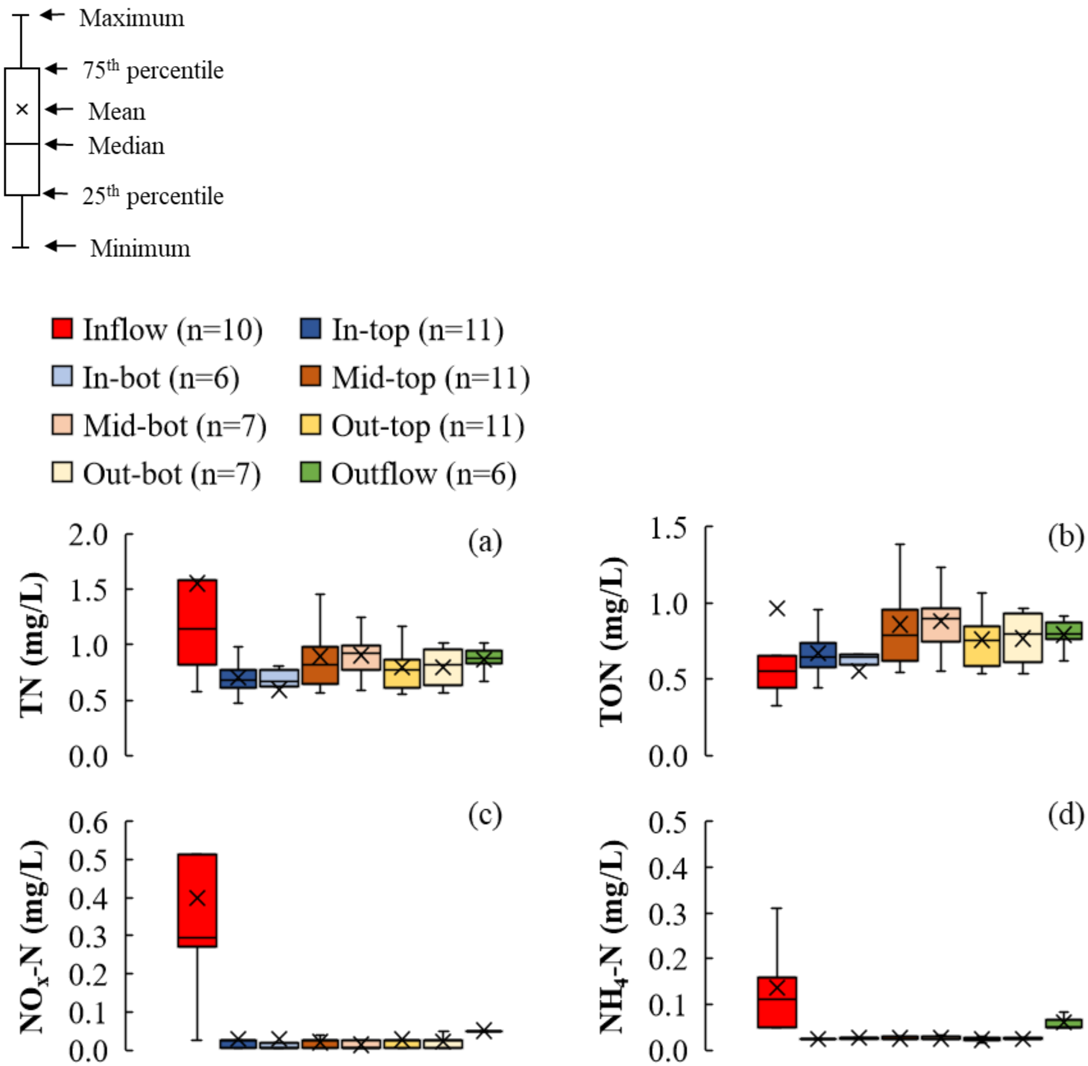

Figure 5-1. Boxplots of nitrogen observed from the inflow, in-pond, and outflow of the Rocky Ridge wetland for 2018; In, Mid, and Out are the in-pond sampling locations (inlet, middle, outlet); top and bot are the sampling top layer and bottom layer; the numbers in the parentheses are sample sizes.

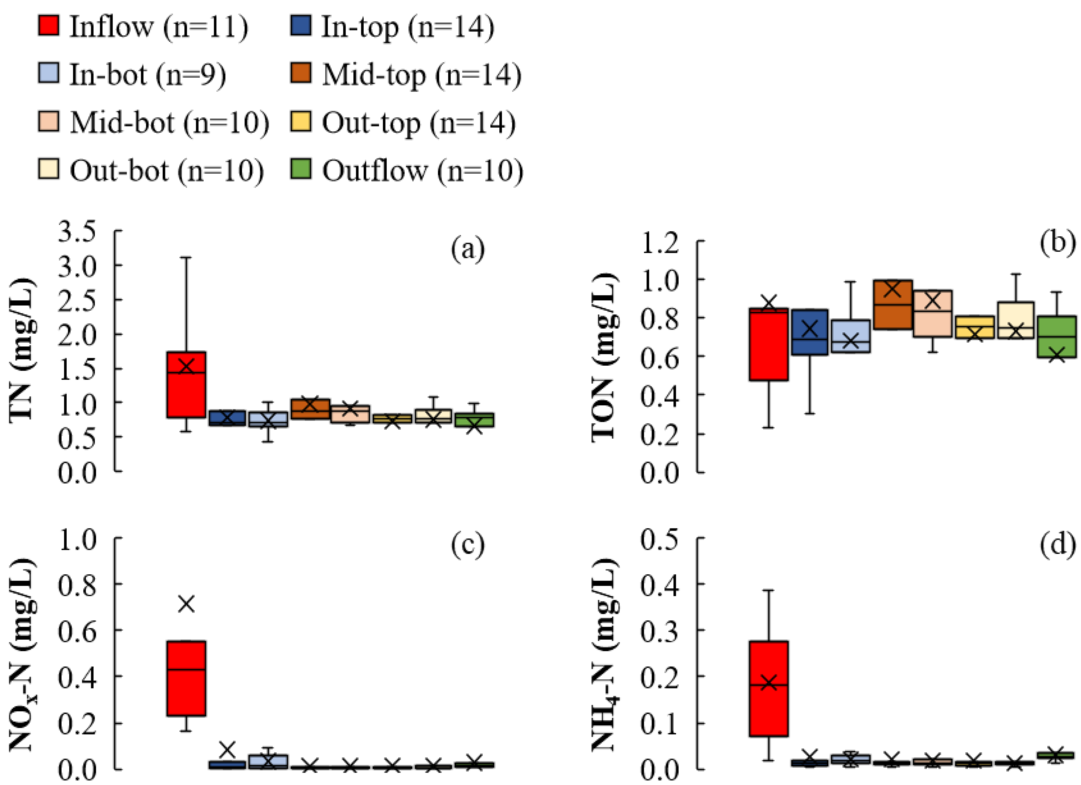

Figure 5-2. Boxplots of nitrogen observed from the inflow, in-pond, and outflow of the Rocky Ridge wetland for 2019; In, Mid, and Out are the in-pond sampling locations (inlet, middle, outlet); top and bot are the sampling top layer and bottom layer; the numbers in the parentheses are sample sizes.

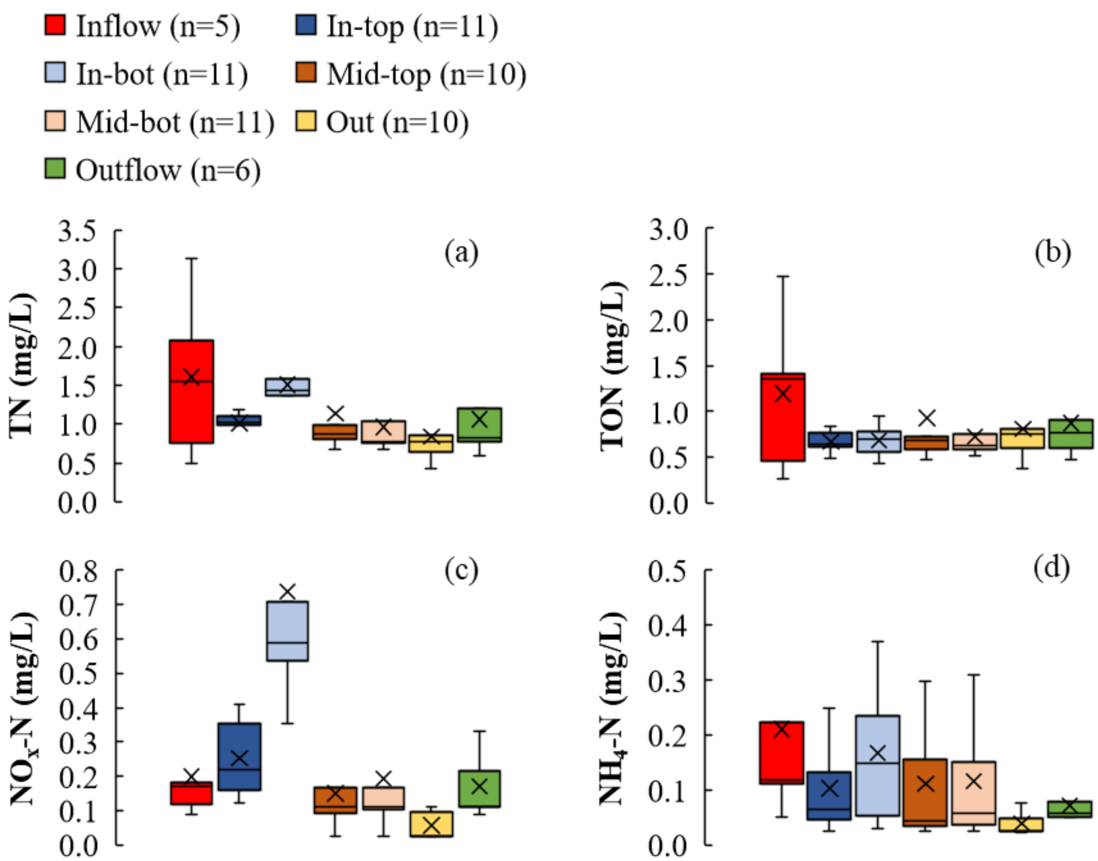

Figure 5-3. Boxplots of nitrogen observed from the inflow, in-pond, and outflow of the Royal Oak wetland for 2018; In, Mid, and Out are the in-pond sampling locations (inlet, middle, outlet); top and bot are the sampling top layer and bottom layer; the numbers in the parentheses are sample sizes.

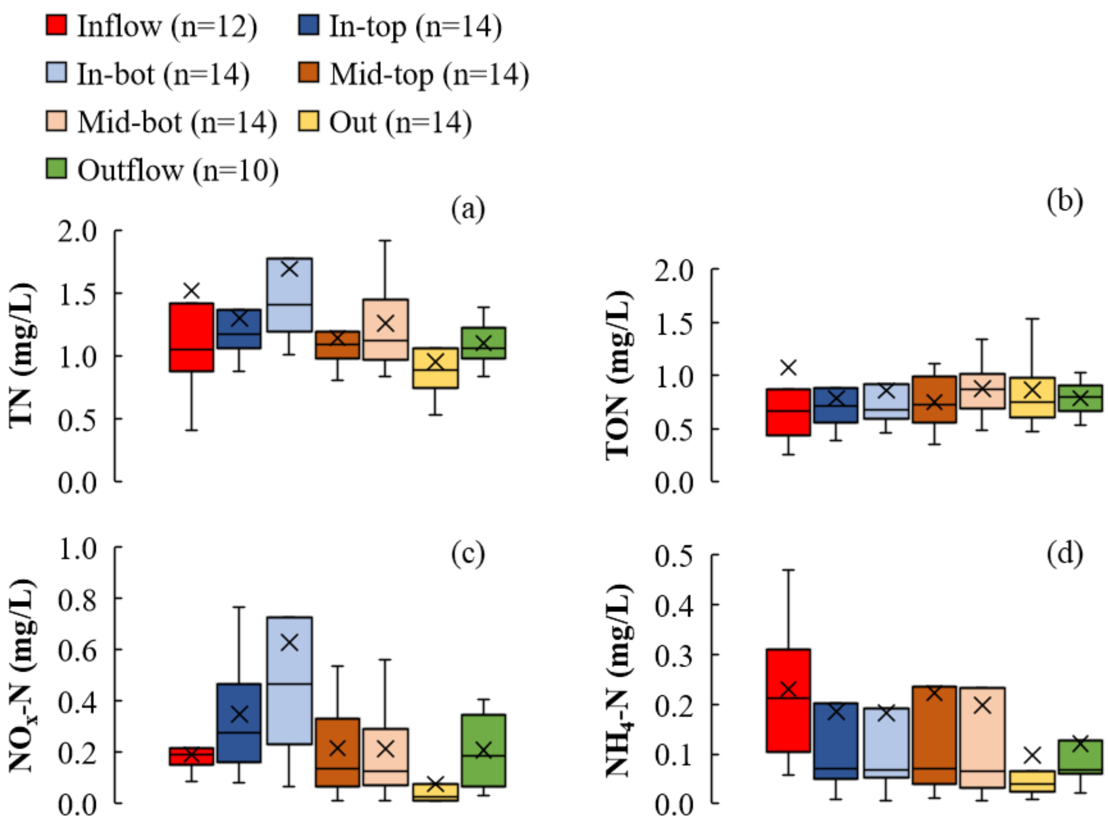

Figure 5-4. Boxplots of nitrogen observed from the inflow, in-pond, and outflow of the Royal Oak wetland for 2019; In, Mid, and Out are the in-pond sampling locations (inlet, middle, outlet); top and bot are the sampling top layer and bottom layer; the numbers in the parentheses are sample sizes.

Phosphorus

The boxplots of the phosphorus concentration from the inflow to the pond to the outflow in these two wetlands for two years are shown in Figure 5-5 and Figure 5-6. The inflow TP concentration of the RO wetland was much higher than the RR wetland during monitoring periods, suggesting that fertilization might occur in the RO watershed (Winston et al., 2013).

In the RR wetland, the range and median values of the inflow concentration were almost the same for TP in two years, Figure 5-5. They were less than the middle and outlet sampling sites and the outflow in 2018, Figure 5-5a, but they were higher than in the pond and the outflow in 2019, Figure 5-5c. In the RO wetland, the mean values of the inflow concentrations of TP and TRP were higher than the median values, showing the data to be right skewed, Figure 5-6. The variabilities, mean and median values of TP concentrations in the inflow were higher than in the pond and the outflow during these monitoring seasons. Over the entire study period 2018-19, the range, mean and median values of concentrations were not notably different among the pond sampling sites and the outlet for TP (Figure 5-6a and Figure 5-6c) and TRP (Figure 5-6b and Figure 5-6d).

There were no differences in the concentrations of TP or TRP between the inflow and the inlet in the RR wetland ($p > 0.05$). On the contrary, the concentrations of TP and TRP decreased from the inflow to the inlet in the RO wetland ($p < 0.001$). No significant differences in concentrations of TP and TRP had been tested between the outlet and outflow for both wetlands ($p > 0.05$).

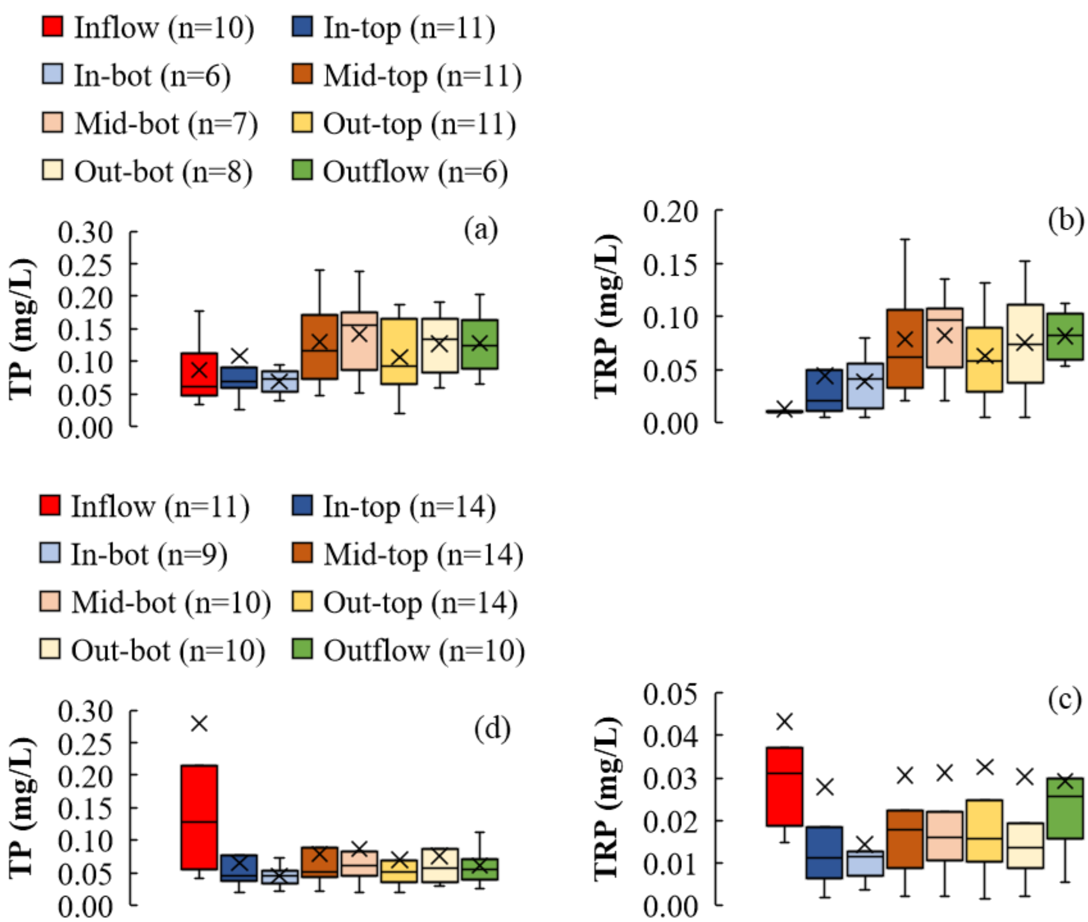

Figure 5-5. Boxplots of phosphorus observed from the inflow, in-pond, and outflow of the Rocky Ridge wetland: (a) and (b) are for 2018 and (c) and (d) are for 2019; In, Mid, and Out are the in-pond sampling locations (inlet, middle, outlet); top and bot are the sampling top layer and bottom layer; the numbers in the parentheses are sample sizes.

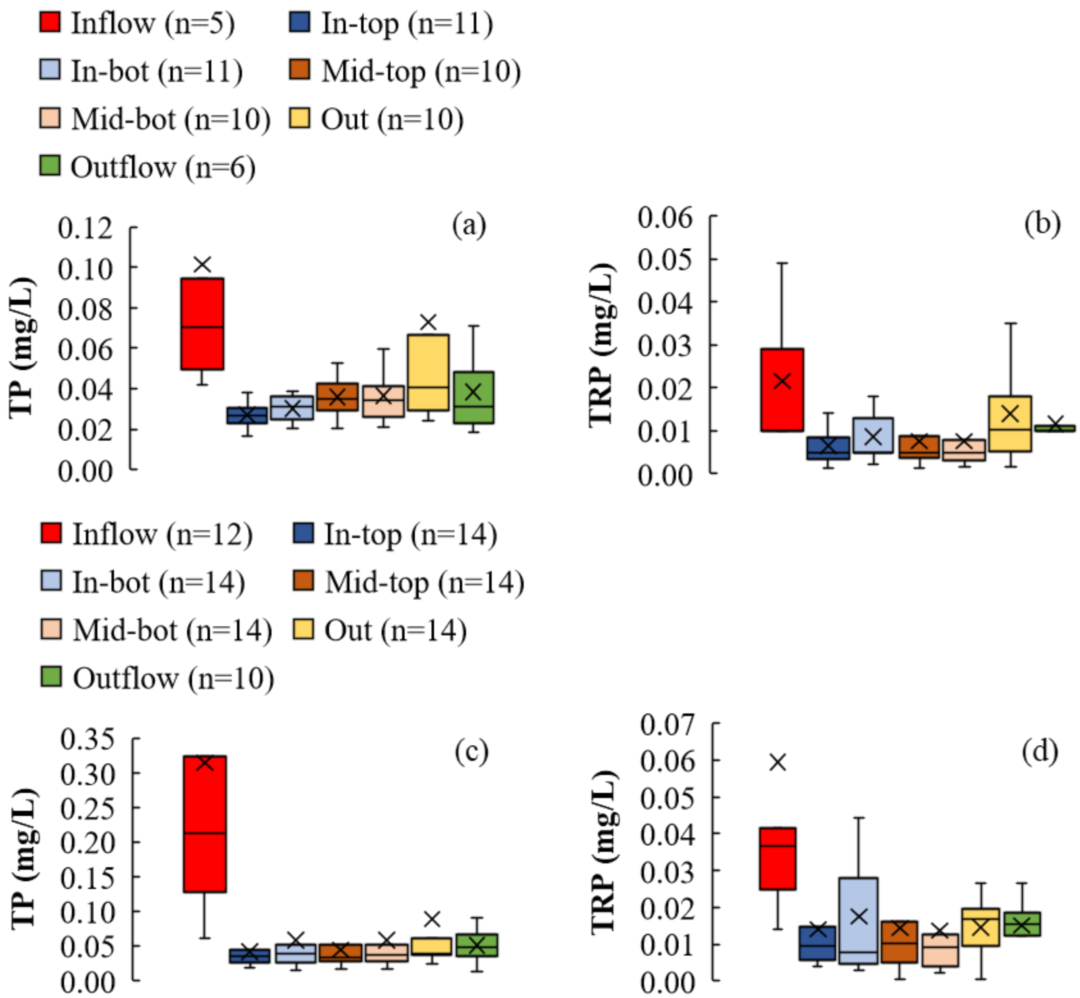

Figure 5-6. Boxplots of phosphorus observed from the inflow, in-pond, and outflow of the Royal Oak wetland: (a) and (b) are for 2018 and (c) and (d) are for 2019; In, Mid, and Out are the in-pond sampling locations (inlet, middle, outlet); top and bot are the sampling top layer and bottom layer; the numbers in the parentheses are sample sizes.

5.1.2 Spatial and Temporal Variability of Nutrients

Rocky Ridge Wetland

Nitrogen

In Rocky Ridge wetland, single samples were collected from the water column in some sampling sites as described in the methodology section. Figures 5-7 and Figure 5-8 show the observed nitrogen in the pool. The concentrations of TN ranged within 0.10 – 1.46 mg/L in 2018 and 0.07 – 1.88 mg/L in 2019, respectively. N stratifications occurred occasionally, and the highest TN concentrations frequently occurred in the middle site. Nitrogen was mainly existing in the pool in organic and dissolved forms, and the concentrations of NH_4-N and NO_x-N were little during the entire study season, within 0.01 – 0.09 mg/L and 0.00 – 0.37 mg/L, respectively, Figure 5-7.

In 2018, The TN concentrations were almost the same in the middle and the outlet, and occasionally negligible nitrogen stratifications were observed in these sites. The TN concentrations increased from 5th June to 16th August before gradually decreasing until 30th August in the middle and the outlet. Of note, there was almost no particle nitrogen in all sites on 18th July. The concentrations of TN, TON (Figure 5-7), and TDN (Figure 5-8) had decreased from 16th August to the end of the monitoring season on 24th October in all sites. In 2019, the concentrations of TN and PN in the middle were usually higher than in the inlet and the outlet, Figure 5-8. The concentrations of TN and PN in all sites raised obviously from 3rd to 30th July. The NO_x-N concentration was suddenly high in the inlet top water on 9th October, Figure 5-7. At the monitoring beginning and the monitoring end, there was almost no difference in the concentrations of TN, TON, TDN, and PN in the outlet. The lowest concentrations of TN in all sites occurred on 3rd July when there was only organic and dissolved nitrogen in the outlet. At this time, the outlet had the highest DO and all sites had approximately 5µg/L of Chl-a concentration, see the following Figure 5-20 and Figure 5-21 in section 5.3.

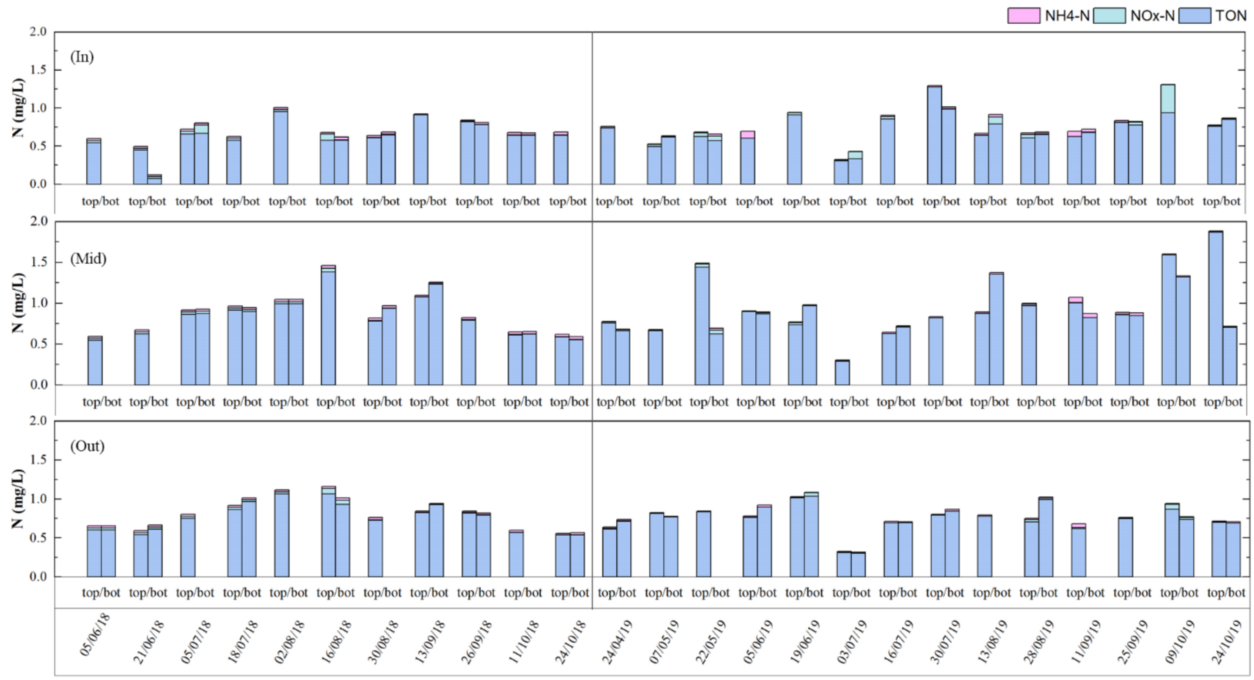

Figure 5-7. The observed nitrogen (NH_4-N, NO_x-N, TON) concentrations in the pond of the Rocky Ridge wetland; In, Mid, and Out are the in-pond sampling locations (inlet, middle, outlet); top and bot are the sampling top layer and bottom layer.

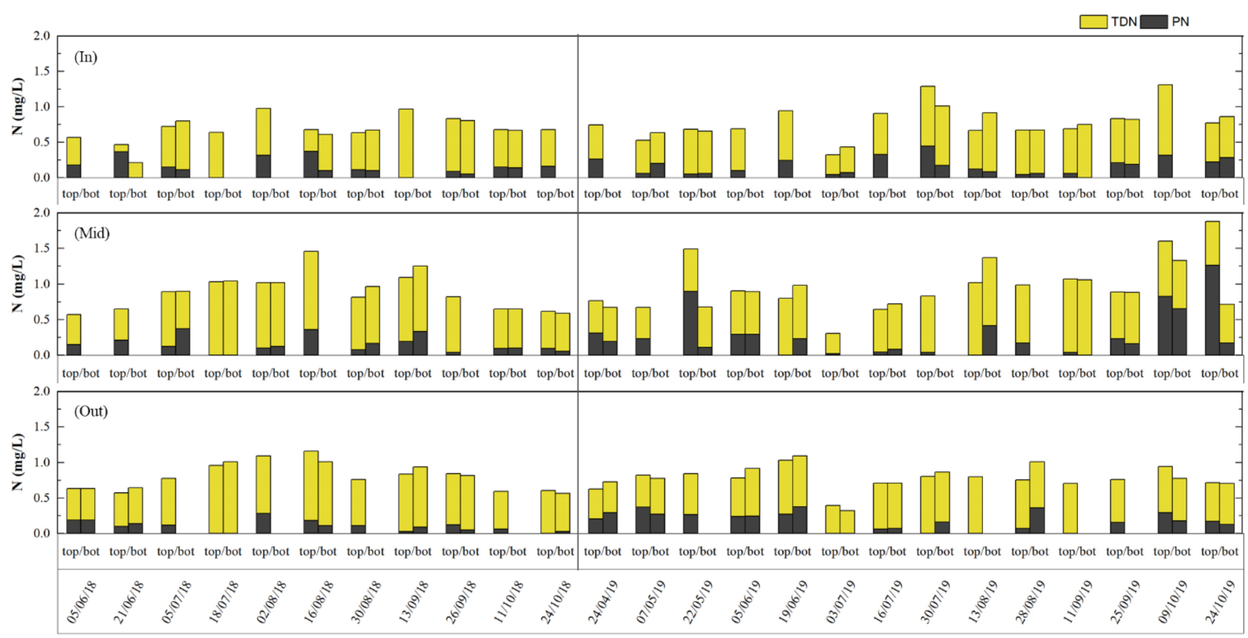

Figure 5-8. The observed nitrogen (TDN and PN) concentrations in the pond of the Rocky Ridge wetland; In, Mid, and Out are the in-pond sampling locations (inlet, middle, outlet); top and bot are the sampling top layer and bottom layer.

Phosphorus

Figures 5-9 and Figure 5-10 show the observed phosphorus in the pool, TP, TRP, URP, TDP and PP were considered. The TP concentration ranged from 0.02 mg/L to 0.30 mg/L in 2018 and from 0.02 mg/L to 0.23 mg/L in 2019.

In 2018, phosphorus was mainly existing in this wetland as dissolved and reactive phosphorus forms, Figure 5-9 and Figure 5-10. The concentrations of TP, TDP, and TRP in the inlet were lower than in the other sites from 5th June to 30th August. The concentrations of TP, TDP, and TRP in all sites had an increased tendency from 5th June to 16th August then decreased until 11st October, and these phosphorus concentrations were almost the same in the middle and the outlet. There was almost no concentration change of TP and TRP in the middle at the monitoring beginning and the end time point, Figure 5-9. A high concentration of TP and PP in the inlet top occurred on 24th October, Figure 5-10.

In 2019, the concentrations of TP and PP were frequently different in different sites, Figure 5-10. The concentrations of TP and PP in the middle had a peak on 9th October, while the concentration peaks of TP, TRP, and TDP in the inlet happened on 19th June. The concentrations of TP, PP, and TRP in the outlet decreased from 24th April to 16th July, except on 19th June when there occurred concentration peaks of TP and TRP. The concentrations of TP, PP, and URP in all sites decreased from 30th July to 28th August then increased until 9th October.

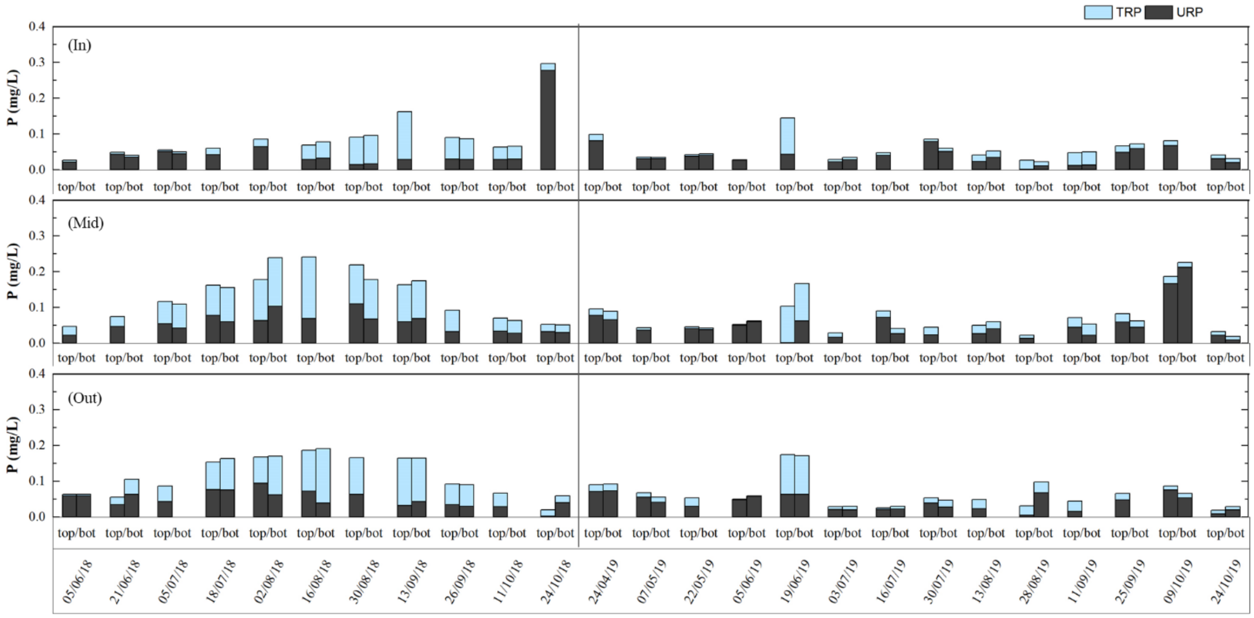

Figure 5-9. The observed phosphorus (TRP and URP) concentrations in the pond of the Rocky Ridge wetland; In, Mid, and Out are the in-pond sampling locations (inlet, middle, outlet); top and bot are the sampling top layer and bottom layer.

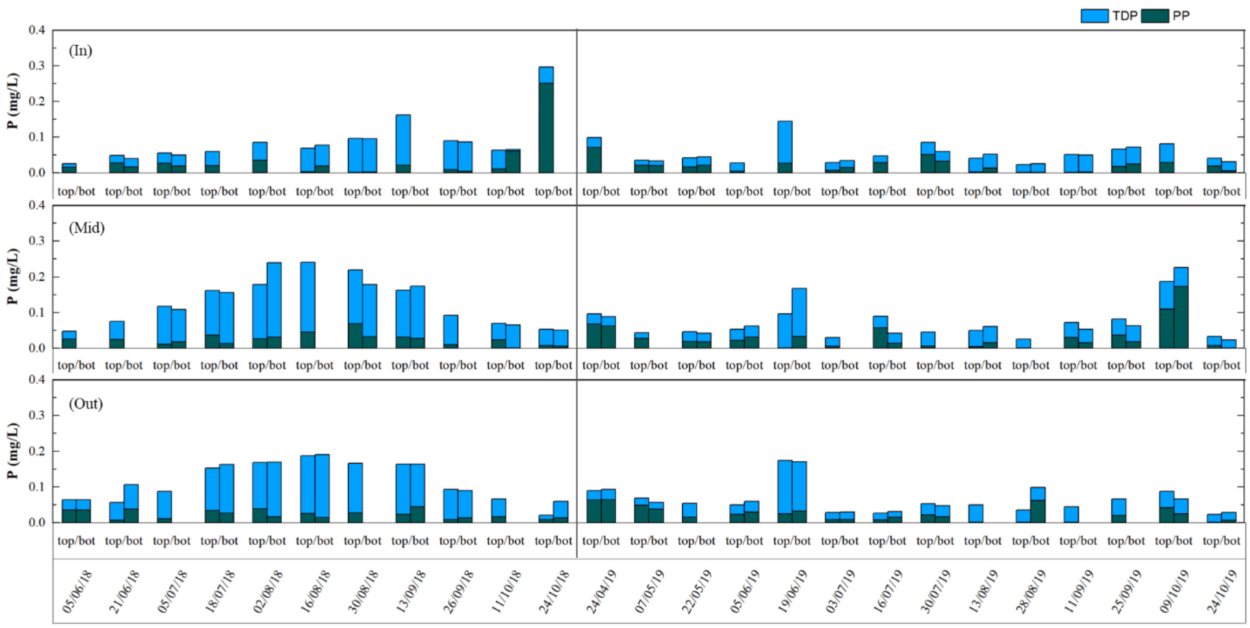

Figure 5-10. The observed phosphorus (TDP and PP) concentrations in the pond of the Rocky Ridge wetland; In, Mid, and Out are the in-pond sampling locations (inlet, middle, outlet); top and bot are the sampling top layer and bottom layer.

Royal Oak Wetland

Nitrogen

Figures 5-11 and Figure 5-12 show the observed nitrogen in the pool. The concentrations of TN ranged within 0.42 – 2.32 mg/L in 2018 and 0.53 – 3.08 mg/L in 2019, respectively. Nitrogen was mainly existing in the pool in dissolved form (Figure 5-12), probably because macrophytes can prevent particle nitrogen release from bed in wetlands (Reddy and D'Angelo, 1997). Contrary to the RR wetland, NH_4-N and NO_x-N were high in the inlet and the middle sites, especially in the inlet bottom, where there is a sedimentation forebay, Figure 5-11. Abundant nitrate/nitrite might result in an anammox process in water (Reddy and D'Angelo, 1997). N stratifications occurred frequently in the inlet, and the concentrations of TN and NO_x-N in the inlet bottom were higher than in the other sites, Figure 5-11. Besides, the stratifications of NOx-N (Figure 5-11) and PN (Figure 5-12) were observed in the inlet and the middle sites, indicating different processes of nitrogen transformation might happen in the top water and the bottom water in these sites. The sustained high concentrations of NO_x-N in the inlet bottom, which can come from the ammonification-nitrification process decomposing organic nitrogen in the bed, can result in anammox and denitrification processes, Figure 5-11.

In 2018, the stratifications of nitrogen concentrations were obvious in the inlet for TN and NO_x-N in the outlet, and nitrogen was mainly constituted by TON in this site, Figure 5-11. The concentrations of TN, TON, and PN declined significantly in the outlet over the entire study period, Figure 5-12. However, the concentrations of TN, TON, and TDN changed little in the middle and the inlet sites in the 2018 season. Of note, there was a concentration peak of TN, PN, and TON in the middle top water on 18th July. Accordingly, a concentration peak of TN, PN, TDN, and TON occurred in the middle bottom water on 16th August. The highest concentrations of NO_x-N in the inlet and the middle occurred on 11th October. The concentrations of NH_4-N in the inlet and the middle had risen from the middle of July to the middle of August. The increase of NH_4-N indicates that the DNRA process or ammonification process had occurred.

In 2019, the PN concentrations in the top water of the inlet and the middle were below 0.2 mg/L from 5th June to 24th October (the end of the monitoring period, Figure 5-12). The stratifications of NOx-N and PN were observed in the inlet and the middle sites and sustained high concentrations of NO_x-N were observed in the inlet bottom. Besides, there were concentration declines for NO_x-N in the inlet bottom and the middle top from 7th to 22nd May and 3rd – 16th July, following the occurrences of concentration peaks. The concentrations of NO_x-N and TN in the inlet decreased from 3rd July to 28th August. The concentrations of TON and TN in the outlet decreased from 22nd May to 03rd July then increased until 13th August, before gradually decreasing until the end of this study period. The concentrations of NH_4-N in the inlet and the middle had a rise from the end of August to the end of September.

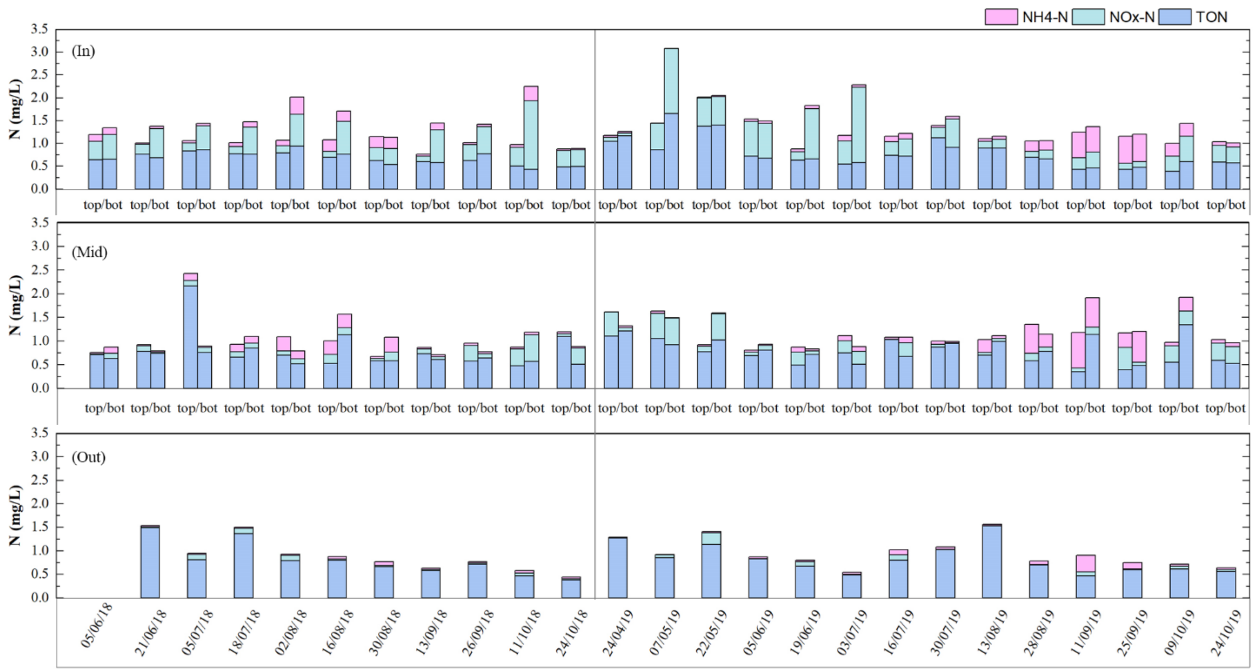

Figure 5-11. The observed nitrogen (NH_4-N, NO_x-N, TON) concentrations in the pond of the Royal Oak wetland; In, Mid, Out are the in-pond sampling locations (inlet, middle, outlet); top, bot is the sampling top layer and bottom layer.

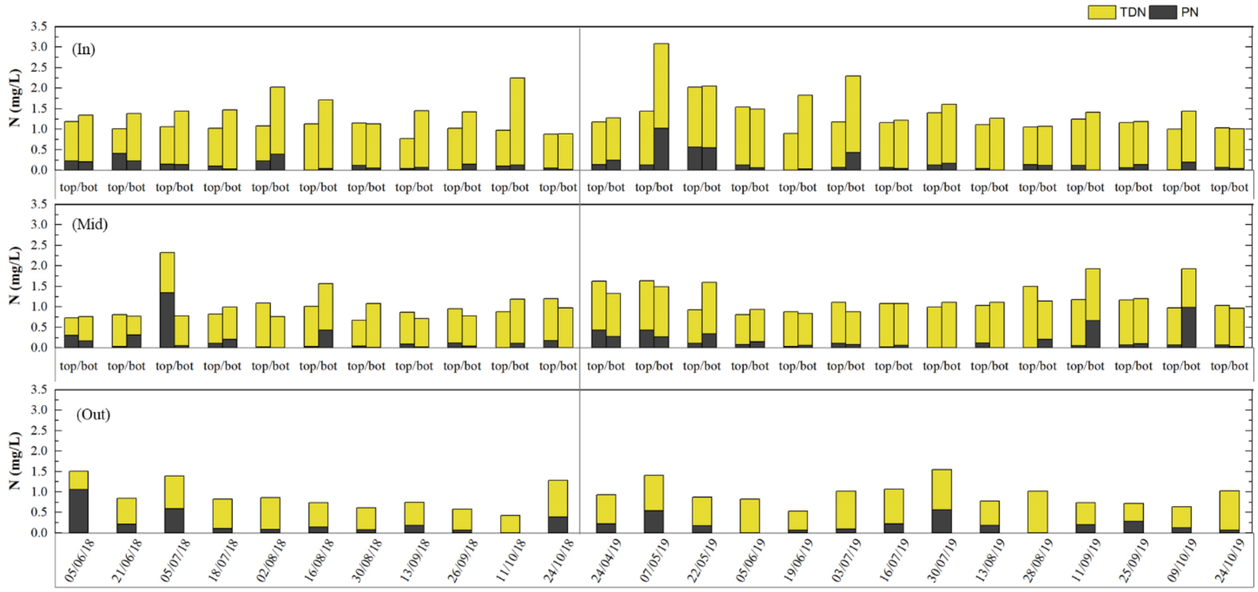

Figure 5-12. The observed nitrogen (TDN and PN) concentrations in the pond of the Royal Oak wetland; In, Mid, Out are the in-pond sampling locations (inlet, middle, outlet); top, bot is the sampling top layer and bottom layer.

Phosphorus

Figures 5-13 and Figure 5-14 show the observed and considered phosphorus in the pool. The TP concentration ranged from 0.02 mg/L to 0.20 mg/L in 2018 and from 0.01 mg/L to 0.28 mg/L in 2019, respectively.

In 2018, phosphorus was mainly in the dissolved (Figure 5-14) and unreactive (Figure 5-13) forms in this wetland. Few concentration differences in TP, TDP, and TRP were observed between the inlet and the outlet, and there were no phosphorus stratifications in these two sites. Most of the concentrations of TP in the inlet and the middle were small and below 0.05 mg/L. The concentrations of TP in the outlet had a peak on 18th July, with a value of ~ 0.2 mg/L. The concentrations of all different phosphorus in the outlet decreased from 18th July until the monitoring ended on 24th October.

In 2019, phosphorus was mainly constituted of particle and unreactive forms in all sites from 24th April (the monitoring beginning) to 22nd May. While phosphorus was mainly existed in the pool in reactive and dissolved forms from the end of August to the end of September. There was almost no discrepancy in phosphorus concentrations between the top and the bottom water in the inlet and the middle sites from 5th June to 25th September. TP concentrations in the inlet and the middle decreased from above 0.05 mg/L at the monitoring beginning to ~ 0.02 mg/L on 30th July, then they raised to around 0.05 mg/L on 25th September, before falling to ~ 0.025 mg/L at the monitoring end. Of note, there were peaks of TP concentration in the middle bottom (~ 0.16 mg/L, mainly is particle form) on 9th October and in the outlet (~ 0.28 mg/L, mainly was particle form) on 13th August, respectively.

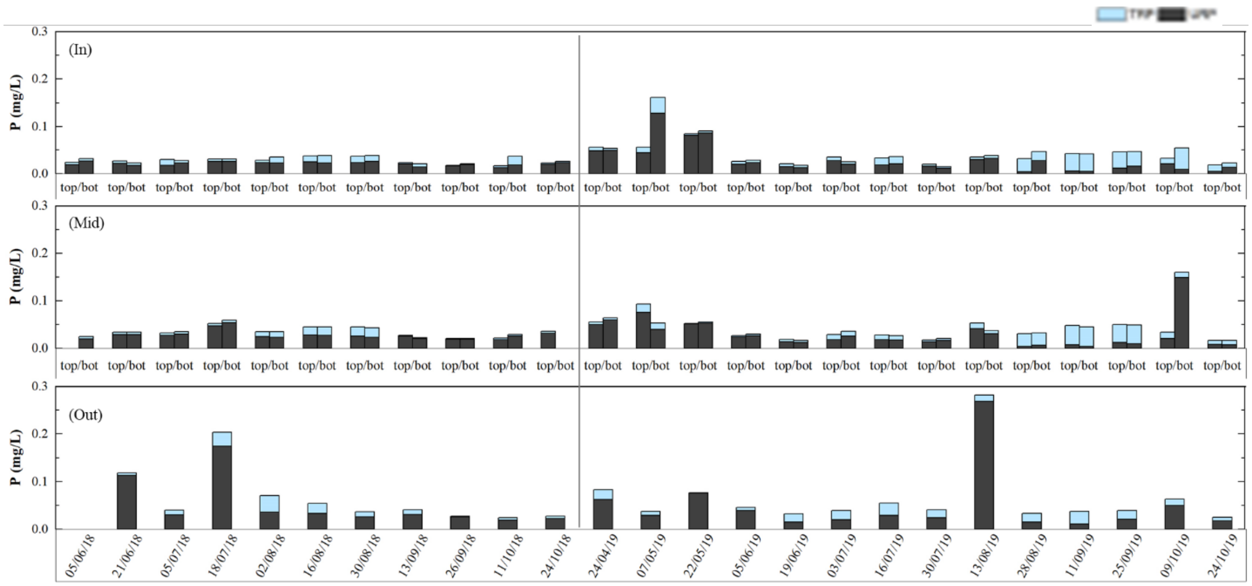

Figure 5-13. The observed phosphorus (TRP and URP) concentrations in the pond of the Royal Oak wetland; In, Mid, Out are the in-pond sampling locations (inlet, middle, outlet); top, bot is the sampling top layer and bottom layer.

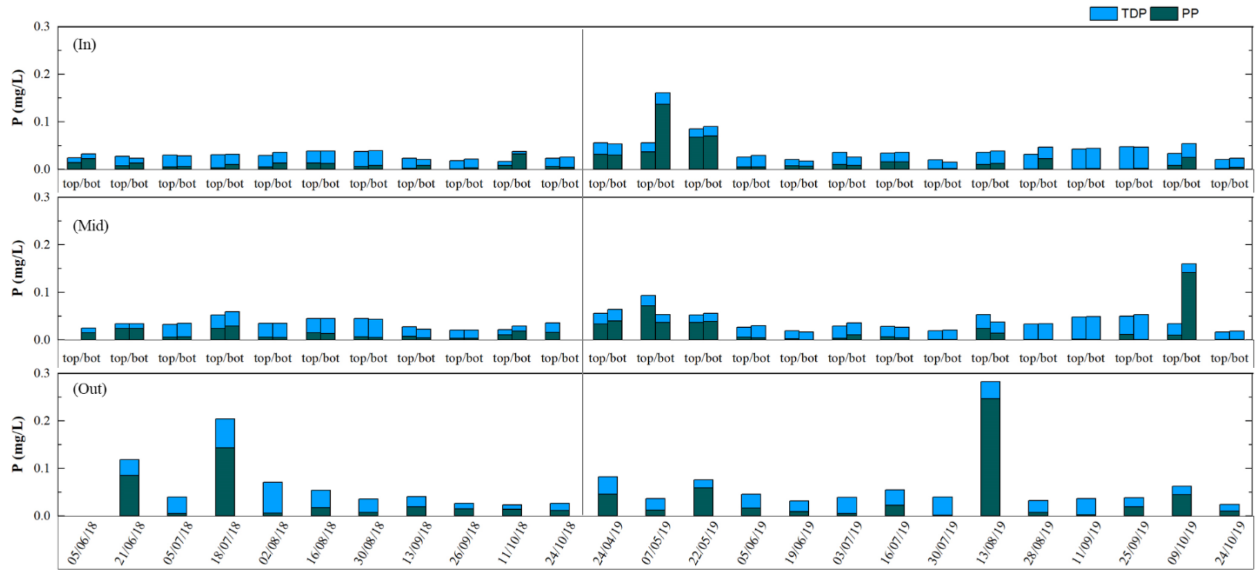

Figure 5-14. The observed phosphorus (TDP and PP) concentrations in the pond of the Royal Oak wetland; In, Mid, Out are the in-pond sampling locations (inlet, middle, outlet); top, bot is the sampling top layer and bottom layer.

Temporal Comparations between Pond and Outflow

Stormwater finally flows away from the wetlands through the outlet sampling location, and the outflow concentrations mainly depend on the concentrations of the outlet locations, no matter how the concentration distributions of the pond would be. The concentrations of nitrogen and phosphorus in the pond were observed regularly and the outflow EMCs were observed randomly because of rainfall events. The concentration comparations of TN and TP between pond and outflows are displayed in Figure 5-15 for the RR wetland and in Figure 5-16 for the RO wetland, respectively. The concentrations in the outlet sampling location were selected to be representative of the pond conditions. It is clear that the outflow concentrations agree well with the pond values.

In the RR wetland, the outflow concentrations of TN and TP locate in or around the pond concentration lines for all events, except one event on 20th June 2019 (red circled in Figure 5-15b), in which outflow had a TN concentration as 0.07 mg/L without organic nitrogen form. Around the date of this deviation event, the TN concentration in the outlet sampling site of the pond was 1.03 mg/L and was mainly in organic nitrogen form, Figure 5-7 (Out). The deviation of TN occurred in this event possibly because of that there was a problem with the measured data. The TN and TP concentrations in the outlet sampling site of the RR wetland fluctuated from early June to middle

July 2019, Figure 5-15b and Figure 5-15d, primarily because of successive rainfall events (Figure 5-17a). These results emphasize the need to study the influence of rainfall on the nutrient cycling in the pond of this wetland.

Similarly, the outflow had almost the same TN and TP concentrations as the pond sampling site of the outlet for all of the events in the RO wetland, except one event on 16th August 2019 (red circled in Figure 5-16d), in which outflow had a TP concentration as 0.013 mg/L being reactive phosphorus form. The TP concentration in the outlet sampling site of the RO wetland had a peak on 13th August 2019 (Figure 5-16d), mainly being unreactive and particle phosphorus forms (Figure 5-13 and Figure 5-14). This deviation phenomenon mainly resulted from the observed algal bloom, Figure 5-22.

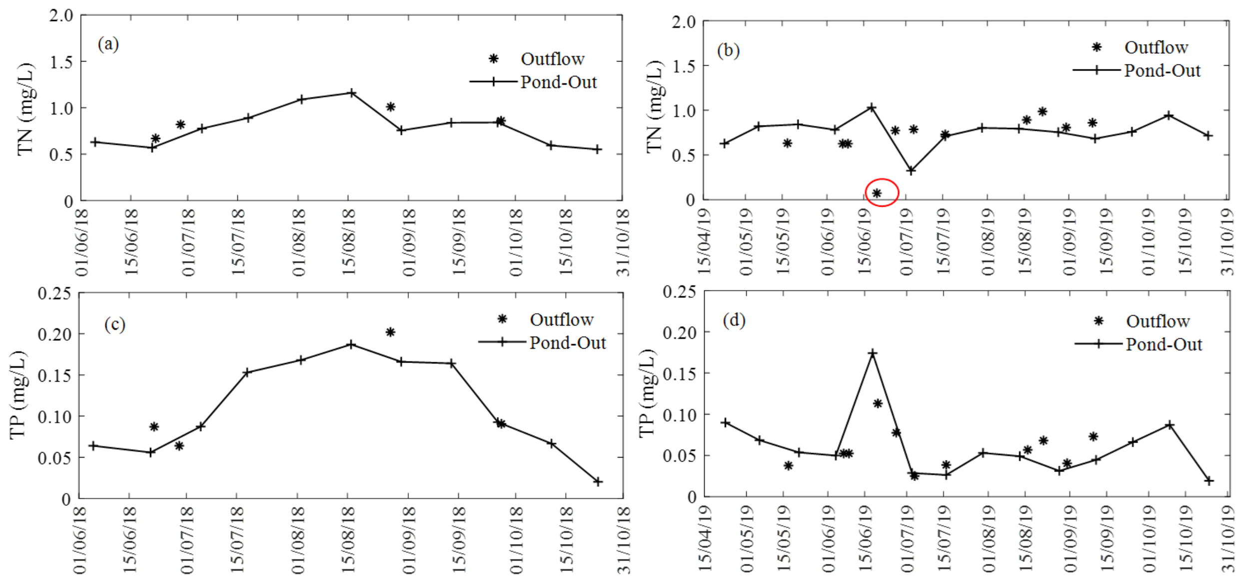

Figure 5-15. The concentrations of total nitrogen and total phosphorus in the pond and the EMCs of total nitrogen and total phosphorus in the outflows for the Rocky Ridge wetland. Pond-Out is the outlet top layer sampling location in the pond.

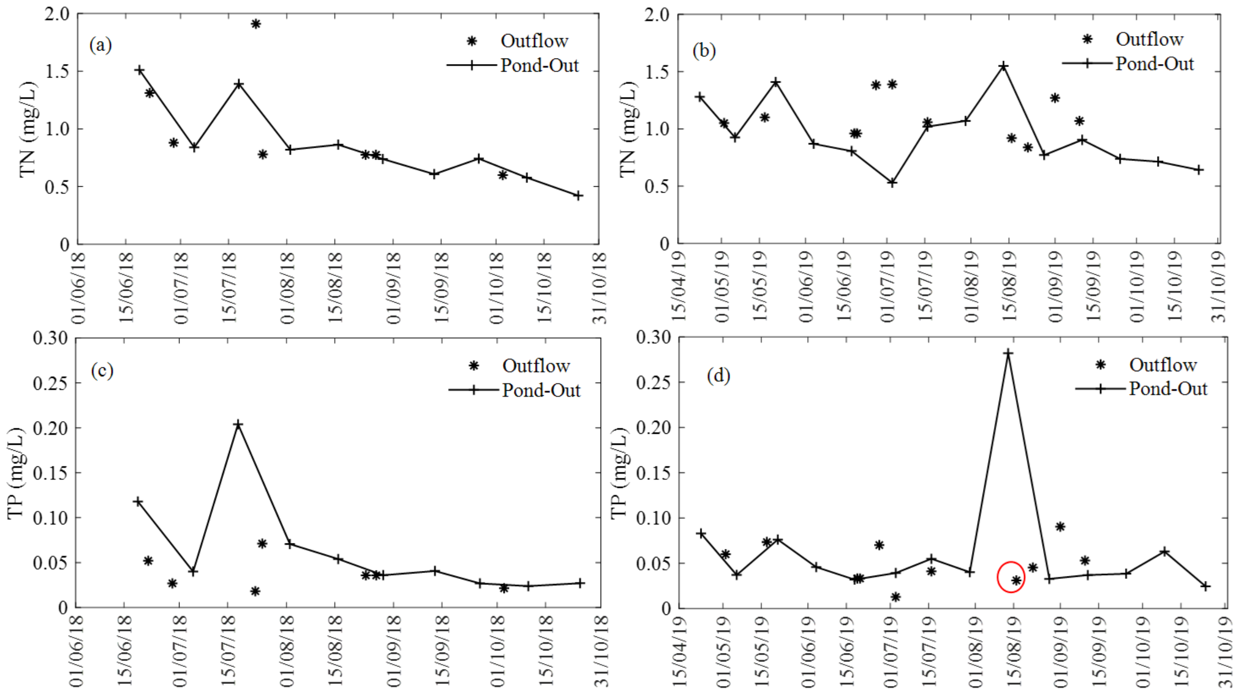

Figure 5-16. The concentrations of total nitrogen and total phosphorus in the pond and the EMCs of total nitrogen and total phosphorus in the outflows for the Royal Oak wetland. Pond-Out is the outlet bottom layer sampling location in the pond.

5.1.3 Event Comparation between Inflow and Outflow

The observed EMCs and event flow volumes are shown in Figure 5-17 for the RR wetland and in Figure 5-18 for the RO wetland.

Nitrogen

For the entire monitoring season, the inflow EMCs of nitrogen and phosphorus were variable in these two wetlands, Figure 5-17 and Figure 5-18. The inflow TN concentrations of the two wetlands in the two monitored seasons varied greatly, that is, RR wetland: 0.58 – 3.65 mg/L, Standard Deviation (S.d) = 0.86 mg/L, Figure 5-17b; RO wetland: 0.41 – 3.83 mg/L, S.d = 0.93 mg/L, Figure 5-18b, respectively. Compared with the International Stormwater Best Management Practices (BMPs) Database Annual Report (Clary et al., 2020), in which the median TN concentration in stormwater for retention wetlands was 1.43 mg/L. The inflows to these two wetlands were relatively clean, and the median concentration of TN was 1.21 mg/L for the RR wetland and 1.10 mg/L for the RO wetland. According to Mann-Whitney U-test, the EMC of TN decreased significantly from the inlet to the outlet in the RR wetland ($p = 0.012$) while not in the RO wetland with $p > 0.05$.

Alberta province (ESRD, 2014) has made a threshold value of TN below 1.0 mg/L, which would be protective or desirable for downstream waters. The median concentration of TN in the outflow from the RR wetland was 0.81 mg/L, with all EMCs below 1.0 mg/L (Figure 5-17b). The exporting TN concentrations from the RR wetland can be considered compiled with the threshold value. The median of the outflow TN concentrations was 1.05 mg/L in the RO wetland, and 8 of 18 EMCs were higher than 1.0 mg/L (Figure 5-18b), there is still needed to improve the ecosystem function of the RO wetland.

For nitrogen fractions, in the RR wetland, TON and NO_x-N were the main nitrogen forms in the inflow of the RR wetland (Figure 5-17b), accounting for 2.6 – 71.0% and 27.4 – 94.8%, respectively, while NH_4-N had small accountant of 1.7 – 27.1%. There were significant decreases observed from the inflow to the outflow for NH_4-N and NO_x-N ($p < 0.001$), thus, organic nitrogen was the major nitrogen form accounting for 81.5 – 97.7% of the outflow (Figure 5-17b), without a significant concentration difference between the inflow and the outflow ($p = 0.3$). In the RO wetland, the major N form in the inflow was TON (Figure 5-18b), with 38.7 – 91.0%. The concentrations of NH_4-N and NO_x-N were relatively small, accounting for 3.2 – 30.3% for NH_4-N and 5.4 – 31.1% for NO_x-N. No statistically significant differences in the concentrations of NO_x-N or TON between the inflow and the outflow were detected ($p > 0.05$), but the concentrations of NH_4-N decreased significantly from the inflow to the outflow, with $p = 0.006$. The NO_x-N and NH_4-N forms could also dominate occasionally in the outflow of the RO wetland, the maximum percent reached 30.4% (NH_4-N) and 38.7% (NO_x-N), even though organic nitrogen was the major nitrogen form, accounting for 55.1 – 94.3%, Figure 5-18b.

Phosphorus

Similarly, the observed TP concentrations of the inflow varied greatly, 0.03 – 0.96 mg/L with S.d = 0.20 mg/L for the RR wetland (Figure 5-17c) and 0.04 – 0.85 mg/L with S.d = 0.20 mg/L for the RO wetland (Figure 5-18c), respectively. Unreactive phosphorus form dominated in the inflow P and accounted for 31.8 – 96.0% in the RR wetland (Figure 5-17c) and 41.8 – 97.1% in the RO wetland (Figure 5-18c), respectively. There was no significant difference in concentrations between the inflow and the outflow for phosphorus ($p > 0.05$ for TP and TRP) in the RR wetland.

Conversely, the concentrations of TP and TRP decreased significantly from the inflow to the outflow ($p < 0.001$ for TP; 0.002 for TRP) in the RO wetland. The outflow concentrations of TP were 0.03 – 0.20 mg/L with S.d = 0.05 mg/L in the RR wetland and were 0.01 – 0.09 mg/L with S.d = 0.02 mg/L in the RO wetland, respectively. The chemistry forms of phosphorus had been altered from the inflows, in which phosphorus mainly existed in particle and unreactive forms in both wetlands (Figure 5-17c and Figure 5-18c), to the outflows, where reactive and dissolved phosphorus had become the prevalent phosphorus in the RR wetland (Figure 5-17c). Relevant to these, the pond environmental conditions had altered the chemistry forms of the inflow phosphorus, probably replacing recalcitrant phosphorus with labile phosphorus forms through intense biological activities (Kadlec and Knight, 1996).

The inflow TP concentrations for the RR wetland were relatively clean, with a median value of 0.06 mg/L, being compared with the inflow median concentration of 0.170 mg/L in the International Stormwater Best Management Practices (BMPs) Database Annual Report (Clary et al., 2020). Consequently, the median concentration of TP in the outflow from the RR wetland was 0.07 mg/L, which was higher than the 0.05 mg/L determined by Alberta province for water protection (ESRD, 2014). The concentration range of the exported TP by this wetland was 0.03 – 0.20 mg/L, which was within the eutrophic to the hyper-eutrophic level endorsed by (EC, 2011), that is, 0.035 – 0.100 mg/L for eutrophic level and > 0.100 mg/L for the hyper-eutrophic level, respectively. However, the inflow TP concentrations for the RO wetland were relatively typical, with a median value of 0.14 mg/L. In comparison, the outflow TP concentrations were within 0.01 – 0.09 mg/L which belongs to mesotrophic to eutrophic levels (EC, 2011), and the median value was 0.04 mg/L which is below the water protection threshold (ESRD, 2014). It could be determined that the RO wetland is capable of removing TP from stormwater.

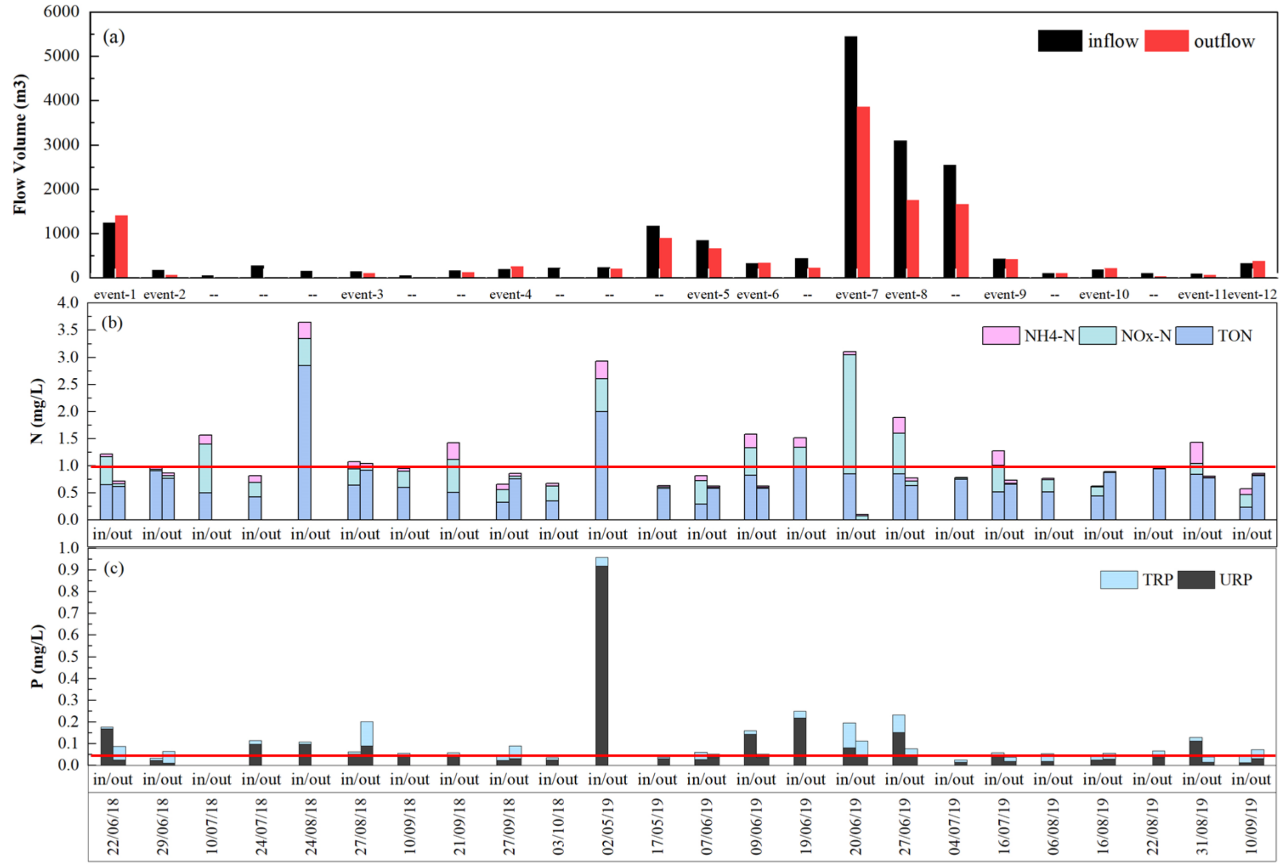

Figure 5-17. Bar charts showing EMCs of nutrients in the inflows and the outflows, and the flow volumes of the Rocky Ridge wetland for 24 storm events. Event-# is the fully captured events; the red line represents the protective threshold values.

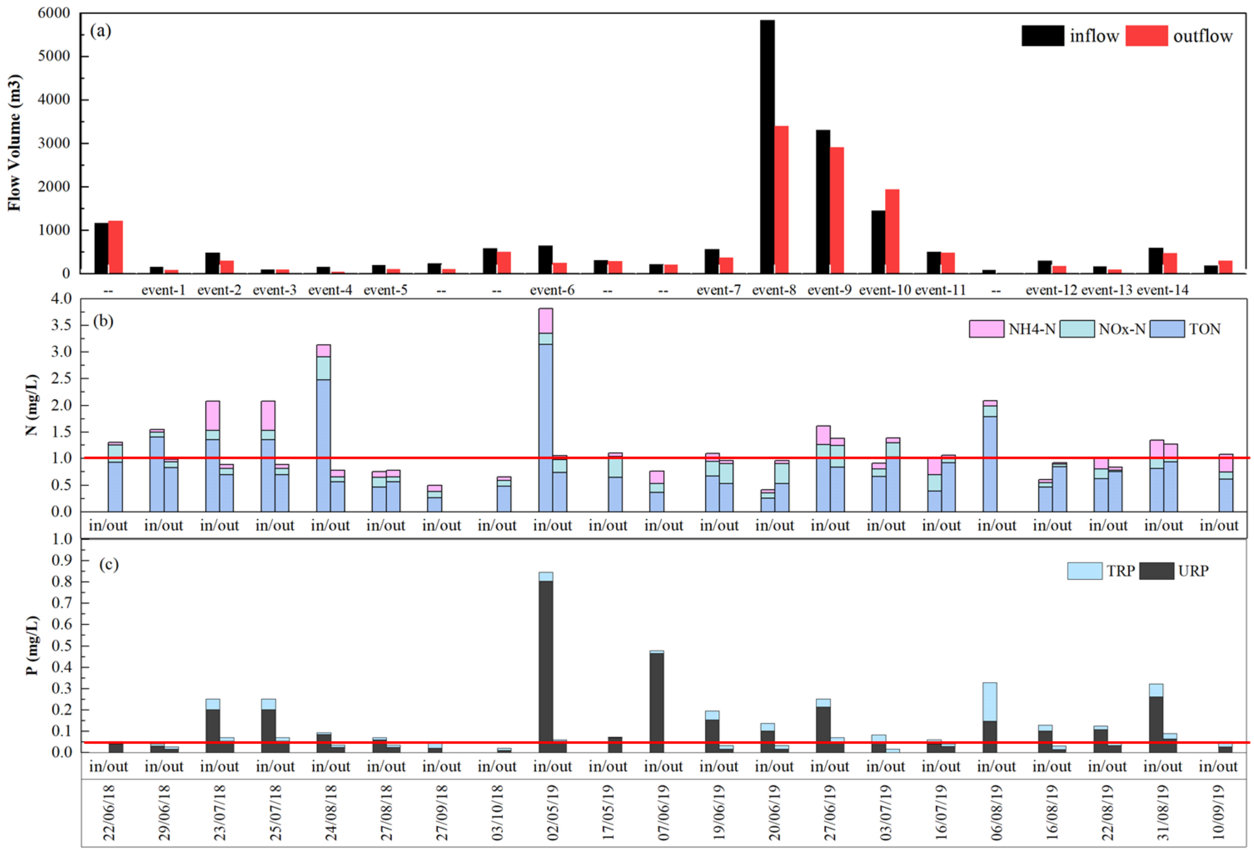

Figure 5-18. Bar charts showing EMCs of nutrients in the inflows and the outflows, and the flow volumes of the Royal Oak wetland for 21 storm events. Event-# is the fully captured events; the red line represents the protective threshold values.

Event Flow Reduction

The nutrient removal efficiency reflects two aspects, which are flow volume and nutrient concentrations. In the fully captured events of these two wetlands, the removal efficiencies of N, P, and their fractions changed widely from negative to positive because of the ineffective combination of the flow reductions and concentration reductions.

There were 5 small events in 2018 with hundred percent removal efficiencies in the RR wetland (Figure 5-17a), in which there was no water flowing away from the RR wetland through the outlet. There was only one small event in 2019 with hundred percent removal efficiencies in the RO wetland, Figure 5-18a. There were 6 events in the RR wetland and 3 in the RO wetland with negative flow reductions, and there was more weir/orifice outflow water than pipe inflow water in these events.

For the fully captured events, the flow volume reductions from the pipe inlet to the weir/orifice outlet of these two wetlands had large variations, changing from -28.4% to 67.7% in the RR wetland and changing from -18.8% to 75.0% in the RO wetland, Table 5-1, respectively. The RO wetland had better performance on flow volume reductions than the RR wetland, comparing the median of flow reductions, Table 5-1. Both wetlands had close median and mean flow reductions, indicating that their event flow reductions distribute normally. The negative reductions could result from imprecise calculations, mainly because the wetlands received new stormwater runoff before the outflow had returned to no-flow conditions, particularly when the antecedent dry periods (ADP) were short such as less than two days (Al-Rubaei et al., 2017). The ineffective flow reductions should also indicate the important improvement that needs to be done to the wetland's hydraulic design.

5.2 Nutrient Removal

5.2.1 Event Removal Efficiency

Given the relatively complex conditions from weather and wetland configurations included in this entire season studies (Table 3-1, Table 4-4, and Table 4-5), the event removal efficiencies (REs) of N, P, and their fractions varied widely, as shown in Table 5-1. The RE-TN ranged from -68.6% to 98.4% of the RR wetland and from -104.1% to 93.8% of the RO wetland, respectively. The median and mean RE-TN of these two wetlands were close, they were 41.6% and 34.1% of the RR wetland, 44.2% and 31.5% of the RO wetland, respectively. In terms of nitrogen fractions, these two wetlands had almost the same median and mean RE-NH_4, RR had a higher median and mean RE-NO_x but RO had a higher median and mean RE-TON, Table 5-1. The RO wetland had better phosphorus reductions than the RR wetland, comparing the median and mean RE of TP and TRP, Table 5-1. The RE-TP ranged from 29.9% to 97.2% of the RO wetland and from -160% to 80.3% of the RR wetland, respectively. The median and mean RE of TP and TRP were almost the same in the RO wetland, which indicates that the event REs of TP and TRP by this wetland distribute normally, Table 5-1. The RR wetland had a negative median and mean RE of TP and TRP and their values were quite different, Table 5-1.

Despite the different nature of hydrologic and nutrients inputs from stormwater runoff, we put our observed performance results into a reviewed analysis carried out by Carleton et al. (2001), who summarized 49 stormwater wetlands treatment performances from 35 studies and reported the event RE range was -49% to 46% for TN, -55% to 87% for TP, -86% to 96% for NH_4-N, and -193% to 94% for NO_x-N, respectively. Land et al. (2016) also reported a median event RE of TN and TP was 37% and 46% from 203 different stormwater wetlands, respectively. Compared to these, both wetlands performed well on nitrogen, especially on NH_4-N and NO_x-N, as the event median RE of these nitrogen fractions was in the upper range of the database reported by Carleton et al. (2001) and Land et al. (2016). The RO wetland also had excellent performance on TP and TRP, with upper ranges and high medians of phosphorus RE. While the RR wetland had a negative median RE of TRP and had a close median RE of TP with the database. Comparing the median and mean values of event nitrogen RE, the RR wetland had better performance on NO_x-N, but the RO wetland had better performance on TON, and they had almost the same performance on NH_4-N and TN.

The comparison between event RE of TN and TP with the relevant HRT, HLR, and rainfall depths are shown in Figure 5-19. In the relatively dry year 2018, the RE of TN and TP exhibited the same fluctuations as HLR in both wetlands. The RE-TN by the RO wetland in events with high rainfall depths was lower than in other events (Figure 5-19d), indicating the nitrogen removal in the RO wetland could be susceptible to rainfall. The RE-TP by the RO wetland was almost stable during the two-year seasons, being the same as RE-TN in 2018 and higher than RE-TN in 2019 (Figure 5-19d). The RE of TN and TP by the RR wetland varied widely in both years, showing almost the same values in 2019 but higher RE-TN than RE-TP in 2018 (Figure 5-19b). In addition to the low or ineffective flow volume reductions, the high negative RE-TP in the RR wetland and RE-TN in the RO wetland could be partially attributed to the existing low inflow concentrations (Figure 5-17 and Figure 5-18).

Table 5-1. Summary of event removal efficiencies of nutrients, n is the observed stormwater events.

Site	/	Flow Reduction	NH_4-N	NO_x-N	TON	TN	TRP	TP
	median (%)	11.9	71.4	94.6	-4.2	41.6	-42.4	41.9
RR	**Mean (%)**	12.8	63.7	87.9	-12.9	34.1	-131.8	12.8
n = 12	**Min (%)**	-28.4	-13.2	35.4	-196.7	-68.6	-691.8	-160.0
	Max (%)	67.7	94.4	99.1	99.9	98.4	78.5	80.3
	median (%)	39.7	74.1	59.3	34.2	44.2	64.9	80.1
RO	**Mean (%)**	29.0	62.4	24.5	17.5	31.5	62.2	77.4
n = 14	**Min (%)**	-33.9	-18.7	-153.8	-141.2	-104.1	30.7	29.9
	Max (%)	75.0	94.3	94.7	94.3	93.8	95.6	97.2

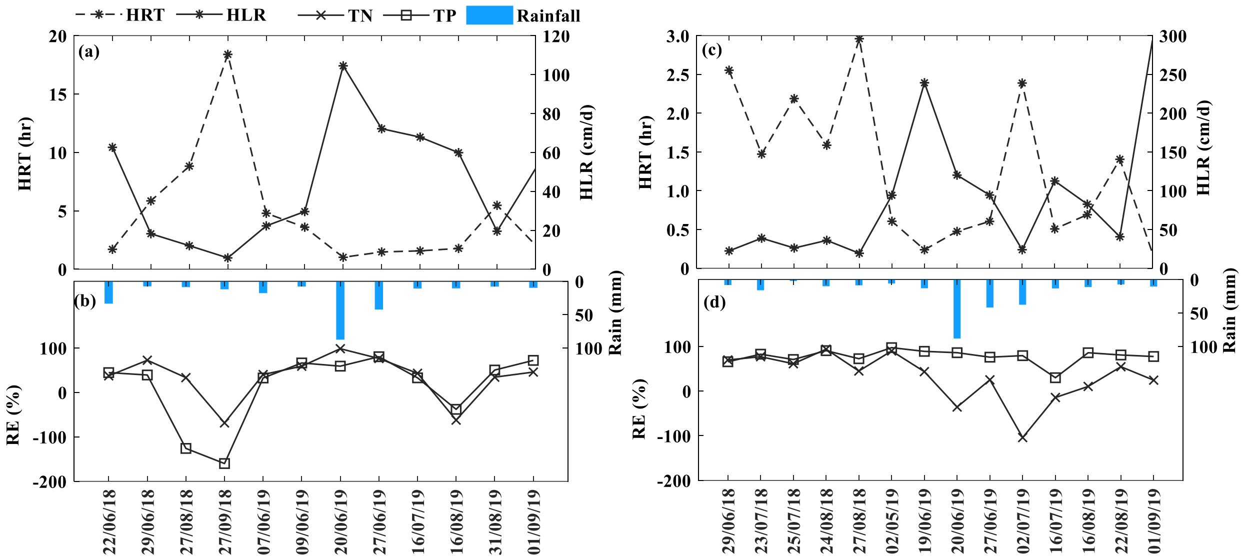

Figure 5-19. Event REs of TN, TP and the relevant HRT, HLR and rainfall depth for the Rocky Ridge wetland (a) and (b) and the Royal Oak wetland (c) and (d).

5.2.2 Annual Reduction

Relative to fully captured events, some events are not fully captured, that is, the samples were only collected from either inflows or outflows in one event, Figure 5-17 and Figure 5-18. To calculate the annual removal rate, all observed mass loads in the outlets and the inlets are summed using the equation 3-8. The performance comparison of the dry and wet season years based on annual nutrient reduction is shown in Table 5-2. Of note, the flow volume reductions by these two wetlands in these two years were almost the same, which indicates the stable hydraulic performance.

The RR wetland had good annual reductions for N, its fractions, and TP in both years, Table 5-2. The RO wetland did not trap nitrogen effectively in both years, except for NH_4-N, but this wetland had good annual performance on phosphorus in both years, Table 5-2. Both wetlands had higher annual reductions of TN and TP in the wet year than the dry year, probably due to the proliferation of vegetation and microbial communities in the wet season (Griffiths et al., 2021). The altered hydrology can shift pond species during wet and dry seasons, which can result in nutrient retention change (Griffiths et al., 2021). However, these reasons remain suppositional given the complex processes in wetlands (Kadlec and Knight, 1996).

According to the annual reductions in Table 5-2, the RR wetland exhibited better performance in removing nitrogen and its fractions than the RO wetland in both years. The RO wetland performed better on TP and TRP than the RR wetland in both years, and it had almost the same phosphorus annual reductions of TP and TRP in the two years, Table 5-2. The RR wetland acted as a TRP source in 2018, while the RO wetland acted as a NO_x-N source in the dry year 2018. Besides, the observed annual TN and TP retention were 3.57 kg-N·ha^{-1}·yr^{-1} and 0.28 kg-P·ha^{-1}·yr^{-1} in 2018 and 39.60 kg-N·ha^{-1}·yr^{-1} and 2.84 kg-P·ha^{-1}·yr^{-1} in 2019 by the RR wetland, and they were 2.43 kg-N·ha^{-1}·yr^{-1} and 0.37 kg-P·ha^{-1}·yr^{-1} in 2018 and 3.51 kg-N·ha^{-1}·yr^{-1} and 5.36 kg-P·ha^{-1}·yr^{-1} in 2019 by the RO wetland, respectively.

The results were compared to Mitsch et al. (2000), who suggested that the sustainable annual removal rates would be 100 – 400 kg-N·ha^{-1}·yr^{-1} and 5 – 50 kg-P·ha^{-1}·yr^{-1}, provided they are optimal locations with adapted design. Besides, the aforementioned Land et al. (2016) reviewed that the median annual removal rates of TN and TP are 930 and 12 kg·ha^{-1}·yr^{-1}, respectively. The annual removal rates of TN and TP of the RR wetland were much lower than the database in both years. However, the annual removal rates of TN and TP are highly variable because they depend on the nutrient forms in the inflow and in-pond conditions (Knight, 1994; Richardson et al., 1997; Land et al., 2016). The absolute mass removal rate of TN and TP have consistently been found to correlate with mass loading rates (Knight, 1994; Richardson et al., 1997). TN and TP could still be removed effectively from both wetlands. The inflows to these two wetlands were relatively clean (Figure 5-17 and Figure 5-18), as aforementioned discussed in section 5.1.3. The phosphorus retention percent of annual inputs from stormwater runoff was 47.0% in 2018 and 66.8% in 2019 by the RR wetland and were 84.1% in 2018 and 83.1% in 2019 by the RO wetland (Table 5 – 2), respectively. The RR wetland could trap TN effectively, with an annual retention percentage of 59.7% in 2018 and 70.1% in 2019, and the RO wetland had annual TN removal efficiency of 48.6% in 2018 and 10.9% in 2019 (Table 5 – 2). It can be concluded that both wetlands can have better performance on nutrients in wet year, and the RR can have better nitrogen performance while the RO can have better performance on phosphorus.

Table 5-2. Summary of annual reductions for nutrients, in/out means the stormwater events in the pipe inlet and the outlet.

Site-Year	Storm Events	Volume pipe In (m^3)	Volume weir/orifice Out (m^3)	Volume Reductions (%)	Rainfall (mm)	Annual Reductions of Nutrients
RR-2018	**in = 10; out = 9**	2652.5	1920.8	27.6	204.6	TN = 59.7%; NH_4-N = 64.4%; NO_x-N = 91.8%; TON = 36.4%; TP = 47.0%; TRP = -287.9%;
RR-2019	**in = 11; out = 11**	15333.7	10773.3	29.7	402.8	TN = 70.1%; NH_4-N = 81.9%; NO_x-N = 96.6%; TON = 23.0%; TP = 66.8%; TRP = 59.3%; TDP = 37.9%;
RO-2018	**in = 6; out = 6**	3070.8	2437.6	20.6	221.8	TN = 48.6%; NH_4-N = 78.5%; NO_x-N = 50.4%; TON = 56.9%; TP = 84.1%; TRP = 64.9%;
RO-2019	**in = 11; out = 11**	14135.6	10866.2	23.1	414.4	TN = 10.9%; NH_4-N = 55.5%; NO_x-N = -52.3%; TON = 13.8%; TP = 83.1%; TRP = 65.3%; TDP = 35.9%;

5.3 Pond Environmental Conditions

Rocky Ridge Wetland

There is no sedimentation forebay in this wetland, and the inlet consists of a sediment vault for the first flush treatment and flow flatten, and of a 750 mm concrete bypass for extreme storm events. There are plenty of submerged plants throughout the wetland. Figure 5-20 and Figure 5-21 show the observed environmental parameters in the pool of the RR wetland.

The water depths increase from the inlet (~ 0.6 m) to the middle (~ 0.70 m), and the outlet (~ 0.75 m) in 2018. While the depths of ~ 0.80 m in the middle are higher than the inlet and outlet which havethe same ~ 0.70 m in 2019, see Secchi depth and Z_{Secchi}:Z_{mix} in Figure 5-20. Nguyen-Quang et al. (2018) states that there is a medium to high risk of harmful algal blooms when Chl-a concentrations > 5µg/L. The occurrences of algal blooms were usually observed in the inlet bottom in 2018, but they were observed in almost all sites in 2019, Figure 5-20. Except for the duration from 3rd July to 13th August in 2019, when algal blooms only occurred in the inlet water column. Most of the mixing depth ratios (Z_{Secchi}:Z_{mix}) were 1.0 during the entire monitoring season, showing that sunlight was frequently available throughout the entire water column. The occasionally low (Z_{Secchi}:Z_{mix}) values coincided with the occurrences of high Chl-a concentrations because of the biogenic turbidity. Slight thermal stratifications were observed from 5th June to 2nd August in 2018, mainly occurring in the inlet and the middle (Figure 5-21, T). While thermal stratifications were only observed in the inlet from 19th June to 30th July in 2019.

The DO concentrations in all sites mainly ranged from 5 – 20 mg/L in 2018 and 3 – 20 mg/L in 2019, respectively, Figure 5-21. Specifically, DO concentrations were different and stratifications were also observed across all the sites on 18th July and on 2nd August in 2018, and the highest DO is in the middle top water. DO concentrations decreased from 5th June to 16th August and then increased during the rest monitoring duration in 2018 almost in all sites. In 2019, DO concentrations experienced an increase from 11th September to 24th October, and they were ununiformly distributed in all sites. Stratifications of DO concentrations were observed frequently in 2019.

pH was ~ 9.0 – 10.5 in 2018 and it was ~ 9.0 – 10.0 in 2019 in the water column, Figure 5-21. In 2018, the pH of the middle and outlet increased from ~ 10.5 on 5th June to ~ 11 on 18th July and then declined to ~ 9 on 13th September, before gradually increasing to ~ 9.5 on 24th October 2018. pH was almost the same across all the sites from 30th August to 24th October. pH in the inlet had stratifications and it was lower than the other sites from 21st June to 2nd August. In 2019, pH was almost uniform in the pond, and it had an increased tendency from 7th May to 19th June, and from 11th September to 9th October.

Temperature (T) was variable over seasonal gradients, ranging within 4 – 24 °C in this wetland in both years, Figure 5-21. Occasional thermal stratifications were observed in the inlet on 21st June 2018, 19th June 2019, 3rd July 2019, and 30th July 2019.

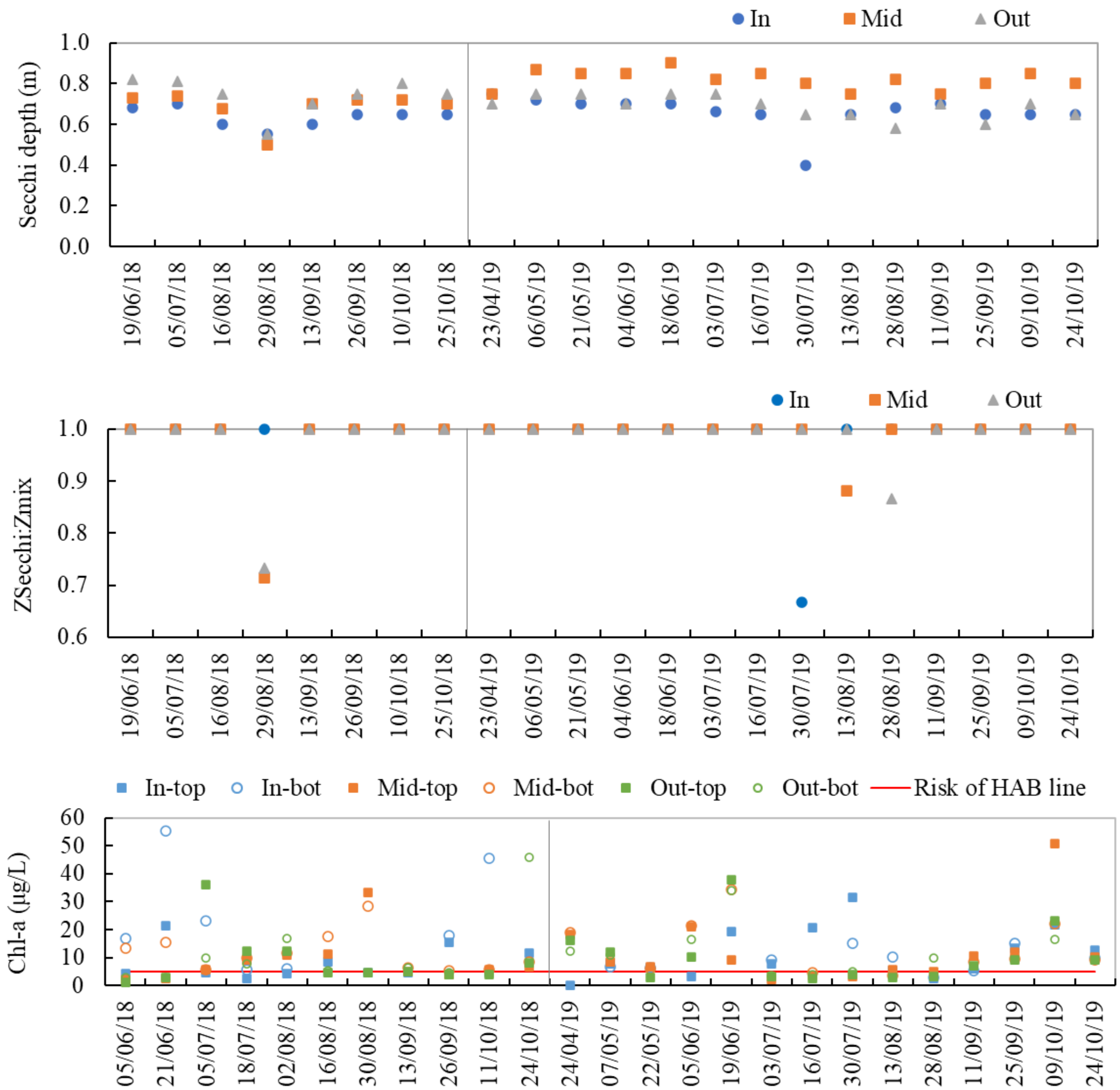

Figure 5-20. The environmental parameters in the pond of the Rocky Ridge wetland for Secchi depth and Chl-a; In, Mid, and Out are the in-pond sampling locations (inlet, middle, outlet); top and bot are the sampling top layer and bottom layer. Z_{secchi} is Secchi depth and Z_{mix} is water column depth.

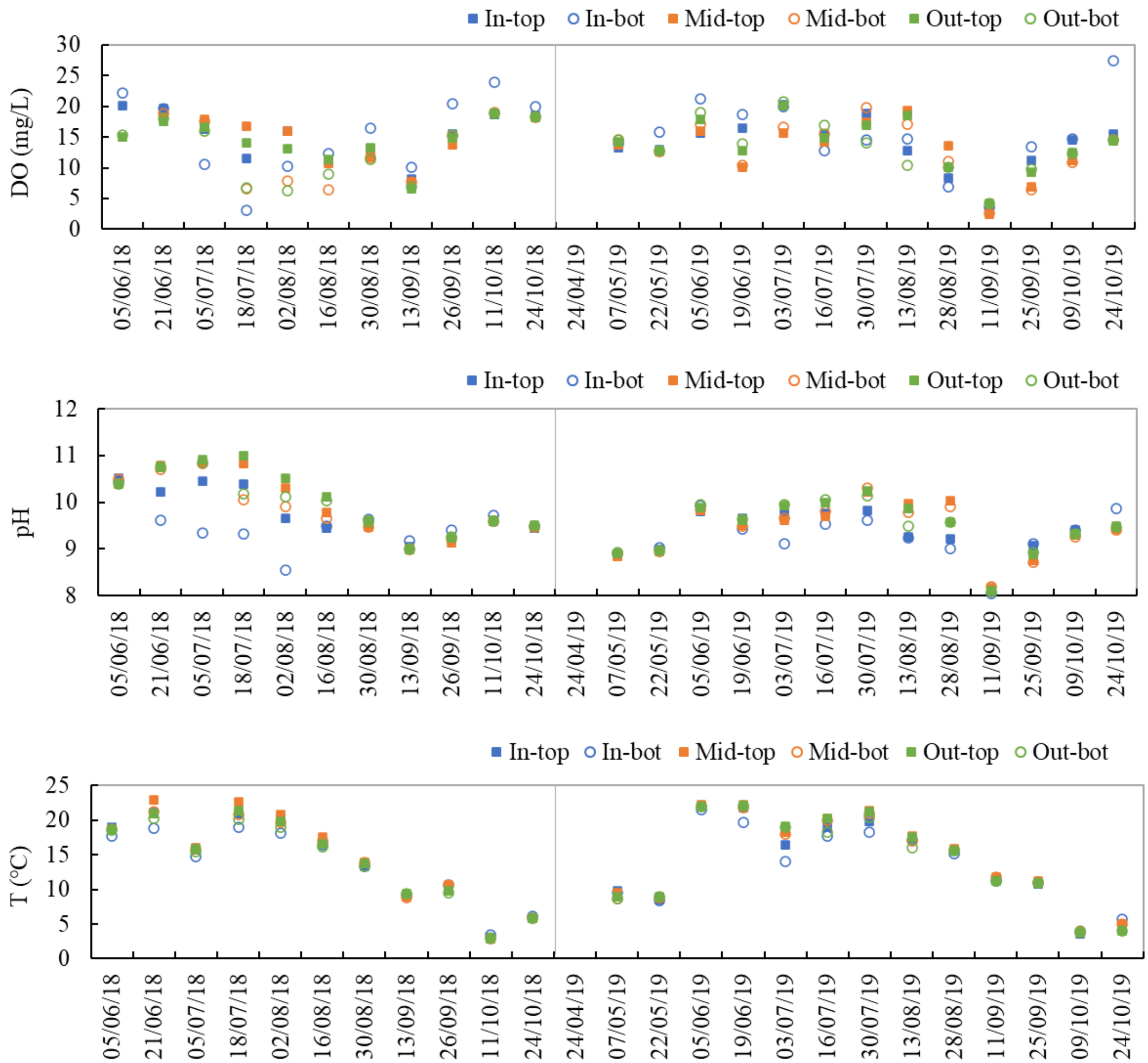

Figure 5-21. The environmental parameters in the pond of the Rocky Ridge wetland for DO, pH, and T; In, Mid, and Out are the in-pond sampling locations (inlet, middle, outlet); top and bot are the sampling top layer and bottom layer.

According to Kendall's Tau_b analysis results, which are summarized in Table 5-3 and Table 5-4 for nitrogen. In 2018, TN exhibited high positive correlations with TP, DOC, TOC, and COD in the middle and the outlet, and it also had a negative correlation with DO in the middle, Table 5-3. Organic nitrogen was positively correlated with COD but was negatively correlated with DO in the middle and the outlet. Besides, organic nitrogen was positively correlated with organic carbon in almost all sites and TDN had a negative correlation with Si in the middle. NO_x-N negatively correlated with dissolved carbon and Ca in all sites. In 2019, TN, PN, and TON had positive correlations with TP in the inlet and the outlet, and TON had a positive correlation with organic carbon in almost all sites, Table 5-4. Chl-a was positively correlated with PN in all sites and with TN in the inlet. COD had positive correlations with TN and TON in the inlet and the outlet. Mn was positively correlated with organic nitrogen in the inlet and with PN in the outlet. Fe was also positively correlated with PN in the outlet. Ca was negatively correlated with DON in the outlet. Besides, TN also had a positive correlation with COD in almost all sites.

For phosphorus, the results are summarized in Table 5-5 and Table 5-6. In 2018, Chl-a was positively correlated with TP, TDP, and TRP in the middle, Table 5-5. pH was negatively correlated with TDP in the inlet. DO had negative correlations with TP, TDP, and TRP in the middle and the outlet. COD had positive correlations with almost all phosphorus forms in the middle and the outlet. Organic carbon had positive correlations with TP, TDP, and TRP in all locations. Si had negative correlations with all phosphorus forms in the middle while it had a negative correlation with PP in the outlet. Ca had a positive correlation with TP, TDP, and TRP in the inlet. In 2019, TP had positive correlations with Chl-a, Mn, and Fe in all sites, Table 5-6. Organic carbon had a positive correlation with TDP, and COD had a positive correlation with TDP in all sites. TRP had a negative correlation with DO in the outlet.

Table 5-3. Correlation analysis results for nitrogen of the Rocky Ridge wetland in 2018. Red color is significant at the 0.01 level (2-tailed); blue color is significant at the 0.05 level (2-tailed); In, Mid, and Out are the in-pond sampling locations (inlet, middle, outlet).

In-Kendall's tau_b Correlations															
	TSS	**TP**	**DIC**	**DOC**	**TDC**	**TOC**	**Ca**	**Fe**	**Mn**	**Si**	**COD**	**DO**	**pH**	**T (°C)**	**Chla μg/L**
TN	0.037	0.353	0.397	0.222	0.406	0.406	0.338	0.118	0.118	0.362	0.24	-0.221	-0.426	-0.338	-0.162
TDN	0.007	0.265	0.368	0.267	0.421	0.465	0.309	-0.059	-0.029	0.125	0.224	-0.279	-0.279	-0.309	-0.103
PN	-0.007	-0.118	-0.191	-0.237	-0.214	-0.229	-0.191	0.059	0.059	0.185	-0.116	0.162	0.279	0.132	-0.162
NH_4-N	0.13	-0.104	-0.152	-0.282	-0.177	-0.353	-0.152	-0.12	-0.056	0.008	-0.387	0.232	0.264	0.008	0.232
NO_x-N	0.3	-0.605	-0.621	-0.519	-0.591	-0.468	-0.605	0.213	-0.131	-0.386	-0.043	-0.164	0.278	0.441	-0.082
TON	0.097	0.368	0.412	0.267	0.435	0.45	0.353	0.074	0.015	0.288	0.255	-0.176	-0.324	-0.353	-0.118
DON	-0.022	0.353	0.397	0.267	0.45	0.465	0.338	-0.059	-0.029	0.125	0.271	-0.25	-0.279	-0.25	-0.162
Mid-Kendall's tau_b Correlations															
	TSS	**TP**	**DIC**	**DOC**	**TDC**	**TOC**	**Ca**	**Fe**	**Mn**	**Si**	**COD**	**DO**	**pH**	**T (°C)**	**Chla μg/L**
TN	-0.047	0.77	0.079	0.612	0.249	0.603	0.013	0.164	0.354	-0.362	0.505	-0.63	-0.066	0.197	0.249
TDN	-0.053	0.564	0.033	0.42	0.229	0.373	0.072	-0.013	0.373	-0.616	0.404	-0.608	-0.046	0.216	0.359
PN	0.047	0.151	-0.21	0.349	-0.013	0.446	-0.223	0.309	-0.079	0.151	0.199	-0.052	0.092	0.026	-0.17
NH_4-N	0.162	-0.087	0.094	-0.196	0.022	-0.152	0.137	-0.044	0.166	0.073	0.015	0.137	-0.226	-0.195	0.325
NO_x-N	0.379	0.167	-0.682	0.095	-0.555	0.174	-0.602	-0.239	-0.333	-0.127	0.08	0.063	0.694	0.492	-0.016
TON	-0.047	0.77	0.079	0.612	0.249	0.603	0.013	0.164	0.354	-0.362	0.505	-0.63	-0.066	0.197	0.249
DON	-0.027	0.538	0.059	0.42	0.255	0.373	0.098	0.013	0.373	-0.59	0.404	-0.608	-0.059	0.216	0.333
Out-Kendall's tau_b Correlations															
	TSS	**TP**	**DIC**	**DOC**	**TDC**	**TOC**	**Ca**	**Fe**	**Mn**	**Si**	**COD**	**DO**	**pH**	**T (°C)**	**Chla μg/L**
TN	0.061	0.746	0.007	0.513	0.139	0.548	0.125	-0.013	0.039	-0.342	0.586	-0.603	0.026	0.157	0.249
TDN	0.195	0.544	0.083	0.301	0.201	0.367	0.189	-0.018	0.112	-0.277	0.536	-0.5	-0.065	0.112	0.418
PN	-0.249	0.139	-0.139	0.171	-0.099	0.152	-0.244	-0.026	-0.171	-0.026	0.047	0	0.236	0.262	-0.38
NH_4-N	0.232	0.146	-0.212	-0.191	-0.159	-0.212	-0.119	-0.206	-0.165	0.046	0.013	0.072	0.204	0.112	0.033
NO_x-N	0.134	0.288	-0.519	0.029	-0.497	0.065	-0.454	-0.311	-0.417	0.101	0.257	-0.229	0.501	0.573	-0.072
TON	0.034	0.719	0.007	0.513	0.165	0.548	0.073	-0.013	0.013	-0.368	0.586	-0.63	0.052	0.184	0.275
DON	0.189	0.525	0.088	0.306	0.206	0.372	0.195	-0.024	0.106	-0.306	0.535	-0.493	-0.059	0.106	0.434

Table 5-4. Correlation analysis results for nitrogen of the Rocky Ridge wetland in 2019. Red color is significant at the 0.01 level (2-tailed); blue color is significant at the 0.05 level (2-tailed); In, Mid, and Out are the in-pond sampling locations (inlet, middle, outlet).

In-Kendall's tau_b Correlations															
	TSS	**TP**	**DIC**	**DOC**	**TDC**	**TOC**	**Ca**	**Fe**	**Mn**	**Si**	**COD**	**DO**	**pH**	**T (°C)**	**Chla µg/L**
TN	0.219	0.523	0.067	0.356	0.159	0.301	-0.032	0.095	0.38	0.254	0.508	0.035	0.286	0.061	0.396
TDN	-0.044	0.412	-0.036	0.396	0.016	0.42	-0.104	0.032	0.23	0.024	0.284	-0.139	0.043	0.121	0.253
PN	0.429	0.391	0.119	0.123	0.234	0.13	0.068	0.147	0.328	0.298	0.471	0.299	0.463	0.03	0.486
NH_4-N	-0.196	-0.072	-0.187	0.358	-0.16	0.445	-0.361	-0.263	-0.103	-0.1	-0.012	-0.208	-0.009	0.226	-0.087
NO_x-N	0.017	0.087	-0.017	-0.17	-0.029	-0.137	0.075	0.046	-0.161	-0.112	-0.138	0.018	-0.1	-0.136	0.054
TON	0.183	0.494	0.087	0.336	0.171	0.265	0.004	0.044	0.399	0.258	0.463	0.03	0.299	0.056	0.415
DON	-0.087	0.383	-0.04	0.462	0.028	0.423	-0.124	-0.044	0.289	0.075	0.311	-0.143	0.074	0.108	0.257
Mid-Kendall's tau_b Correlations															
	TSS	**TP**	**DIC**	**DOC**	**TDC**	**TOC**	**Ca**	**Fe**	**Mn**	**Si**	**COD**	**DO**	**pH**	**T (°C)**	**Chla µg/L**
TN	0.12	0.13	0.072	0.283	0.127	0.413	-0.054	0.047	0.094	0.087	0.352	-0.074	-0.013	-0.212	0.29
TDN	-0.069	0.138	-0.21	0.551	-0.091	0.493	-0.309	0.018	0.072	0.022	0.161	-0.177	0.056	0.082	0.007
PN	0.284	0.142	0.279	-0.113	0.276	0.062	0.211	0.131	0.171	0.192	0.158	0.035	-0.026	-0.295	0.403
NH_4-N	-0.059	-0.102	-0.102	0.241	-0.077	0.19	-0.172	-0.245	-0.153	-0.073	-0.103	-0.226	-0.26	-0.217	-0.161
NO_x-N	-0.13	-0.102	0.111	-0.223	0.033	-0.241	0.121	-0.042	-0.241	-0.251	-0.16	-0.023	0.012	0.059	-0.065
TON	0.142	0.152	0.065	0.275	0.12	0.406	-0.033	0.069	0.116	0.123	0.322	-0.048	-0.004	-0.203	0.297
DON	-0.069	0.123	-0.225	0.551	-0.105	0.478	-0.309	0.004	0.058	0.036	0.161	-0.16	0.074	0.065	-0.007
Out-Kendall's tau_b Correlations															
	TSS	**TP**	**DIC**	**DOC**	**TDC**	**TOC**	**Ca**	**Fe**	**Mn**	**Si**	**COD**	**DO**	**pH**	**T (°C)**	**Chla µg/L**
TN	0.036	0.464	-0.007	0.49	0.13	0.497	-0.044	0.163	0.189	-0.08	0.385	-0.177	0.022	0.169	0.328
TDN	-0.317	0.127	-0.179	0.669	-0.083	0.611	-0.383	-0.218	-0.069	-0.106	0.301	-0.217	0.2	0.312	-0.036
PN	0.305	0.565	0.305	0.069	0.406	0.134	0.291	0.454	0.509	0.196	0.187	-0.255	-0.248	-0.1	0.502
NH_4-N	0.088	-0.08	-0.073	0.201	0	0.267	-0.242	-0.128	-0.007	0.103	0.1	-0.074	0.206	0.1	-0.06
NO_x-N	0.061	0.315	0.242	-0.009	0.272	0.086	0.234	0.216	0.294	0.048	0.114	-0.303	-0.166	-0.048	0.343
TON	0.036	0.478	0.007	0.49	0.145	0.497	-0.044	0.149	0.204	-0.08	0.385	-0.186	0.013	0.177	0.328
DON	-0.32	0.101	-0.24	0.65	-0.145	0.592	-0.415	-0.243	-0.116	-0.116	0.268	-0.152	0.239	0.368	-0.059

Table 5-5. Correlation analysis results for phosphorous of the Rocky Ridge wetland in 2018. Red color is significant at the 0.01 level (2-tailed); blue color is significant at the 0.05 level (2-tailed); In, Mid, and Out are the in-pond sampling locations (inlet, middle, outlet).

	TSS	TN	DIC	DOC	TDC	TOC	Ca	Fe	Mn	Si	COD	DO	pH	T (°C)	Chla μg/L
In-Kendall's tau_b Correlations															
TP	-0.28	0.353	0.544	0.37	0.554	0.45	0.515	-0.06	0.382	0.362	0.271	-0.16	-0.46	-0.4	0.015
TDP	-0.34	0.324	0.485	0.459	0.539	0.48	0.485	0.029	0.353	0.125	0.317	-0.4	-0.49	-0.28	-0.015
PP	0.307	0.059	-0.16	-0.34	-0.19	-0.35	-0.13	0.059	-0.09	0.066	-0.21	0.074	0.103	0.044	-0.044
TRP	-0.49	0.306	0.657	0.631	0.682	0.59	0.657	-0.08	0.351	0.23	0.305	-0.18	-0.43	-0.35	0.076
Mid-Kendall's tau_b Correlations															
	TSS	**TN**	**DIC**	**DOC**	**TDC**	**TOC**	**Ca**	**Fe**	**Mn**	**Si**	**COD**	**DO**	**pH**	**T (°C)**	**Chla μg/L**
TP	-0.03	0.77	0.052	0.586	0.223	0.564	-0.04	0.046	0.249	-0.47	0.625	-0.58	0	0.223	0.485
TDP	-0.06	0.743	0.066	0.612	0.262	0.59	-0.03	0.007	0.223	-0.51	0.598	-0.56	0.013	0.262	0.511
PP	0.113	0.428	-0.01	0.507	0.157	0.472	-0.13	0.007	0.118	-0.52	0.571	-0.33	-0.01	0.289	0.328
TRP	-0.08	0.734	0.007	0.616	0.203	0.608	-0.06	-0.01	0.268	-0.56	0.563	-0.53	-0.02	0.242	0.464
Out-Kendall's tau_b Correlations															
	TSS	**TN**	**DIC**	**DOC**	**TDC**	**TOC**	**Ca**	**Fe**	**Mn**	**Si**	**COD**	**DO**	**pH**	**T (°C)**	**Chla μg/L**
TP	-0.01	0.746	0.083	0.49	0.178	0.509	0.13	0.065	0.112	-0.31	0.566	-0.62	-0.07	0.112	0.194
TDP	0	0.706	0.071	0.49	0.189	0.509	0.166	0.03	0.112	-0.24	0.578	-0.65	-0.09	0.1	0.253
PP	-0.16	0.25	-0.11	0.176	-0.05	0.171	-0.2	-0.1	-0.19	-0.51	0.162	-0.18	0.235	0.235	-0.094
TRP	-0.02	0.632	0.195	0.529	0.313	0.572	0.265	0.13	0.212	-0.29	0.559	-0.62	-0.19	-0.02	0.258

Table 5-6. Correlation analysis results for phosphorous of the Rocky Ridge wetland in 2019. Red color is significant at the 0.01 level (2-tailed); blue color is significant at the 0.05 level (2-tailed); In, Mid, and Out are the in-pond sampling locations (inlet, middle, outlet).

	TSS	TN	DIC	DOC	TDC	TOC	Ca	Fe	Mn	Si	COD	DO	pH	T (°C)	Chla μg/L
In-Kendall's tau_b Correlations															
TP	0.111	0.523	0.087	0.241	0.21	0.296	0.02	0.321	0.399	0.298	0.407	-0.01	0.048	0.065	0.415
TDP	-0.24	0.42	0.143	0.47	0.274	0.431	-0.15	0.083	0.36	0.242	0.351	-0.2	-0.02	0.065	0.123
PP	0.437	0.349	0.04	-0.1	0.107	0.036	0.155	0.401	0.186	0.123	0.279	0.299	0.203	-0.04	0.518
TRP	-0.42	0.167	0.072	0.377	0.195	0.226	-0.16	-0.2	0.329	0.187	0.144	-0.3	-0.1	0.074	-0.012
Mid-Kendall's tau_b Correlations															
	TSS	**TN**	**DIC**	**DOC**	**TDC**	**TOC**	**Ca**	**Fe**	**Mn**	**Si**	**COD**	**DO**	**pH**	**T (°C)**	**Chla μg/L**
TP	0.301	0.13	0.159	0.312	0.338	0.384	0.127	0.519	0.529	0.275	0.293	-0.26	-0.2	0.1	0.464
TDP	0.051	0.316	-0.07	0.613	0.109	0.584	-0.11	0.255	0.279	0.185	0.437	-0.15	0	0.113	0.243
PP	0.509	0.083	0.236	-0.03	0.32	0.105	0.262	0.531	0.461	0.243	0.062	-0.25	-0.24	-0.13	0.483
TRP	-0.02	0.033	-0.03	0.352	0.145	0.229	-0.01	0.233	0.272	0.127	0.092	-0.22	-0.09	0.156	0.025
Out-Kendall's tau_b Correlations															
	TSS	**TN**	**DIC**	**DOC**	**TDC**	**TOC**	**Ca**	**Fe**	**Mn**	**Si**	**COD**	**DO**	**pH**	**T (°C)**	**Chla μg/L**
TP	0.225	0.464	0.327	0.2	0.42	0.279	0.196	0.454	0.575	0.211	0.224	-0.27	-0.18	0.039	0.573
TDP	-0.21	0.403	0.237	0.465	0.287	0.487	0.018	0.131	0.222	0.084	0.515	-0.37	-0.19	0.043	0.238
PP	0.495	0.312	0.247	-0.04	0.283	0.069	0.204	0.49	0.48	0.218	0.011	-0.09	-0.08	0.117	0.51
TRP	-0.22	0.268	0.102	0.265	0.196	0.272	0.182	0.011	0.247	-0.01	0.128	-0.47	-0.23	0.013	0.123

Royal Oak Wetland

The observed environmental parameters in the pool of the RO wetland are shown in Figure 5-22 and Figure 5-23. The depth decreased from the inlet (~ 1.2 m) to the middle (~ 0.9 m in 2018, ~

0.7 m in 2019) to the outlet (~ 0.6 m) in the pool, see Secchi depth and Z_{Secchi}:Z_{mix} in Figure 5-22. A sedimentation forebay is in the front of the inlet pipe, and the transparency of the inlet was low occasionally, see Z_{Secchi}:Z_{mix} in Figure 5-22. Most of the mixing depth ratios (Z_{Secchi}:Z_{mix}) were 1.0 across all the sampling sites over the whole study season, showing that light availability extends throughout the entire mixed layer in this wetland. High concentrations of Chl-a mainly occurred occasionally in the middle bottom and the outlet site in 2018 and in the outlet in 2019, respectively. The occurrences of algal blooms were not as frequent as in the RR wetland. In wetlands, algal photosynthesis can be suppressed with dense covers of emergent macrophytes, mainly due to the light limitations resulting from shadows of aquatic macrophytes and nutrient limitations resulting from competition with aquatic macrophytes (Kadlec and Knight, 1996).

DO and pH can be directly affected by aquatic plants' photosynthesis/respiration in wetlands (Kadlec and Knight, 1996). Across the whole pool, the ranges of DO concentration were ~ 4 – 25 mg/L in 2018 and 3 – 20 mg/L in 2019 (Figure 5-23, DO), and pH were 7 – 9 in 2018 and 7.5 – 9 in 2019 (Figure 5-23, pH), respectively. The DO concentration and pH decreased from the monitoring beginning (21st June 2018, 7th May 2019) then gradually increased from middle August (16th in 2018, 13th in 2019) until the monitoring ended in late October. The DO concentrations in the outlet tended to be lower than in the other sites frequently during these two study seasons. The bottom water usually had slightly higher DO concentrations than the top water in the middle and the outlet, especially in 2018. The middle had higher pH while the inlet bottom had a lower pH in both years. The outlet had lower pH than the middle and the inlet top water but had almost the same as the inlet bottom in both years.

Temperature (T) was variable over seasonal gradients, ranging from 4 – 24 °C in this wetland in both years, Figure 5-23 (T). No thermal stratification was observed in the middle, but occasional thermal stratifications were observed in the inlet during six fieldwork trips, they were on 21st June 2018, 18th July 2018, 5th June 2019, 19th June 2019, 3rd July 2019, and 9th October 2019. No T differences were observed between the middle water column and the inlet top water, but T in the outlet was slightly lower than the other sites in both years.

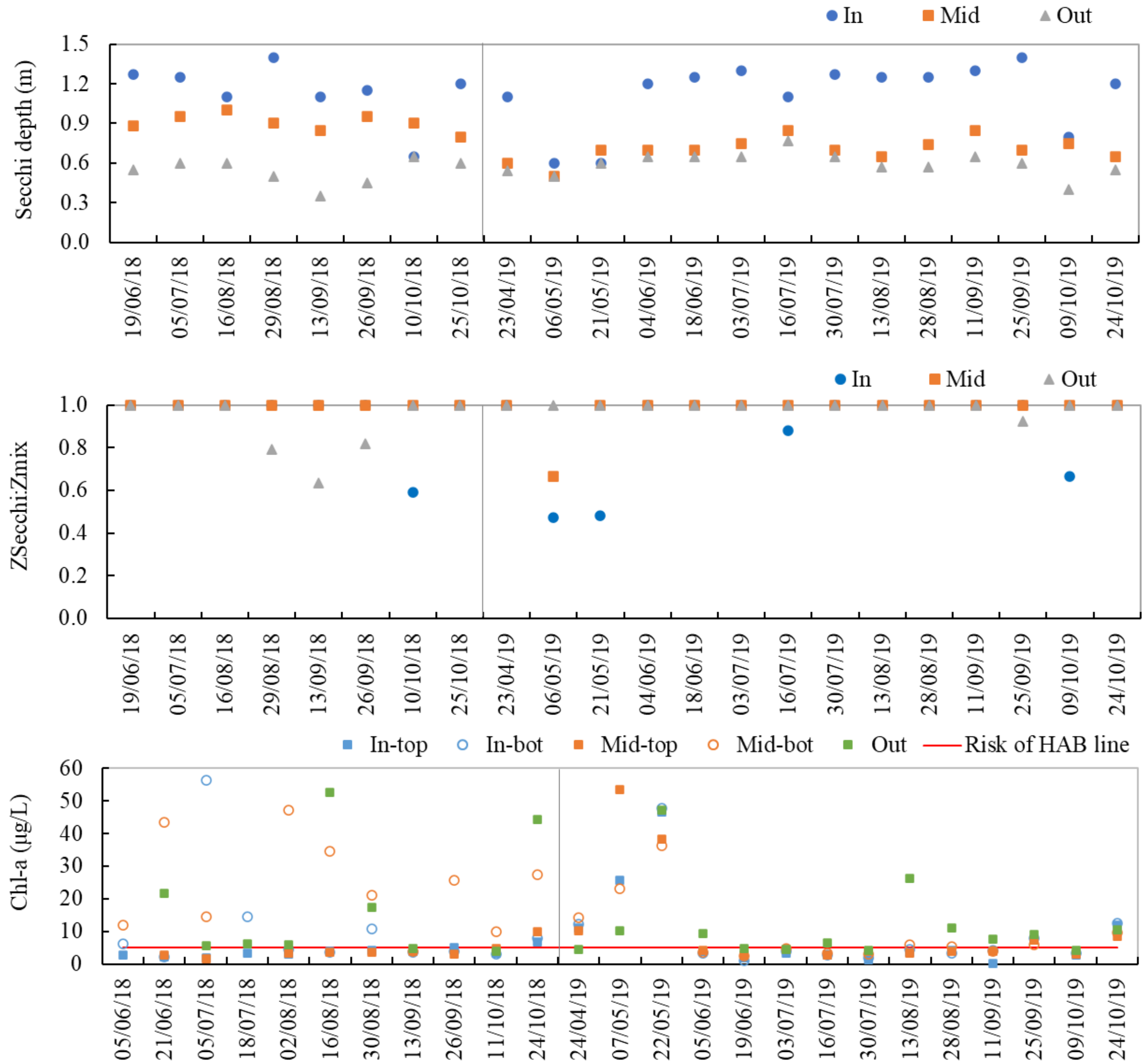

Figure 5-22. The environmental parameters in the pond of the Royal Oak wetland for Secchi depth and Chl-a;In, Mid, Out are the in-pond sampling locations (inlet, middle, outlet); top, bot is the sampling top layer and bottom layer. Z_{secchi} is Secchi depth and Z_{mix} is water column depth.

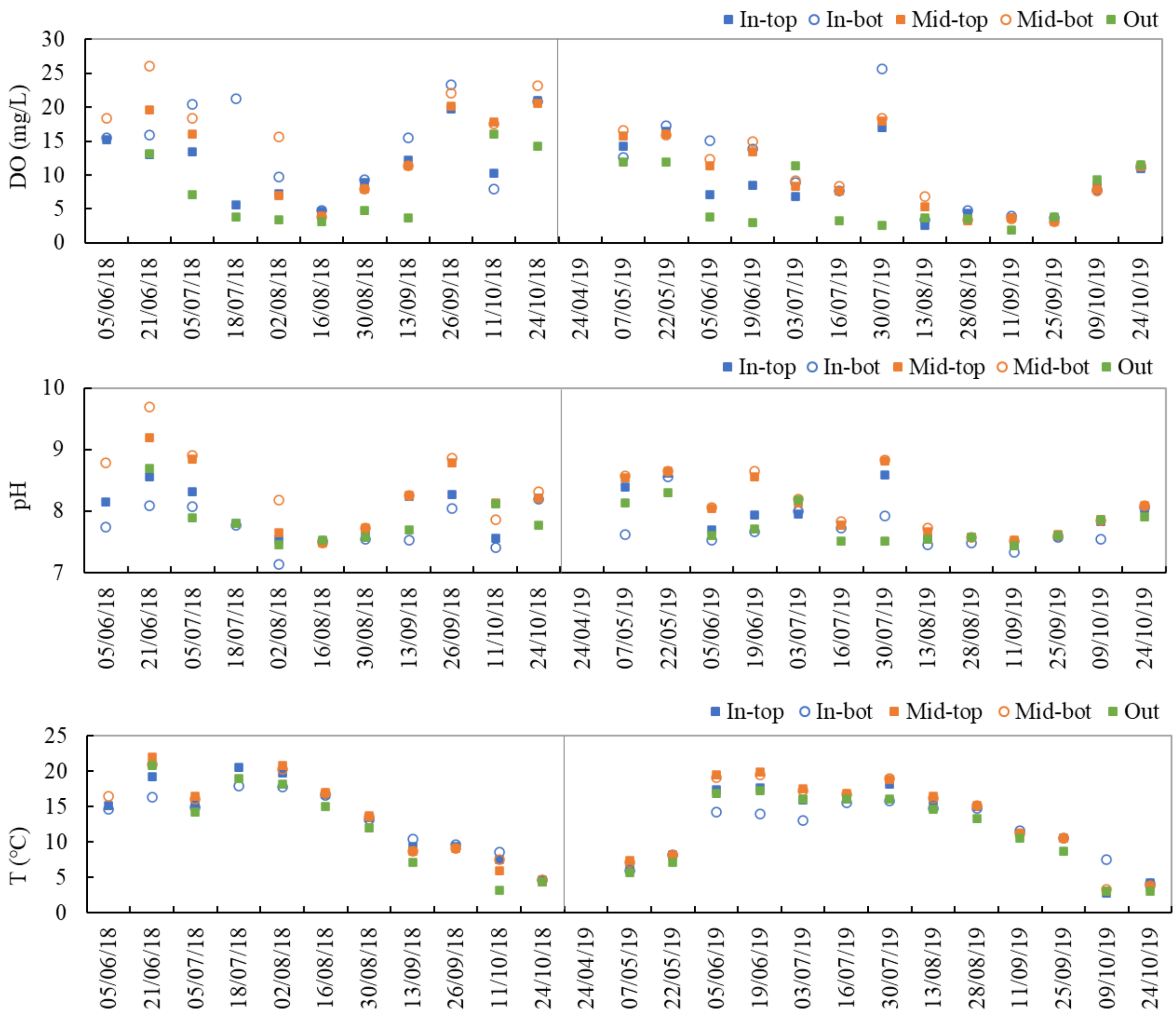

Figure 5-23.The environmental parameters in the pond of the Royal Oak wetland for DO, pH, and T; In, Mid, Out are the in-pond sampling locations (inlet, middle, outlet); top, bot is the sampling top layer and bottom layer.

The correlation analysis results are summarized in Table 5-7 and Table 5-8 for nitrogen. In 2018 (Table 5-7), NH_4-N exhibited negative correlations with DO and pH in the inlet and the middle. TON had positive correlations with T and organic carbon in all locations. Fe correlated with TN in the inlet, and Mn correlated with NH_4-N in the inlet top and the middle, respectively. Of note, high iron concentrations can be favourable for DNRA (Burgin and Hamilton 2007; Kessler, 2018). In 2019 (Table 5-8), TN exhibited a high positive correlation with TP but a negative correlation with T in the middle. and Chl-a correlated with TN and PN positively in this site as well. Besides, in the middle, NH_4-N showed negative correlations with DO and pH but positive correlations with Mn and Si; TON had a slight correlation with DO while PN and NO_x-N had negative correlations with Si. These results possibly indicate that alga grew well in the middle site in 2019. NH_4-N was related to Si positively in the inlet bottom and the outlet, and it also negatively correlated with DO in the inlet bottom.

The correlation analysis results are summarized in Table 5-9 and Table 5-10 for phosphorus. In 2018 (Table 5-9), TP had high correlations with Fe in the inlet top and the middle, with Mn in all sites, and with T and organic carbon in the outlet, respectively. TP also exhibited a correlation with dissolved organic carbon in the middle and the outlet. TDP had a positive correlation with DO but a negative correlation with pH in the inlet middle, while TRP exhibited a positive correlation with DO but a negative correlation with pH in the inlet bottom and the outlet. TRP also had positive correlations with Fe and Mn in the inlet and the middle. In 2019 (Table 5-10), in the inlet, TDP was negatively correlated with DO and pH, but it positively correlated with Mn at the bottom of the inlet. Fe correlated with TRP positively in the bottom of the inlet, showing possible co-precipitation or dissolution occurred there. Some melic parameters, like Al, Fe, Ca, and Mn, were related to phosphorus adsorption/desorption and precipitation/dissolution (Reddy and D'Angelo, 1994). These precipitation processes typically occurred at high concentrations of either phosphate or the metalloid cations, under some circumstances but may re-dissolve under altered conditions (Kadlec and Knight, 1996; Rhue and Harris, 1999). TP had a positive correlation with TN and Chl-a had a negative correlation with T in the middle. Meanwhile, Chl-a correlated with PP positively in this site. Additionally, TRP and TDP exhibited negative correlations with pH, DO, and COD but positive correlations with Si, and Mn in the middle. There were almost no significant correlations that had been tested in the outlet.

Table 5-7. correlation analysis results for Nitrogen of the Royal Oak wetland in 2018. Red color is significant at the 0.01 level (2-tailed); blue color is significant at the 0.05 level (2-tailed); In, Mid, and Out are the in-pond sampling locations (inlet, middle, outlet); top and bot are the sampling top layer and bottom layer.

In-top-Kendall's tau_b Correlations															
	TSS	**TP**	**DIC**	**DOC**	**TDC**	**TOC**	**Ca**	**Fe**	**Mn**	**Si**	**COD**	**DO**	**pH**	**T (°C)**	**Chl-a µg/L**
TN	0.17	0.404	-0.114	0.187	-0.13	0.037	0	0.611	0.477	-0.404	0.094	-0.183	-0.257	0.294	-0.147
TDN	0	0.345	0.245	0.019	0.22	-0.018	0.2	0.404	0.345	-0.055	-0.112	-0.2	-0.345	0.091	0.2
PN	0.262	0.018	-0.623	0.241	-0.624	0.164	-0.273	0.037	0.091	-0.455	0.262	0.055	0.055	0.273	-0.564
NH_4-N	0.037	0.418	0.094	0.13	0.073	0.127	0.055	0.477	0.636	-0.273	0.112	-0.491	-0.564	0.236	-0.018
NO_x-N	0.094	-0.44	-0.152	-0.486	-0.204	-0.44	0.22	-0.315	-0.22	0.11	-0.321	0.44	0.037	-0.404	0.073
TON	0.224	0.491	-0.472	0.833	-0.404	0.709	-0.527	0.55	0.345	-0.636	0.374	-0.273	0.018	0.818	-0.527
DON	-0.037	0.382	0.245	0.315	0.294	0.309	-0.127	0.44	0.164	-0.018	-0.037	-0.309	-0.091	0.273	0.091
In-bottom-Kendall's tau_b Correlations															
	TSS	**TP**	**DIC**	**DOC**	**TDC**	**TOC**	**Ca**	**Fe**	**Mn**	**Si**	**COD**	**DO**	**pH**	**T (°C)**	**Chl-a µg/L**
TN	0.261	0.164	0.018	0.236	0.055	0.491	0.055	0.734	0.455	-0.127	0.187	-0.236	-0.564	0.309	-0.273
TDN	0.221	0.2	-0.018	0.2	0.018	0.455	0.018	0.697	0.491	-0.091	0.224	-0.273	-0.527	0.273	-0.309
PN	0.101	-0.055	-0.273	0.236	-0.309	0.127	-0.018	-0.073	0.018	-0.2	0	-0.018	-0.127	0.164	-0.2
NH_4-N	0.181	0.491	-0.018	0.055	0.091	0.236	0.018	0.587	0.564	-0.164	0.262	-0.564	-0.891	0.127	-0.164
NO_x-N	0.06	0.055	0.127	-0.018	0.091	0.164	0.091	0.404	0.491	0.055	0.037	-0.345	-0.455	0.127	-0.6
TON	0.06	-0.091	0.055	0.709	0.091	0.6	-0.127	0.11	-0.091	-0.309	-0.075	0.236	0.055	0.564	0.2
DON	-0.06	-0.018	0.345	0.418	0.382	0.455	-0.127	0.183	-0.018	-0.091	-0.075	0.236	-0.018	0.418	0.273
Mid-Kendall's tau_b Correlations															
	TSS	**TP**	**DIC**	**DOC**	**TDC**	**TOC**	**Ca**	**Fe**	**Mn**	**Si**	**COD**	**DO**	**pH**	**T (°C)**	**Chl-a µg/L**
TN	0.329	0.427	0.305	0.033	0.358	-0.034	-0.033	0.211	0.377	-0.129	0.01	-0.193	-0.488	-0.135	0.029
TDN	0.207	0.281	0.421	-0.11	0.417	-0.189	0.091	0.154	0.321	0.005	-0.063	-0.235	-0.578	-0.282	0.129
PN	0.139	0.074	-0.377	0.268	-0.287	0.338	-0.191	0.197	0.22	-0.278	0.122	0.059	0.177	0.258	-0.094
NH_4-N	0.11	0.311	0.155	0.102	0.228	0.02	0.228	0.408	0.697	-0.102	0.094	-0.518	-0.689	0.065	0.125
NO_x-N	0.163	0.146	0.242	-0.313	0.207	-0.346	0.111	-0.03	0.091	0.055	-0.159	-0.048	-0.316	-0.399	0.133
TON	-0.01	0.164	-0.21	0.606	-0.1	0.593	-0.358	0.364	0.072	-0.377	0.35	-0.053	0.194	0.45	-0.181
DON	-0.062	0.227	0.162	0.339	0.253	0.304	-0.215	0.249	0.024	-0.215	0.204	-0.205	-0.1	0.018	0.041
Out-Kendall's tau_b Correlations															
	TSS	**TP**	**DIC**	**DOC**	**TDC**	**TOC**	**Ca**	**Fe**	**Mn**	**Si**	**COD**	**DO**	**pH**	**T (°C)**	**Chl-a µg/L**
TN	0.023	0.6	-0.467	0.689	-0.333	0.674	-0.111	0.244	0.422	-0.156	0.449	-0.222	0.056	0.833	0.278
TDN	0.159	0.422	-0.111	0.511	0.111	0.494	-0.022	-0.022	0.244	-0.422	0.18	-0.556	-0.389	0.5	0.056
PN	0.023	0.422	-0.556	0.6	-0.422	0.584	-0.022	0.067	0.244	0.022	0.629	0	0.167	0.722	0.167
NH_4-N	0.44	-0.119	0.119	-0.024	0.119	-0.048	0.119	0.501	0.167	0.167	-0.048	0.183	-0.122	-0.243	0.365
NO_x-N	-0.147	0.201	-0.602	0.43	-0.43	0.435	-0.717	-0.258	0.143	-0.43	0.058	-0.035	0.035	0.174	-0.382
TON	-0.023	0.556	-0.511	0.733	-0.378	0.719	-0.156	0.2	0.378	-0.111	0.494	-0.167	0.111	0.778	0.222
DON	0.068	0.422	-0.2	0.511	0.022	0.494	-0.022	-0.022	0.244	-0.422	0.18	-0.611	-0.333	0.556	0.111

Table 5-8. correlation analysis results for Nitrogen of the Royal Oak wetland in 2019. Red color is significant at the 0.01 level (2-tailed); blue color is significant at the 0.05 level (2-tailed); In, Mid, and Out are the in-pond sampling locations (inlet, middle, outlet); top and bot are the sampling top layer and bottom layer.

In-top-Kendall's tau_b Correlations

	TSS	TP	DIC	DOC	TDC	TOC	Ca	Fe	Mn	Si	COD	DO	pH	T (°C)	Chl-a µg/L
TN	0.316	0.425	-0.256	-0.056	-0.211	-0.067	0.1	0.112	-0.211	-0.211	0.068	0.142	0.194	0.116	0.211
TDN	0.201	0.376	-0.231	-0.099	-0.231	-0.155	-0.033	0.155	-0.165	-0.143	0.089	0.154	0.205	0.026	0.121
PN	0.475	0.313	-0.1	-0.011	-0.1	0.022	0.367	-0.067	-0.078	-0.233	-0.045	0.182	0.156	0.052	0.367
NH_4-N	-0.38	-0.022	0.165	-0.187	0.077	-0.133	-0.297	-0.044	0.319	0.473	-0.313	-0.513	-0.462	-0.231	-0.275
NO_x-N	0.246	-0.022	-0.187	-0.143	-0.187	-0.243	-0.121	-0.066	-0.473	-0.451	0.156	0.359	0.41	-0.077	0.121
TON	0.469	0.177	-0.099	0.253	0.033	0.309	0.407	0.155	-0.077	-0.187	0.291	0.333	0.333	0.256	0.253
DON	0.335	0.044	-0.055	0.341	0.077	0.354	0.407	0.11	-0.077	-0.143	0.358	0.41	0.359	0.333	0.165

In-bottom-Kendall's tau_b Correlations

	TSS	TP	DIC	DOC	TDC	TOC	Ca	Fe	Mn	Si	COD	DO	pH	T (°C)	Chl-a µg/L
TN	0.199	0.099	-0.165	0.165	-0.099	0.121	-0.033	0.055	-0.275	-0.385	0.144	0.436	0.256	-0.103	-0.099
TDN	0.144	-0.044	-0.066	0.177	-0.044	0.088	-0.066	0.133	-0.11	-0.243	0.134	0.323	0.142	-0.065	-0.11
PN	0.354	0.407	-0.121	0.209	-0.055	0.209	0.055	-0.121	-0.187	-0.341	0.5	0.359	0.385	-0.282	0.341
NH_4-N	-0.354	-0.033	0.055	-0.407	-0.011	-0.319	-0.165	0.231	0.253	0.538	-0.411	-0.564	-0.333	0.026	-0.187
NO_x-N	0.221	-0.187	-0.011	0.231	0.055	0.099	0.033	0.121	-0.297	-0.363	0.078	0.487	0.308	-0.103	-0.209
TON	0.331	0.231	-0.165	0.385	-0.099	0.385	0.143	-0.077	-0.055	-0.341	0.389	0.333	0.154	0.256	0.077
DON	0.066	0.011	-0.121	0.341	-0.055	0.341	0.143	-0.121	0.033	-0.165	0.211	0.256	0.128	0.282	-0.011

Mid-Kendall's tau_b Correlations

	TSS	TP	DIC	DOC	TDC	TOC	Ca	Fe	Mn	Si	COD	DO	pH	T (°C)	Chl-a µg/L
TN	0.155	0.59	-0.24	-0.219	-0.298	-0.195	0.045	0.069	0.13	-0.027	-0.241	-0.173	-0.238	-0.563	0.452
TDN	-0.013	0.353	-0.189	-0.142	-0.268	-0.144	-0.096	0.056	0.074	0.098	-0.254	-0.077	-0.124	-0.367	0.263
PN	0.394	0.407	-0.26	-0.144	-0.339	-0.093	0.098	-0.085	-0.061	-0.37	-0.035	0.046	-0.018	-0.237	0.381
NH_4-N	-0.376	0.008	0.12	-0.12	0.13	-0.122	-0.138	0.072	0.456	0.384	-0.34	-0.692	-0.555	-0.249	-0.114
NO_x-N	0.307	0.066	-0.317	-0.166	-0.353	-0.139	-0.144	-0.003	-0.282	-0.438	-0.07	0.272	0.214	-0.383	0.242
TON	0.394	0.349	-0.164	0.021	-0.132	0.098	0.183	0.079	0.05	-0.132	0.153	0.298	0.16	-0.046	0.249
DON	0.197	0.037	-0.074	0.165	-0.021	0.199	0.135	0.011	-0.045	-0.063	0.159	0.378	0.222	0.292	-0.074

Out-Kendall's tau_b Correlations

	TSS	TP	DIC	DOC	TDC	TOC	Ca	Fe	Mn	Si	COD	DO	pH	T (°C)	Chl-a µg/L
TN	0.167	0.473	-0.099	0.099	-0.055	0.253	-0.209	-0.055	0.128	-0.187	-0.044	-0.256	-0.308	0.103	0.143
TDN	-0.033	0.253	-0.099	0.055	-0.055	0.209	-0.297	-0.055	0.051	-0.055	-0.088	-0.385	-0.436	0.231	0.143
PN	0.544	0.56	0.077	-0.077	0.077	-0.011	0.011	-0.011	-0.077	-0.231	0.11	0.308	0.154	-0.308	0.143
NH_4-N	-0.167	-0.275	0.165	-0.033	0.121	-0.055	-0.033	0.121	-0.103	0.604	-0.155	-0.487	-0.436	0.026	-0.165
NO_x-N	0.064	-0.088	-0.341	-0.164	-0.341	-0.164	0.088	0.467	0.058	-0.088	-0.165	0.086	0.115	-0.115	0.038
TON	0.256	0.516	-0.011	0.187	0.033	0.253	0.011	-0.143	0.128	-0.319	0.133	0.026	-0.077	0.077	0.187
DON	-0.122	0.319	0.055	0.341	0.143	0.451	-0.275	-0.165	0.051	-0.253	0.066	-0.256	-0.308	0.359	-0.011

Table 5-9. correlation analysis results for phosphorous of the Royal Oak wetland in 2018. Red color is significant at the 0.01 level (2-tailed); blue color is significant at the 0.05 level (2-tailed); In, Mid, and Out are the in-pond sampling locations (inlet, middle, outlet); top and bot are the sampling top layer and bottom layer.

In-top-Kendall's tau_b Correlations

	TSS	TN	DIC	DOC	TDC	TOC	Ca	Fe	Mn	Si	COD	DO	pH	T (°C)	Chl-a μg/L
TP	0.299	0.404	0.019	0.537	0.073	0.491	-0.236	0.807	0.636	-0.273	0.449	-0.491	-0.273	0.527	-0.091
TDP	0.299	0.257	0.019	0.5	0.073	0.491	-0.236	0.661	0.418	-0.127	0.486	-0.418	-0.055	0.382	-0.018
PP	-0.037	0.294	-0.208	-0.167	-0.183	-0.2	0.018	0.11	0.164	-0.164	-0.187	-0.018	-0.236	-0.091	-0.2
TRP	0.258	0.622	-0.2	0.294	-0.156	0.327	-0.327	0.778	0.559	-0.327	0.396	-0.405	-0.327	0.289	-0.25

In-bottom-Kendall's tau_b Correlations

	TSS	TN	DIC	DOC	TDC	TOC	Ca	Fe	Mn	Si	COD	DO	pH	T (°C)	Chl-a μg/L
TP	0.141	0.164	-0.309	0.127	-0.2	0.164	-0.345	0.294	0.491	-0.309	0.411	-0.564	-0.382	0.127	0.055
TDP	-0.287	-0.019	-0.019	0.204	0.056	0.13	-0.315	0.093	0.056	-0.019	0	-0.13	-0.019	0.167	0.352
PP	0.181	0.418	-0.345	0.018	-0.309	0.055	0.055	0.33	0.382	-0.345	0.299	-0.455	-0.418	0.164	-0.345
TRP	-0.043	0.52	-0.135	0.019	-0.096	0.135	-0.135	0.564	0.713	-0.096	0.456	-0.79	-0.713	0.135	-0.289

Mid-Kendall's tau_b Correlations

	TSS	TN	DIC	DOC	TDC	TOC	Ca	Fe	Mn	Si	COD	DO	pH	T (°C)	Chl-a μg/L
TP	0.149	0.427	0.079	0.434	0.185	0.385	-0.063	0.515	0.455	-0.19	0.366	-0.433	-0.383	0.223	0.105
TDP	-0.021	0.312	0.264	0.24	0.337	0.117	0.087	0.405	0.298	-0.058	0.357	-0.496	-0.475	0.024	0.024
PP	0.273	0.167	-0.158	0.287	-0.086	0.309	-0.105	0.187	0.249	-0.115	0.083	0	-0.012	0.235	-0.012
TRP	0.038	0.236	-0.125	0.322	-0.05	0.218	-0.096	0.656	0.468	-0.292	0.363	-0.392	-0.321	0.283	0.127

Out-Kendall's tau_b Correlations

	TSS	TN	DIC	DOC	TDC	TOC	Ca	Fe	Mn	Si	COD	DO	pH	T (°C)	Chl-a μg/L
TP	-0.023	0.6	-0.156	0.733	-0.022	0.764	-0.244	0.289	0.644	-0.289	0.494	-0.444	-0.167	0.833	0.167
TDP	-0.114	0.511	-0.244	0.644	-0.022	0.629	-0.333	0.111	0.467	-0.467	0.315	-0.556	-0.389	0.722	0.167
PP	0.296	0.244	0.2	0.2	0.156	0.225	0.2	0.378	0.378	0.067	0.27	0	0.278	0.167	0.167
TRP	0.092	0.225	-0.045	0.449	0.18	0.432	-0.27	0.09	0.449	-0.405	0.205	-0.704	-0.704	0.423	0.085

Table 5-10. correlation analysis results for phosphorous of the Royal Oak wetland in 2019. Red color is significant at the 0.01 level (2-tailed); blue color is significant at the 0.05 level (2-tailed); In, Mid, and Out are the in-pond sampling locations (inlet, middle, outlet); top and bot are the sampling top layer and bottom layer.

In-top-Kendall's tau_b Correlations															
	TSS	**TN**	**DIC**	**DOC**	**TDC**	**TOC**	**Ca**	**Fe**	**Mn**	**Si**	**COD**	**DO**	**pH**	**T (°C)**	**Chl-a μg/L**
TP	0.382	0.425	-0.398	-0.11	-0.398	-0.056	-0.022	0.3	0.243	-0.088	-0.101	-0.245	-0.09	-0.426	0.398
TDP	-0.223	-0.078	0.209	-0.187	0.209	-0.088	0.055	0.133	0.319	0.516	-0.246	-0.641	-0.538	-0.256	-0.055
PP	0.559	0.367	-0.495	0.077	-0.363	0.066	-0.033	0.11	0.011	-0.363	0.112	0.231	0.282	0.051	0.209
TRP	-0.101	-0.201	0.022	-0.199	-0.066	-0.211	-0.287	0.1	0.331	0.376	-0.494	-0.452	-0.477	-0.323	-0.044
In-bottom-Kendall's tau_b Correlations															
	TSS	**TN**	**DIC**	**DOC**	**TDC**	**TOC**	**Ca**	**Fe**	**Mn**	**Si**	**COD**	**DO**	**pH**	**T (°C)**	**Chl-a μg/L**
TP	0.376	0.099	-0.495	0.011	-0.473	0.011	-0.319	0.297	0.363	-0.099	0.389	-0.231	-0.154	-0.41	0.495
TDP	0	-0.231	-0.209	-0.231	-0.231	-0.099	-0.385	0.407	0.56	0.319	0.144	-0.564	-0.487	-0.128	0.253
PP	0.552	0.209	-0.341	0.385	-0.231	0.385	-0.033	0.231	0.209	-0.341	0.478	0.026	0.103	-0.154	0.297
TRP	0.078	-0.155	-0.265	-0.11	-0.287	-0.199	-0.442	0.575	0.42	0.265	-0.101	-0.503	-0.4	-0.271	0.11
Mid-Kendall's tau_b Correlations															
	TSS	**TN**	**DIC**	**DOC**	**TDC**	**TOC**	**Ca**	**Fe**	**Mn**	**Si**	**COD**	**DO**	**pH**	**T (°C)**	**Chl-a μg/L**
TP	0.266	0.59	-0.191	-0.096	-0.212	-0.082	0.093	0.116	0.215	0.011	-0.03	-0.2	-0.166	-0.446	0.497
TDP	-0.384	0.117	0.106	-0.048	0.138	-0.093	-0.114	0.085	0.422	0.451	-0.27	-0.583	-0.606	-0.059	-0.095
PP	0.596	0.309	-0.218	0.016	-0.228	0.05	0.109	0.132	-0.045	-0.228	0.153	0.12	0.129	-0.2	0.365
TRP	-0.237	0.216	-0.024	-0.083	0.019	-0.197	-0.095	0.23	0.35	0.432	-0.447	-0.557	-0.53	-0.262	-0.04
Out-Kendall's tau_b Correlations															
	TSS	**TN**	**DIC**	**DOC**	**TDC**	**TOC**	**Ca**	**Fe**	**Mn**	**Si**	**COD**	**DO**	**pH**	**T (°C)**	**Chl-a μg/L**
TP	0.433	0.473	-0.187	0.099	-0.099	0.165	-0.253	0.165	0.128	-0.231	0.066	0.077	-0.026	0.026	-0.121
TDP	-0.278	0.385	0.033	0.407	0.121	0.473	-0.473	-0.451	0.128	0.121	0	-0.436	-0.487	0.385	-0.297
PP	0.678	0.341	-0.187	-0.121	-0.187	-0.055	-0.165	0.297	-0.077	-0.407	-0.066	0.308	0.154	-0.154	0.143
TRP	-0.211	-0.055	-0.099	0.055	-0.099	0.033	-0.429	-0.011	-0.051	0.341	-0.398	-0.41	-0.41	0.256	-0.297

5.4 Discussions

5.4.1 Factors on Event Performance

In this section, event-7 on 20th June 2019 for the RR wetland and event-10 on 02nd July 2019 for the RO wetland were eliminated. Event-7 of the RR wetland was the biggest storm event with 87.20 mm rainfall depth, but the observed N concentrations in the outlet were supposed to be unreasonable, as discussed in section 5.1.4 (Figure 5-17b). Event-10 of the RO wetland was a large storm event with 37.40 mm rainfall depth and had the longest rainfall duration of 38.50 hrs. It was the only fully captured event which had negative flow reduction. The total weir/orifice outflow of 1943.75 m^3 was over the total pipe inflow of 1451.78 m^3 in this event, resulting in the smallest flow volume reduction as well as the minimum RE of N and its fractions, Figure 5-18a and Table 5-1.

Regression analysis between event RE of TN and TP and inflow EMCs are shown in Figure 5-24, RE-TN increased as the relevant inflow concentration increased in both wetlands ($R^2 = 0.58$ for the RR wetland, Figure 5-24a; $R^2 = 0.69$ for the RO wetland, Figure 5-24d; $p < 0.01$). Specifically, the RE of NH_4-N, NO_x-N, and TON also exhibited a positive relationship with the relevant inflow concentration in the RR wetland ($R^2 = 0.53$ for NH_4-N; $R^2 = 0.65$ for NO_x-N; $R^2 = 0.65$ for TON; $p <0.01$), and the same correlation was observed for TON in the RO wetland ($R^2 = 0.56$, $p = 0.003$). These relationships indicate the importance of inflow quality on the removal capacity of these two wetlands on nitrogen. Several authors have reported a positive relationship between the influent concentration and nutrient removal efficiency (Kadlec and Knight, 1996; Braskerud et al., 2005; Land et al., 2016). However, no significant positive relationship between the RE of TP and TRP and the influent concentrations was observed in either wetland.

A significant linear relationship between RE of TP and TSS ($R^2 = 0.67$, $p = 0.002$, Figure 5-27c) in the RR wetland was observed, which is understandable because most P is primarily in a particulate form and sedimentation is an important phosphorus removal pathway (Kadlec and Knight, 1996). The RE of TN and TP also exhibited a significantly positive linear relationship ($R^2 = 0.53$, $p = 0.01$, Figure 5-24c) in the RR wetland, indicating that increasing the TP-RE could partially increase the RE-TN in this wetland. Conversely, no significant correlation was found among the RE of TP, TN, and TSS in the RO wetland. This is probably because the event flow volume reduction of the RR wetland was variable from negative to a hundred percent, Figure 5-17a, and the good event removal efficiency of the RR wetland was determined by both flow reductions and concentration reductions. The RO wetland had effective flow volume reductions with positive values for almost all events, Figure 5-18a, and the good removal efficiency by the RO wetland was mainly dependent on the concentration reductions. The common role of flow reduction in the event efficiency made the RE-TN and RE-TP had a positive correlation in the RR wetland, even though the flow concentrations were variable. In the RO wetland, the independent role of flow concentrations of nitrogen and phosphorus did not result in a significant correlation in the RE-TN and RE-TP.

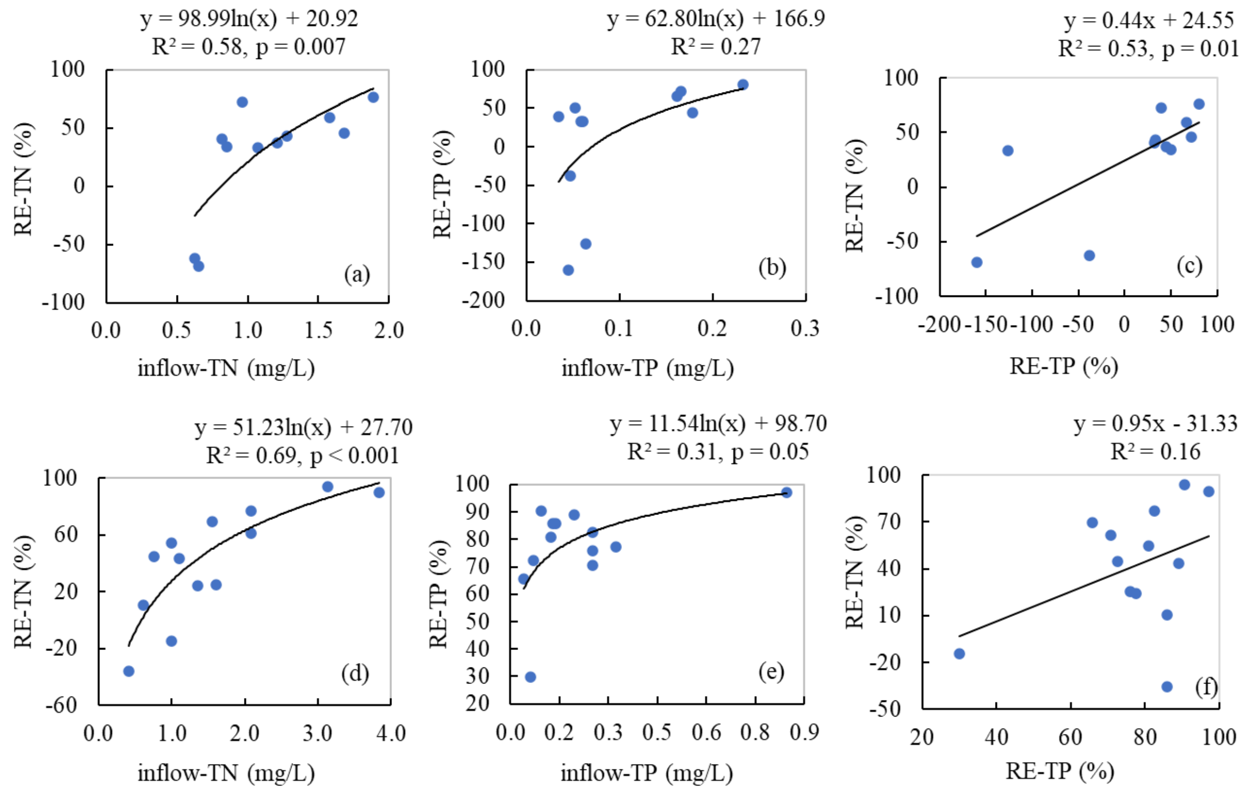

Figure 5-24. Scatter plots showing the event REs vs. inflow EMCs of TN and TP for the Rocky Ridge wetland (a) – (c) and the Royal Oak wetland (d) – (f).

Weather Characteristics vs. Hydraulic Parameters

PCA loading plots were used to provide an overview of how the factor variables affected the N/P removal performance of the studied wetlands (Figure 5-25). One biplot displays the PC1 vs. PC2 for every wetland, respectively. An acute angle between vectors indicates a positive correlation and an obtuse angle of close to 180º exhibits a negative correlation.

In the Rocky Ridge wetland, the first two principal components (PC1 and PC2) account for 35.9% and 19.0% of the data variance, respectively, shown in Figure 5-25a. There is a strong correlation between event RE of TN and TON as the angles between these two vectors are very small and they have almost the same length, which is reasonable since organic nitrogen is the main nitrogen form in the inflows, Figure 5-25a. The vectors of RE-TRP and RE-NO_x are small and should not exhibit any correlations with other vectors. The evaporation rate (E_p) and T_{air} have acute angles with the event RE of TSS, TP, TON, and TN. The rainfall parameters Rde, MRI, and ARI have acute angles with the event RE of TSS and TP, while Rdu and ADP have acute angles with the event RE of TN, TON, and NH_4-N. The hydraulic parameters Vol_R and HLR have acute angles with the event RE of TSS and TP, while HRT has obtuse angles with the event RE of N, P and their fractions. The angles between HRT and the event RE of TP and TSS are close to 180º.

According to the regression analysis, the event RE-TP could increase moderately with increasing T_{air} and E_p, with $R^2 = 0.38$ ($p < 0.05$) and 0.36 ($p = 0.05$, Figure 5-26c), respectively. While the event RE of TN and TON could increase significantly with the increasing E_p ($R^2 = 0.64$ and 0.71, respectively, $p < 0.01$. Figure 5-26a and Figure 5-26b). The RE-TON had also been observed with a moderately positive correlation with air temperature ($R^2 = 0.37$, $p < 0.05$). Air temperature mainly had an influence on pond biological activities with strong seasonal dependence, but its effect on the treatment performance of constructed wetlands is a highly debated topic in literature (Vymazal, 2011). Our finding is consistent with Land et al. (2016) in the positive correlation between TP removal and air temperature. The TP reduction can be impacted by the increasing HRT negatively ($R^2 = 0.66$, $p = 0.003$, Figure 5-27a) but it can be favored by the higher HLR ($R^2 = 0.49$, $p = 0.02$, Figure 5-27b). This finding orients the necessity of P release in the pool exploration of the RR wetland. People also suggest that high fluctuations of hydraulic loading are not recommended in the removal of phosphorus (Lin et al., 2002; Wood et al., 2008).

In the Royal Oak wetland, the first two principal components (PC1 and PC2) account for 38.9% and 23.0% of the data variance, respectively, leading to 61.9% in total, Figure 5-25b. The event RE of N fractions locate mainly close to HRT and ADP, meanwhile, the angles between RE-TON and factors of E_p and T_{air}, RE-TN and factors of HLR and MRI are close to 180º. The rainfall parameters (ARI, Rde and Rdu) and Vol_R locate relatively close to RE of P fractions, but they have the opposite direction to the RE-NO_x. Besides, the angles between factors of E_p and T_{air} and RE of P fractions are close to 180º.

In terms of single factors, the event RE-NO_x decreased significantly with the increase of Rdu ($R^2 = 0.51$, $p = 0.006$, Figure 5-27d) and Rde ($R^2 = 0.81$, $p < 0.001$, Figure 5-27e), demonstrating the nitrogen removal pathways in this wetland are susceptible to interference of rainfall depths and duration. In addition to this result, the minimum event RE of TN, NH_4-N, and NO_x-N occurred along with the longest rainfall duration of 38.5 hrs in event-10, and the maximum event RE of NH_4-N and TRP occurred in the event-2 which has the minimum average rainfall intensity.

The hydraulic parameter Vol_R had negative correlations with the event RE of TN and NO_x-N, Figure 5-25b, especially on RE-NO_x which had strong correlations with it as $R^2 = 0.85$ (Schober and Schwarte, 2018), Figure 5-27f. There were positive correlations among the event RE of TN, TON, TSS, and COD, Figure 5-25b, indicating that the pond bio-assimilation and the accompanying sedimentation could be the major N removal pathways in this wetland. These results suggest that the RO wetland should have a larger pool volume to prolong HRT thus enhancing nitrogen removal theoretically. People recommended that retention wetlands should have enough long HRT to allow particles to settle out to remove nutrients effectively (Nayeb et al., 2021).

Opposite to the RR wetland, E_p had negative correlation with the event RE of TN ($R^2 = 0.41$, p = 0.02, Figure 5-26d), TON ($R^2 = 0.56$, p = 0.003, Figure 5-26e) and TP ($R^2 = 0.43$, p = 0.02, Figure 5-26f) by the RO wetland. People demonstrated that high evapotranspiration (ET) could be a sensitive and important hydrological process in the water budget for treatment wetlands in hot climate countries (Masi and Martinuzzi, 2007; Jiang and Chui, 2022). High ET corresponding to warm temperature can also act to concentrate contaminants remaining in water (Kadlec and Wallace, 2008). Periods of high ET could result in increased contaminant concentrations in the effluent (Liolios et al., 2014) and cause lower concentration reductions (Kadlec and Reddy, 2001).

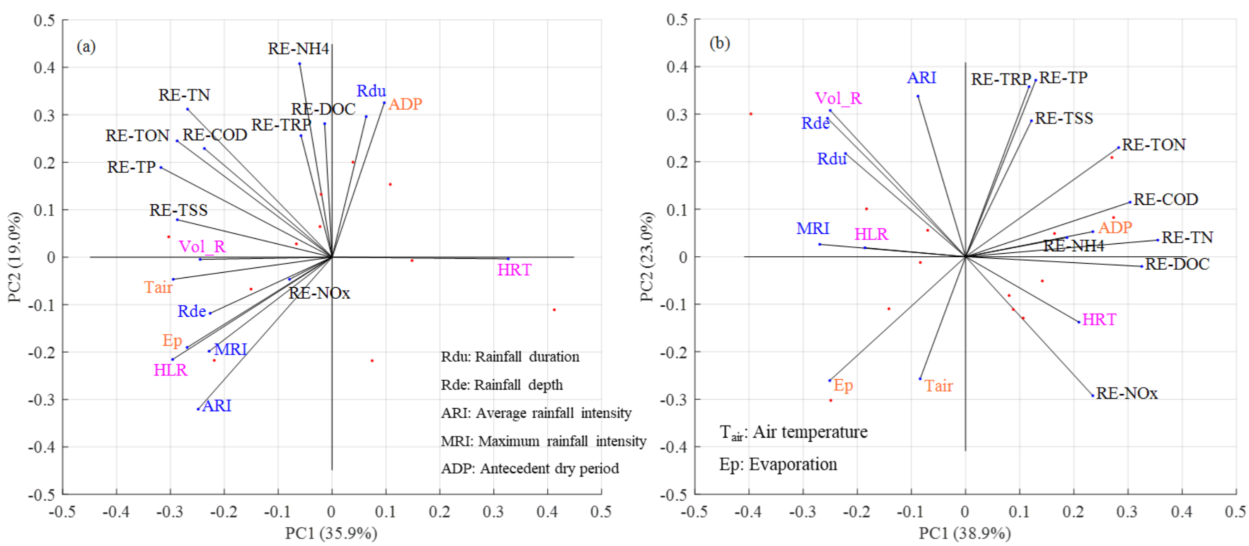

Figure 5-25. Biplot representation of Principal Component Analysis for event REs and factors for the Rocky Ridge wetland and the Royal Oak wetland; the red dots mean observed data, and black lines and blue dots mean the vectors of parameters.

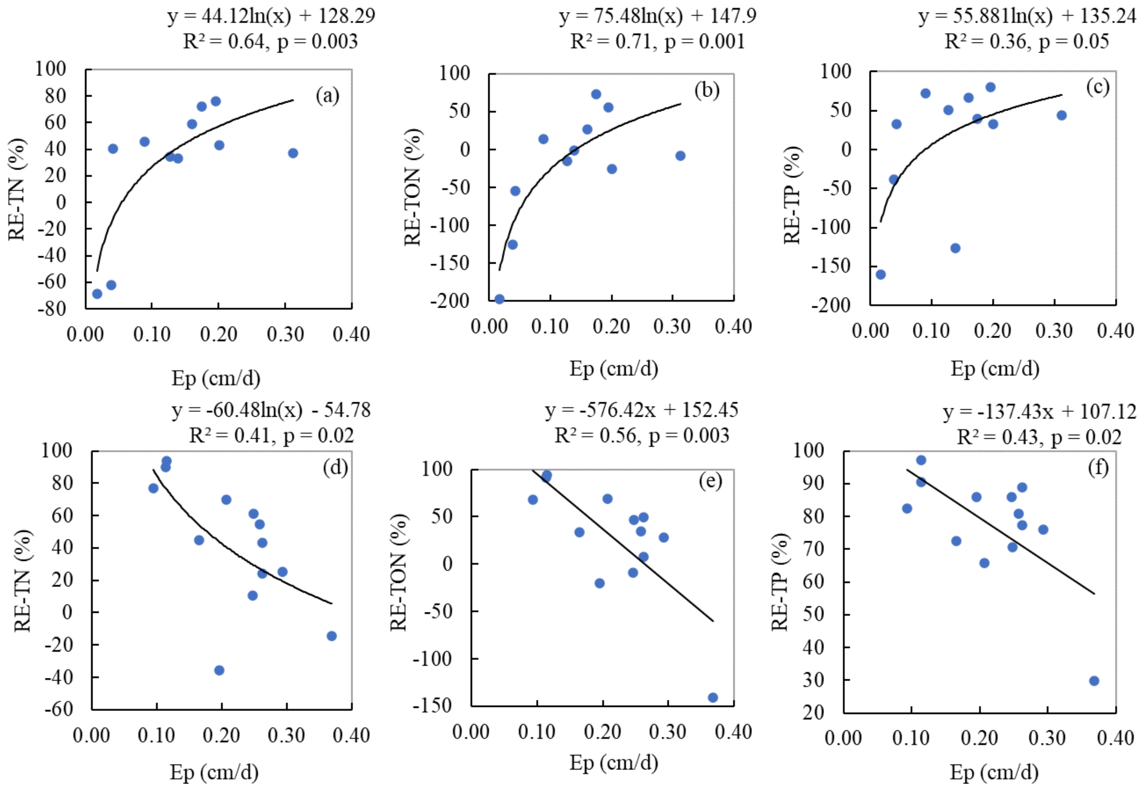

Figure 5-26. Scatter plots showing the REs vs. E_p for the Rocky Ridge wetland (a) – (c) and the Royal Oak wetland (d) – (f).

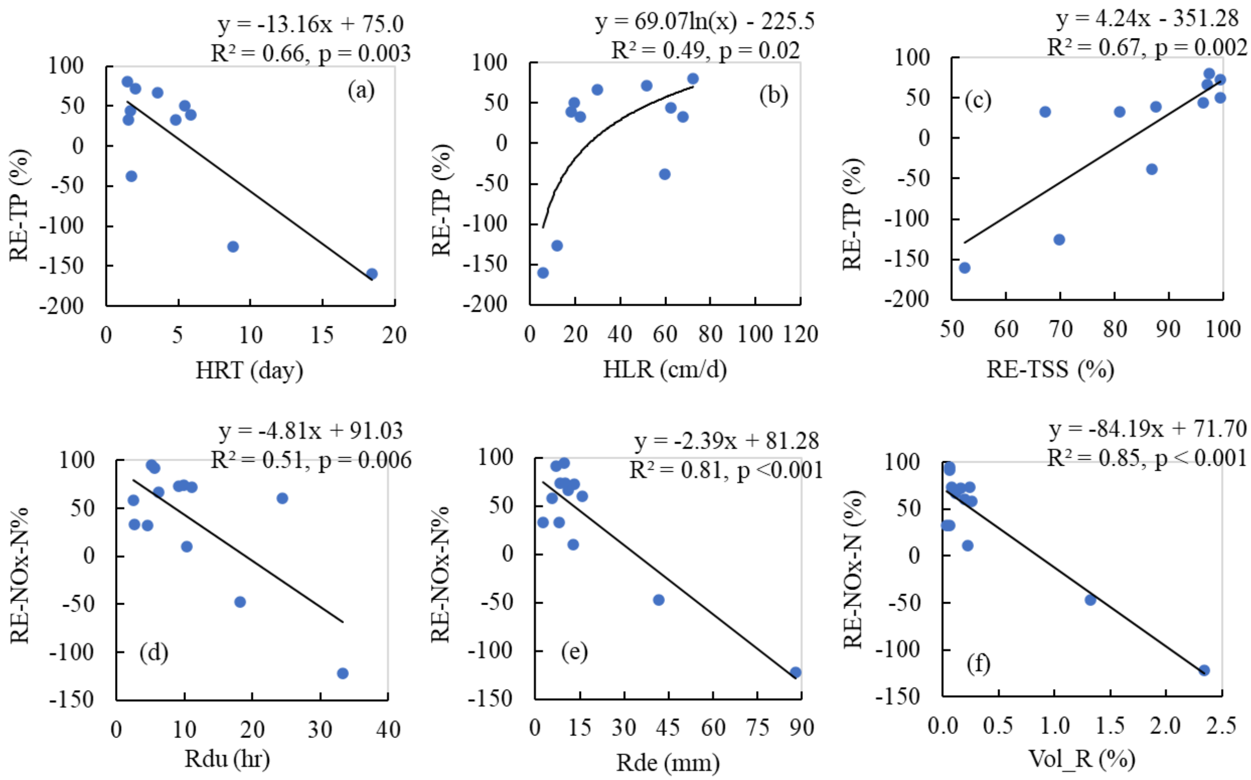

Figure 5-27. Scatter plots showing the event REs vs. factors for the Rocky Ridge wetland (a) – (b) and the Royal Oak wetland (d) – (f), with high R^2. RE-TP vs. RE-TSS for the Rocky Ridge wetland (c).

5.4.2 Comparisons Between Wetlands

The RR wetland had high DO (5 – 20 mg/L in 2018 and 3 – 20 mg/L in 2019) and pH (~ 9.0 – 10.5 in 2018 and ~ 9.0 – 10.0 in 2019) in the water column; thus, alkalinity water bodies can enhance ammonia volatilization but hamper denitrification or DNRA process (Kadlec and Knight, 1996). The positive correlation between TN and TP reduction suggests that the major processes of nutrient retention in the RR wetland should be vegetation uptake and accompanying sedimentation rather than microbial activity. Across the whole RO wetland, the ranges of DO concentrations were around 4 – 25 mg/L in 2018 and 3 – 20 mg/L in 2019, and pH values were 7 – 9 in 2018 and 7.5 – 9 in 2019, respectively. The neutral pH conditions in the bottom water layer, probably caused by the depleted oxygen used for aerobic respiration, could also counteract parts of oxygen production by photosynthesis (Kadlec and Knight, 1996). The pH and DO levels were not suitable for denitrification or DNRA but favored ammonification (Kadlec and Knight, 1996). Still, the plant roots and their attached biofilms can be important mechanisms of biological denitrification

(Kadlec and Knight, 1996). The relatively poor annual removal of TN, NO_x-N, and TON but good NH_4-N removal in the RO wetland suggests that organic decomposition and nitrification should be the major processes.

There is still little understanding of how different plant species influence nutrient uptake and storage in surface flow constructed wetlands (Griffiths et al., 2021). Besides, plant communities are subjected to a wide range of hydraulic and nutrient loads independently, since the hydrology of wetlands is predominantly driven by stormwater events (Dierberg et al., 2002). The elevation in pH was observed in the RR wetland with submerged plants throughout the pond; this finding is consistent with other studies (Reddy et al., 1987; Dierberg et al., 2002), in which people found submerged vegetation can use DO and bicarbonate ions, thereby raising pH in the water column and promoting the removal of P via coprecipitation. Elevated pH can lead to $CaCO_3$ supersaturation, then may facilitate P-Ca coprecipitation in turn (Dierberg et al., 2002). However, the RR wetland did not have stable or better P reduction than the RO wetland (Figure 5-19, Table 5-1), it had better N removal (Figure 5-19, Table 5-1). Additionally, the chemistry forms of the influent phosphorus were altered by the RR wetland in the dry year (Figure 5-17c), probably replacing recalcitrant phosphorus with labile phosphorus forms through biological activities (Song et al., 2015).

From aforementioned discussions, the event RE of TP had a positive correlation with the HRT and a negative correlation with HLR in the RR wetland, while the event RE of NO_x-N had negative correlations with Vol_R in the RO wetland, Figure 5-27. The implications for water quality from rainfall are not inconsequential, as internal mixing patterns would blur the effects of the rainfall on water quality (Kadlec and Wallace, 2008). In this study, it is demonstrated that the rainfall depth and duration exhibited negative correlations with the event RE of NO_x-N and TN in the RO wetland, Figure 5-27. There was no correlation between rainfall parameters and the RE of nutrients found in the RR wetland.

In the RR wetland, the good removal performance was determined by both flow reductions and concentration reductions, and it was exporting variable TP mainly in reactive form, Figure 5-17c, section 5.1.3. If event-3 and event-4 were eliminated in the regression analysis, there were no correlations would be observed between the RE-TP and HRT or HLR. These two small events had the largest HRT and the smallest HLR and higher outflow concentrations than the inflow, Table

4-4, Table 4-5 and Figure 5-17. It indicates that small and clean rainfall events which have low flow rates can reduce the reliability of phosphorus removal assessment by the RR wetland. The RO wetland had effective flow reductions, and it was exporting variable TN concentrations, Figure 5-18. The good removal performance by this wetland was mainly determined by the concentration reductions, section 5.1.3. Without the event-8 and event-9 considered in the regression analysis, correlations between the RE of TN and NO_x-N with rainfall or hydraulic parameters cannot be got. Event-8 and event-9 had the largest rainfall depths and average intensities, Table 4-4, Table 4-5, and Figure 5-27. The interference from large rainfall events on the nitrogen removal by the RO wetland needs to be explored in the future.

The impacts of evaporation on water quality performance should be examined in the future. As discussed in chapter 4, evaporation volume can be negligible in the event water budgets (Table 4-6). However, the evaporation rate exhibited a contrary correlation with nitrogen and phosphorus removal in these two wetlands, Figure 5-26.

5.5 Summary

Rocky Ridge Wetland

In the RR wetland with plenty of submerged plants throughout the pond, 85% of the mixing depth ratios (Secchi depth of water column depth, Z_{Secchi}:Z_{mix}) values were 1.0 across all locations, showing that sunlight was frequently available throughout the entire water column. This wetland had high DO (~ 5 – 20 mg/L in 2018 and ~ 3 – 20 mg/L in 2019) and pH (~ 9.0 – 10.5 in 2018 and ~ 9.0 – 10.0 in 2019) in the water column. Under the high DO level and alkalinity pH conditions, NO_x-N from stormwater can be transformed into ammonium in the pool, and the product NH_4-N ions can also be converted to NH_3 gas in alkalinity water bodies (pH > 9.3, Białowiec et al., 2011), thus, the ammonia volatilization removal pathway could occur in this wetland. Alkaline water bodies can hamper denitrification or DNRA process (Kadlec and Knight, 1996; Białowiec et al., 2011). Besides, high DO concentrations and pH (Figure 5-21) cannot be favourable to the precipitation/dissolution processes, for instance, Fe-phosphate precipitates best at a theoretical pH of 5.3 (Headley et al., 2005; Langergraber, 2005).

Organic nitrogen was the main nitrogen form in the pool of the RR wetland, and there was almost little NH_4-N in the pool (Figure 5-7). The concentrations of TP, PP, and URP increased with the occurrences of algal blooms and even resembled the pattern in DO and pH variables in 2019,

Figure 5-10 and Figure 5-21. Additionally, the concentration peaks of TN, TON, and PN occurred along with the occurrences of algal bloom, Figure 5-7 and Figure 5-8 in section 5.3. It could be illustrated that plant/microbial uptake has an important role in nutrient cycling. Photosynthesis needs soluble phosphate and inorganic nitrogen and then transforms them into organically particle nutrients tending to settle down. This corresponds well with (Vymazal, 1995) that algae can significantly influence nutrient cycling in areas with open water. The relatively high annual removal of TP, TN and its fractions (Table 5-2) and the high correlation between RE-TN and RE-TP suggests that the major processes of nutrient retention in the pool should be vegetation uptake and accompanying sedimentation rather than microbial activity.

Inflow phosphorus mainly existed in particle and unreactive forms (Figure 5-17c), but the chemical forms of phosphorus had been altered in the pool of the RR wetland, and the reactive and dissolved phosphorus became the prevalent phosphorus forms in the pool (Figure 5-9 and Figure 5-10) and the outflow (Figure 5-17c) as well. The outflow concentrations of TN, NH_4-N, and NO_x-N from this wetland were stably lower than the inflow concentrations. There was no significant difference in concentrations between the inflows and outflows for TON, TP and TRP. TN concentrations exported were never higher than 0.1 mg/L, but TP concentrations were not always below 0.05 mg/L (Figure 5-17). The good removal performance by this wetland was determined by both flow reductions and concentration reductions. The ineffective flow reductions are also indicating the important improvement that needs to be done to this wetland's hydraulic design. TN concentrations exported were never higher than 0.1 mg/L, but TP concentrations were never below 0.05 mg/L.

Royal Oak Wetland

The RO wetland mainly has mature emergent macrophytes in the pool. Similarly, the light availability frequently extended throughout the entire mixed layer in the wetland, with 92% of (Z_{Secchi}:Z_{mix}) values being 1.0 across all locations. Across the whole pool, the ranges of DO concentrations were ~ 4 – 25 mg/L in 2018 and ~ 3 – 20 mg/L in 2019, and pH were ~ 7.0 – 9.0 in 2018 and ~7.5 – 9.0 in 2019, respectively. The neutral pH conditions in the bottom water layer, probably caused by the depleted oxygen used for aerobic respiration, could also counteract parts of oxygen production by photosynthesis (Kadlec and Knight, 1996). The pH and DO levels were not suitable for denitrification or DNRA but favour ammonification (Kadlec and Knight, 1996). Still, the plant roots and their attached biofilms can be important mechanisms of biological denitrification (Kadlec and Knight, 1996). The relatively poor annual removal of TN, NO_x-N, and TON but good NH_4-N removal in this wetland suggest that organic decomposition and nitrification should be the major processes in the pool.

The nitrogen stratifications of TN, NO_x-N and PN were frequent in the inlet sampling location of the pool, where the sedimentation forebay locates, indicating the different processes of nitrogen transformation that happen in the top water and bottom water of the inlet sampling site, Figure 5-11 and Figure 5-12. NO_x-N and NH_4-N in the pool were related and were higher than the inflows in 2018-2019, especially in the inlet bottom layer, Figure 5-11 and Figure 5-12. The sediment forebay designed for sediment removal can be a nitrogen source in the pool, especially NH_4-N and NO_x-N can come from decomposable organic nitrogen through ammonification and nitrification processes, and they can be transported to other locations in the wetland. The sustained high NO_x-N and NH_4-N would be removed by ammonia volatilization, plant/microbial uptake, denitrification, and even anammox (Reddy and D'Angelo, 1997). However, the environmental conditions of high DO and neutral pH in the pool make these removal pathways hardly realized, Figure 5-23. The phenomenon that the increase of NH_4-N concentrations along with the decrease of NO_x-N concentrations in the inlet bottom during the study season in 2019 (Figure 5-11) indicates that the DNRA process or ammonification process can occur there.

The prevalence of phosphorus form was different in different years in the pool (Figure 5-13 and Figure 5-14), even though the particle and unreactive phosphorus forms were always the major phosphorus in the inflows, see Figure 5-18c. Sedimentation and the related physicochemical processes in the pool can reduce particulate phosphorus. The environmental conditions can alter the chemical forms of phosphorus, probably replacing recalcitrant phosphorus with labile phosphorus form through intense biological activities (Kadlec and Knight, 1996). There were differences in phosphorus concentrations in the different sites, Figure 5-13 and Figure 5-14. This corresponds with variations in environmental conditions (Figure 5-22 and Figure 5-23) and the biological activities in different sites. Similarly, plant/microbial assimilation can also influence the phosphorus dynamic in the pool of this wetland because the occurrences of TP and PP concentration peaks (Figure 5-13 and Figure 5-14) are accompanied by the algal blooms being indicated by the high Chl-a concentrations (Figure 5-22). Phosphorus in the water column can be retained by algae assimilation and sedimented back to the bottom or can be assimilated into tissue phosphorus by emerged plants (Kadlec and Knight, 1996).

This wetland exported TP concentrations below the protective value 0.05 mg/L and TN concentrations not always below the protective value 0.1 mg/L (Figure 5-18). The outflow concentrations of NH_4-N, TP, and TRP from the pool were significantly lower than the inflow concentrations. While there were no statistically significant differences in the concentrations of NO_x-N, TON, or TN between the inflows and the outflows. This wetland had good performance on the flow volume reductions, and the good removal performance was mainly determined by the concentration reductions.

6 Conclusions and Future Study

This study examined the effectiveness of two created wetlands built for treating urban stormwater nutrients in a cold temperate region. The water budget analysis was done to guarantee the reliability of flow data. The nutrient performance was considered in two aspects: loading mass removal and concentration reductions.

It is indicated that annual flow into these studied wetlands was mainly through the inlet pipes and the outflow was through evaporation and weir/orifice control in RR wetland but mainly over weir/orifice control in RO wetland. Inflow and outflow through the RO wetland were much larger than the water budget components associated with rainfall and evaporation. Evaporation had a certain important effect on the water budget in these two wetlands annually, especially in 2018 with less annual rainfall depths. The residuals of the annual water budget were reasonably within 3% in the RR wetland and 1% in the RO wetland in both years. However, rainfall and evaporation were minor components of the flow when considering individual storm events. The event error in the closure of the event water budget for the RR wetland ranged from -37.2% to 13.6%, and for the RO wetland ranged from -8.8% to 46.8%.

The nutrient concentrations in the inflows of these two wetlands were highly variable. However, the exported TN concentrations from the RR wetland can be below or comply with Alberta's discharge water protection threshold value of 1.0 mg/L. Most of the exported TP concentrations from the RO wetland were below the threshold value of 0.05 mg/L. Stably good performance still can not be guaranteed throughout the monitoring seasons, considering the exported concentrations of all nutrients from these two wetlands. TN loading into the RR wetland was retained at approximately 59.7% in 2018 and 70.1% in 2019. Nevertheless, the RO wetland trapped 48.6% of TN inflow loadings in 2018 and only trapped 10.9% in 2019. Both wetlands could effectively remove TP from stormwater, given the annual TP reductions were 47.0% in 2018 and 66.8% in 2019 by the RR wetland and 84.1% in 2018 and 83.1% in 2019 by the RO wetland.

Both wetlands had better removal of N and P in the wet year 2019, while the event REs of TN and TP exhibited the same fluctuations as the hydraulic loading rate in the dry year 2018. The event RE-TN ranged from -68.6% to 98.4% of the RR wetland and from -104.1% to 93.8% of the RO wetland. The event RE-TP ranged from 29.9% to 97.2% of the RO wetland and from -160% to 80.3% of the RR wetland. The event removal efficiencies of TN were positively correlated with the inflow concentrations in these two wetlands. The evaporation volume could be negligible in the event water budgets and the evaporation rate was lower than the maximum rainfall intensity and hydraulic loading rate in both wetlands. However, the evaporation rate exhibited a contrary correlation with the event removal of nitrogen and phosphorus in these two wetlands.

For the RR wetland, the nutrient removal could be attributed to TSS reduction since the RE-TP had positive correlations with RE-TN and RE-TSS. The removal of TP was influenced by air temperature, evaporation rate, hydraulic loading rate and hydraulic retention time. The major processes of nutrient retention in the pool should be vegetation uptake and accompanying sedimentation rather than microbial activity. For the RO wetland, the interference from rainfall characteristics played important role in nitrogen removal in the pool, as the rainfall duration and depth had significant negative correlations with the event RE-NO_x. The event RE of TN and TP increased with the increased evaporation rate. Sedimentation forebay can result in the release of dissolved nutrients from the sediment to the water column, like NO_x-N. Organic decomposition and nitrification were assumed to be the major processes for pool annual nitrogen removal in this wetland.

There is still little understanding of how different plant species influence nutrient uptake and storage in surface flow constructed wetlands (Griffiths et al., 2021). Besides, plant communities are subjected to a wide range of hydraulic and nutrient loads independently, since the hydrology of wetlands is predominantly driven by stormwater events (Dierberg et al., 2002). In this study, submerged plants are present throughout the entire RR wetland while matured emergent macrophytes are the dominant plant in the RO wetland. The elevation in pH was observed in the RR wetland, and this finding is consistent with other studies (Reddy et al., 1987; McConnaughey et al., 1994; Dierberg et al., 2002), in which people found submerged vegetation can use DO and bicarbonate ions and raise pH in the water column and promote the removal of P via coprecipitation. Because elevated pH can lead to $CaCO_3$ supersaturation, it may facilitate P-Ca coprecipitation in turn (Dierberg et al., 2002). Although the RR wetland did not have stable or better P reduction than the RO wetland, it had better N removal. Additionally, the chemistry forms of the inflow phosphorus were altered by the RR wetland in the dry year, probably replacing recalcitrant phosphorus with labile phosphorus forms through biological activities (Song et al., 2015).

Regarding future work, the fate of influent nutrients and nutrients' cycling in the pond should be studied to guarantee uniformly good performance of both wetlands, especially understanding the stability of the pond ecosystem. It should also focus on understanding how design features like sedimentation forebay, depth distributions, and vegetation types affect the nutrients cycling in the pool. The RR wetland's ineffective flow reductions require further study, and its good removal performance is determined by both flow reductions and concentration reductions. Small and clean rainfall events which have low flow rates can reduce the reliability of phosphorus removal assessment by the RR wetland. However, the RO wetland had good performance on the flow volume reductions, and the good removal performance is mainly determined by the concentration reductions. The interference from large rainfall events on the nitrogen removal by the RO wetland needs to be explored in the future.

7 References

Ahilan, S., Mingfu, G., Nigel, W., Andrew, S., Deonie, A., Scott, A., Heather, H., and Vladimir, Kr., 2019. "Modelling the Long-Term Suspended Sedimentological Effects on Stormwater Pond Performance in an Urban Catchment." Journal of Hydrology 571 (September 2018): 805 – 18. https://doi.org/10.1016/j.jhydrol.2019.02.002.

Akratos, C. S., and Vassilios, T. 2007., "Effect of Temperature, HRT, Vegetation and Porous Media on Removal Efficiency of Pilot-Scale Horizontal Subsurface Flow Constructed Wetlands." Ecological Engineering 29: 173 – 91. https://doi.org/10.1016/j.ecoleng.2006.06.013.

Al-Rubaei, Ahmed., Malin E., Maria V., and Godecke T. B. 2017., "Effectiveness of a 19-Year-Old Combined Pond-Wetland System in Removing Particulate and Dissolved Pollutants." Wetlands 37 (3): 485 – 96. https://doi.org/10.1007/s13157-017-0884-6.

Al-Rubaei, Ahmed M., Malin E., Maria V., and Godecke T. B. 2016., "Long-Term Hydraulic and Treatment Performance of a 19-Year-Old Constructed Stormwater Wetland - Finally Maturated or in Need of Maintenance?" Ecological Engineering 95: 73 – 82. https://doi.org/10.1016/j.ecoleng.2016.06.031.

Azim, A., Mohamed, A., Mohamed, I., and Diwedar, A. I., 2015. "The Discharge Coefficient for a Compound Sharp Crested V-Notch Weir." Asian Journal of Engineering and Technology 03 (05): 2321 – 2462.

Barbosa, A. E., Fernandes, J. N., and David L. M., 2012. "Key Issues for Sustainable Urban Stormwater Management." Water Research 46 (20): 6787 – 98. https://doi.org/10.1016/j.watres.2012.05.029.

Baskar, G., and Thattai, D. V. 2014., "Effect of Vegetation and Retention Time on Wastewater Treatment in Pilot Scale Constructed Wetlands in a Tropical Campus." BIOINFO Environment and Pollution 4 (2). http://bioinfopublication.org/journal.php?opt=index&jouid=BPJ0000198.

Bavor, H. J., Davies, C. M., and Sakadevan, K., 2001. "Stormwater Treatment: Do Constructed Wetlands Yield Improved Pollutant Management Performance over a

Detention Pond System?" Water Science and Technology 44 (11 – 12): 565–70. https://doi.org/10.2166/wst.2001.0881.

Bayley, M. L., Davison, L., and Headley, T. R., 2003. "Nitrogen Removal from Domestic Effluent Using Subsurface Flow Constructed Wetlands: Influence of Depth, Hydraulic Residence Time and Pre-Nitrification." Water Science and Technology 48 (5): 175 – 82. https://doi.org/10.2166/wst.2003.0313.

Bertino, A., 2010. "Study on One-Stage Partial Nitritation-Anammox Process in MBBRs: A Sustainable Nitrogen Removal."

Białowiec, A., Wojciech, J., and Peter, F. R., 2011. "Nitrogen Removal from Wastewater in Vertical Flow Constructed Wetlands Containing LWA / Gravel Layers and Reed Vegetation." Ecological Engineering 37: 897 – 902. https://doi.org/10.1016/j.ecoleng.2011.01.013.

Borne, K. E., 2014. "Floating Treatment Wetland Influences on the Fate and Removal Performance of Phosphorus in Stormwater Retention Ponds." Ecological Engineering 69: 76 – 82. https://doi.org/10.1016/j.ecoleng.2014.03.062.

Borne, K. E., Fassman, E. A., and Tanner, C. C., 2013. "Floating Treatment Wetland Retrofit to Improve Stormwater Pond Performance for Suspended Solids, Copper and Zinc." Ecological Engineering 54: 173 – 82. https://doi.org/10.1016/j.ecoleng.2013.01.031.

Boyd, C. E., 1969. "Production, Mineral Nutrient Absorption, and Biochemical Assimilation by Justicia Americana and Alternanthera Philoxeroides." Archiv Fur Hydrobiologie.

Braskerud, B. C., Tonderski, K. S., Wedding, B., Bakke, R., Blankenberg, A.G, Ulén, B., and Koskiaho, J., 2005. "Can Constructed Wetlands Reduce the Diffuse Phosphorus Loads to Eutrophic Water in Cold Temperate Regions?" Journal of Environmental Quality 34 (6): 2145 – 55. https://doi.org/10.2134/jeq2004.0466.

Brient, L., Lengronne, M., Bertrand, E., Rolland, D., Sipel, A., Steinmann, D., Baudin, I., Legeas, M., Rouzic, B. L., and Bormans, M., 2008. "A Phycocyanin Probe as a Tool for Monitoring Cyanobacteria in Freshwater Bodies." Journal of Environmental Monitoring 10 (2): 248 – 55. https://doi.org/10.1039/b714238b.

Brix, H., 1997. “Do Macrophytes Play a Role in Constructed Treatment Wetlands?” Water Science and Technology 35 (5): 11 – 17. https://doi.org/https://doi.org/10.1016/S0273-1223(97)00047-4.

Brodrick, S. J., Cullen, P., and Maher, W., 1988. “Denitrification in a natural wetland receiving secondary treatment effluent Stephanie.” Water Research 22 (4): 431 – 39.

Bulgakov, N. G. and Levich, A. P., 1999. “The Nitrogen:Phosphorus Ratio as a Factor Regulating Phytoplankton Community Structure.” Archiv Für Hydrobiologie 146 (1): 3 – 22. https://doi.org/10.1127/archiv-hydrobiol/146/1999/3.

Burgin, A. J., and Hamilton, S. K., 2007. “Have We Overemphasized the Role of Denitrification in Aquatic Ecosystems? A Review of Nitrate Removal Pathways.” Front Ecol Envi 5 (2): 89 – 96.

Carey, R. O., Hochmuth, G. J., Martinez, C. J., Boyer, T. H., Dukes, M. D., Toor, G. S., and Cisar, J. L. 2013. “Evaluating Nutrient Impacts in Urban Watersheds: Challenges and Research Opportunities.” Environmental Pollution 173: 138 – 49. https://doi.org/10.1016/j.envpol.2012.10.004.

Carleton, J. N., Grizzard, T. J., Godrej, A. N., and Post, H.E. 2001. “Factors Affecting the Performance of Stormwater Treatment Wetlands.” Water Research 35 (6): 1552 – 62. https://doi.org/10.1016/S0043-1354(00)00416-4.

Caselles-osorio, A., Villafañe, P., Caballero, V., and Manzano, Y. 2011. “Efficiency of Mesocosm-Scale Constructed Wetland Systems for Treatment of Sanitary Wastewater Under Tropical Conditions.” Water Air Soil Pollut 220: 161 – 71. https://doi.org/10.1007/s11270-011-0743-7.

Cerezo, R. G., Sua´rez, M. L., and Vidal-Abarca, M. R. 2001. “The Performance of a Multi-Stage System of Constructed Wetlands for Urban Wastewater Treatment in a Semiarid Region of SE Spain.” Ecological Engineering 16 (4): 501 – 17. https://doi.org/10.1016/S0925-8574(00)00114-2.

Chanson, H. and Wang, H. 2013. “Unsteady Discharge Calibration of a Large V-Notch Weir.” Flow Measurement and Instrumentation 29: 19 – 24. https://doi.org/10.1016/j.flowmeasinst.2012.10.010.

Chazarenc, F., Gagnon, V., Comeau, Y., and Brisson, J. 2009. "Effect of Plant and Artificial Aeration on Solids Accumulation and Biological Activities in Constructed Wetlands." Ecological Engineering 35: 1005 – 10. https://doi.org/10.1016/j.ecoleng.2008.07.008.

Chrétien, F, Gagnon, P., Thériault, G., and Guillou, M. 2016. "Performance Analysis of a Wet-Retention Pond in a Small Agricultural Catchment." Journal of Environmental Engineering 142 (4): 04016005. https://doi.org/10.1061/(asce)ee.1943-7870.0001081.

Chyan, D. J., Chang, C. J., and Lee, M. H. 2006. "Discussion of 'Design and Calibration of a Compound Sharp-Crested Weir' by J. Martínez, J. Reca, M. T. Morillas, and J. G. López." J. Hydraul. Eng. 132 (2): 868 – 71.

Chyan, J. M., Lin, C. J., Lin, Y. C., and Yi, C. Y. 2016. "Improving Removal Performance of Pollutants by Artificial Aeration and Flow Rectification in Free Water Surface Constructed Wetland." International Biodeterioration and Biodegradation 113 (September): 146 – 54. https://doi.org/10.1016/j.ibiod.2016.04.034.

Clary, J., Jonathan, J., Leisenring, M., Hobson, P., and Strecker, E. 2020. International Stormwater BMP Database: 2020 Summary Statistics.

Collins, K. A., Lawrence, T. J., Stander, E. K., Jontos, R. J., Kaushal, S. S., Newcomer, T. A., Grimm, N. B., and Ekberg, M. L. C. 2010. "Opportunities and Challenges for Managing Nitrogen in Urban Stormwater: A Review and Synthesis." Ecological Engineering 36 (11): 1507 – 19. https://doi.org/10.1016/j.ecoleng.2010.03.015.

Connolly, R., Zhao Y. Q., Guang, Z., Sun, G. Z., and Allen, S. 2004. "Removal of Ammoniacal-Nitrogen from an Artificial Landfill Leachate in Downflow Reed Beds." Process Biochemistry 39 (2): 1971 – 76. https://doi.org/10.1016/j.procbio.2003.09.020.

Cooper, P. F. 1996. Reed Beds and Constructed Wetlands for Wastewater Treatment. WRC Publications. Water Research Centre (Great Britain). https://doi.org/10.3390/w2030530.

Cui, J, and Jiang, C. L. 2013. "A Sustainability Strategy of Integrated Highway Wetlands for Urban Water Management in China." Desalination and Water Treatment 51 (31 – 33): 6166 – 71. https://doi.org/10.1080/19443994.2013.780693.

Cui, L. H., Ouyang, Y., Lou, Q., Yang, F. L., Chen, Y., Zhu, W. L., and Luo, S. M. 2010. "Removal of Nutrients from Wastewater with Canna Indica L. under Different Vertical-

Flow Constructed Wetland Conditions.” Ecological Engineering 36 (8): 1083 – 88. https://doi.org/10.1016/j.ecoleng.2010.04.026.

Demin, O. A. and Dudeney, A. W. L. 2003. “Nitrification in Constructed Wetlands Treating Ochreous Mine Water.” Mine Water and the Environment 22: 15 – 21. https://doi.org/https://doi.org/10.1007/s102300300003.

Diamantini, E., Lutz, S. R., Mallucci, S., Majone, B., Merz, R., and Bellin, A. 2018. “Driver Detection of Water Quality Trends in Three Large European River Basins.” Science of the Total Environment 612: 49 – 62. https://doi.org/10.1016/j.scitotenv.2017.08.172.

Dierberg, F. E., DeBusk, T. A., Jackson, S. D., Chimney, M. J., and Pietro, K. 2002. “Submerged Aquatic Vegetation-Based Treatment Wetlands for Removing Phosphorus from Agricultural Runoff: Response to Hydraulic and Nutrient Loading.” Water Research 36 (6): 1409 – 22. https://doi.org/10.1016/S0043-1354(01)00354-2.

Dong, H. Y., Qiang, Z. M., Li, T. G., Jin, H., and Chen, W. D. 2012. “Effect of Artificial Aeration on the Performance of Vertical-Flow Constructed Wetland Treating Heavily Polluted River Water.” Journal of Environmental Sciences 24 (4): 596 – 601. https://doi.org/10.1016/S1001-0742(11)60804-8.

Drake, C. W., Jones, C. S., Schilling, K. E., Amado, A. A., and Weber, L. J. 2018. “Estimating nitrate-nitrogen Retention in a Large Constructed Wetland Using High-Frequency, Continuous Monitoring and Hydrologic Modeling.” Ecological Engineering 117 (July): 69 – 83. https://doi.org/10.1016/j.ecoleng.2018.03.014.

Drizo, A., Frost, C. A., Grace, J., and Smith, K. A. 2000. “Phosphate and Ammonium Distribution in a Pilot-Scale Constructed Wetland with Horizontal Subsurface Flow Using Shale as a Substrate.” Wat. Res. 34 (9): 2483 – 90.

Drizo, A., Frost, C. A., Smith, K. A., Grace, J. 1997. “Phosphate and Ammonium Removal by Constructed Wetlands with Horizontal Subsurface Flow, Using Shale as a Substrate.” Water Science and Technology 35 (5): 95 – 102. https://doi.org/https://doi.org/10.1016/S0273-1223(97)00057-7.

Dunalska, J. A., Grochowska, J., Wiśniewski, G., and Napiórkowska-Krzebietke, A. 2015. “Can We Restore Badly Degraded Urban Lakes?” Ecological Engineering 82: 432 – 41. https://doi.org/10.1016/j.ecoleng.2015.05.037.

Dunne, E. J., Culleton, N., O’Donovan, G., Harrington, R., and Olsen, A. E. 2005. “An Integrated Constructed Wetland to Treat Contaminants and Nutrients from Dairy Farmyard Dirty Water.” Ecological Engineering 24 (3): 219 – 32. https://doi.org/10.1016/j.ecoleng.2004.11.010.

Dunne, E. J., and Reddy, K. R. 2005. “Phosphorus Biogeochemistry of Wetlands in Agricultural Watersheds.” Nutrient Management in Agricultural Watershed: A Wetlands Solution. https://doi.org/10.3920/978-90-8686-558-1.

Ellis, J. B., Shutes, R. B. E., Revitt, D. M. Environment Agency. 2003. Guidance for Constructed Wetlands. Environment Agency.

Environment, Alberta. 2001. Municipal Policies and Procedures Manual.

Environment Canada. 2011. Water Quality Status and Trends of Nutrients in Major Drainage Areas of Canada: Technical Summary. Environment Canada.

ESRD. 2014. Environmental Quality Guidelines for Alberta Surface Waters. Water Policy Branch, Policy Division. https://doi.org/10.1002/2014GB005021.

Eylon, S., Thompson, T. L., Karpiscak, M. M., Freitas, R. J., Zauderer, J. 1998. “Nitrogen Accumulation in A Constructed Wetland for Dairy Wastewater Treatment.” The Journal of the American Water Resources Association 37 (2): 315 – 25. https://doi.org/https://doi.org/10.1111/j.1752-1688.2001.tb00971.x.

Fenton, J. D. 1992. “Reservoir Routing.” Hydrological Sciences Journal 37 (3): 233 – 46. https://doi.org/10.1080/02626669209492584.

García, J., Rousseau, D. P. L., Morató, J., Lesage, E., Matamoros, V., and Bayona, J. M. 2010. “Contaminant Removal Processes in Subsurface-Flow Constructed Wetlands: A Review.” Critical Reviews in Environmental Science and Technology 40 (7): 561 – 661. https://doi.org/10.1080/10643380802471076.

Ge, Z. G., Feng, C. M., Wang, X. P., and Zhang, J. B. 2016. “Seasonal Applicability of Three Vegetation Constructed Floating Treatment Wetlands for Nutrient Removal and Harvesting Strategy in Urban Stormwater Retention Ponds.” International Biodeterioration and Biodegradation 112: 80 – 87. https://doi.org/10.1016/j.ibiod.2016.05.007.

Ghasemzadeh, F., Kouchakzadeh, S., and Belaud, G. 2020. “Unsteady Stage-Discharge Relationships for Sharp-Crested Weirs.” Journal of Irrigation and Drainage Engineering 146 (6): 04020009. https://doi.org/10.1061/(asce)ir.1943-4774.0001468.

Griffiths, L. N., Haupt, T. N., Zhang, L., and Mitsch, W. J. 2021. “Role of Emergent and Submerged Vegetation and Algal Communities on Nutrient Retention and Management in a Subtropical Urban Stormwater Treatment Wetland.” Wetlands Ecology and Management 29 (2): 245 – 64. https://doi.org/10.1007/s11273-020-09781-6.

Guardo, M. 1999. “Hydrologic Balance for a Subtropical Treatment Wetland Constructed for Nutrient Removal.” Ecological Engineering 12 (3 – 4): 315 – 37. https://doi.org/10.1016/S0925-8574(98)00076-7.

Haberl, R., Perfler, R., and Mayer, H. 1995. “Constructed Wetlands in Europe.” Water Science and Technology 32 (3): 305 – 15. https://doi.org/https://doi.org/10.1016/0273-1223(95)00631-1.

Hagerthey, S. E, Cole, J. J., and Kilbane, D. 2010. “Aquatic Metabolism in the Everglades: Dominance of Water Column Heterotrophy.” Limnol. Oceanogr 55 (2): 653 – 66.

Hamid, S., Gharehbaghi, A., Mehdizadeh, S., Kaya, B., and Behmanesh, J. 2017. “Experimental Investigation of Discharge Coefficient over Novel Kind of Sharp-Crested V-Notch Weir.” Flow Measurement and Instrumentation 54 (2017): 236 – 42. https://doi.org/10.1016/j.flowmeasinst.2017.02.008.

Hammer, D.E., and Kadlec, R. H. 1983. “Design Principles for Wetland Treatment Systems.”

Härdle, W. K., and Simar, L. 2013. Applied Multivariate Statistical Analysis. Applied Multivariate Statistical Analysis. https://doi.org/10.1007/978-3-642-17229-8.

Headley, T. R., Herity, E., and Davison, L. 2005. "Treatment at Different Depths and Vertical Mixing within a 1-m Deep Horizontal Subsurface-Flow Wetland." Ecological Engineering 25: 567 – 82. https://doi.org/10.1016/j.ecoleng.2005.07.012.

Healy, M., and Cawley, A. M. 2002. "Wetlands and Aquatic Processes Nutrient Processing Capacity of a Constructed Wetland in Western Ireland." J. Environ. Qual. 31 (5): 1739 – 47. https://doi.org/10.2134/jeq2002.1739.

Heiner, B., Barfuss, S. L., and Johnson, M. C. 2011. "Conditional Assessment of Flow Measurement Accuracy." Journal of Irrigation and Drainage Engineering 137 (6): 367 – 74. https://doi.org/10.1061/(asce)ir.1943-4774.0000309.

Herouvim, E., Akratos, C. S., Tekerlekopoulou, A., and Vayenas, V. D. 2011. "Treatment of Olive Mill Wastewater in Pilot-Scale Vertical Flow Constructed Wetlands." Ecological Engineering 37 (6): 931 – 39. https://doi.org/10.1016/j.ecoleng.2011.01.018.

Hoang, T., Nhat, L., Huu, N., and Brix, H. 2011. "Treatment of High-Strength Wastewater in Tropical Constructed Wetlands Planted with Sesbania Sesban: Horizontal Subsurface Flow versus Vertical Downflow." Ecological Engineering 37 (5): 711 – 20. https://doi.org/10.1016/j.ecoleng.2010.07.030.

Holford, I. C. R., and Patrick, W. H. 1979. "Effects of Reduction and PH Changes on Phosphate Sorption and Mobility in an Acid Soil." Soil Science Society of America Journal 43 (2): 292 – 97. https://doi.org/10.2136/sssaj1979.03615995004300020010x.

Huett, D. O., Morris, S. G., Smith, G., and Hunt, N. 2005. "Nitrogen and Phosphorus Removal from Plant Nursery Runoff in Vegetated and Unvegetated Subsurface Flow Wetlands." Water Research 39: 3259 – 72. https://doi.org/10.1016/j.watres.2005.05.038.

Hushchyna, K., and Nguyen-quang, T. 2017. "Using the modified Redfield ratio to estimate harmful algal blooms." ENVIRONMENTAL PROBLEMS 2 (2).

ISCO, Teledyne. 2016. "2150 Area Velocity Flow Module and Sensor Installation and Operation Guide."

Ivanovsky, A., Belles, A., Criquet, J., Dumoulin, D., Noble, P., Alary, C., and Billon, G. 2018. "Assessment of the Treatment Efficiency of an Urban Stormwater Pond and Its Impact on the Natural Downstream Watercourse." Journal of Environmental Management 226 (August): 120 – 30. https://doi.org/10.1016/j.jenvman.2018.08.015.

Jefferson, A. J., Bhaskar, A. S., Hopkins, K. G., Fanelli, R., Avellaneda, P. M., and McMillan, S. K. 2017. "Stormwater Management Network Effectiveness and Implications for Urban Watershed Function: A Critical Review." Hydrological Processes 31 (23): 4056 – 80. https://doi.org/10.1002/hyp.11347.

Jiang, L., and Chui, T. F. 2022. "A Review of the Application of Constructed Wetlands (CWs) and Their Hydraulic, Water Quality and Biological Responses to Changing Hydrological Conditions." Ecological Engineering 174 (May 2021). https://doi.org/10.1016/j.ecoleng.2021.106459.

Johnson, F. A., and Green, C. S. 1977. "The Calibration of Sharp Crested Weirs by the Pondage Drawdown Method." Journal of Hydrology 33 (3 – 4): 363 – 73. https://doi.org/10.1016/0022-1694(77)90046-4.

Kadlec, R. H., and Knight, R. L. 1996. Treatment Wetlands. Feb. 1, 1996. 1st edition. CRC-Press.

Kadlec, R. H., and Reddy, K. R. 2001. "Temperature Effects in Treatment Wetlands." Water Environment Research 73 (5): 543 – 57. https://doi.org/10.2175/106143001x139614.

Kadlec, R. H., and Wallace, S. D. 2008. Treatment Wetlands Second Edition. CRC Press Taylor & Francis Group. 2nd ed. Boca Raton London New York CRC: CRC Press. https://doi.org/10.1097/00010694-199706000-00008.

Kantawanichkul, S., Kladprasert, S., and Brix, H. 2009. "Treatment of High-Strength Wastewater in Tropical Vertical Flow Constructed Wetlands Planted with Typha Angustifolia and Cyperus Involucratus." Ecological Engineering 35: 238 – 47. https://doi.org/10.1016/j.ecoleng.2008.06.002.

Kaseva, M. E. 2004. "Performance of a Sub-Surface Flow Constructed Wetland in Polishing Pre-Treated Wastewater - a Tropical Case Study." Water Research 38: 681–87. https://doi.org/10.1016/j.watres.2003.10.041.

Katayon, S., Fiona, Z., Megat, M. J., Noor, M., Halim, G. A., Ahmad, J., Fiona, Z., Noor, M. J., Halim, G. A., and Ahmad, J. 2008. "Treatment of Mild Domestic Wastewater Using

Subsurface Constructed Wetlands in Malaysia." International Journal of Environmental Studies 65 (1): 87 – 102. https://doi.org/10.1080/00207230601125192.

Keffala, C, and Ghrabi, A. 2005. "Nitrogen and Bacterial Removal in Constructed Wetlands Treating Domestic Wastewater." Desalination 185 (May): 383 – 89. https://doi.org/10.1016/j.desal.2005.04.045.

Kessler, A J. 2018. "Biogeochemical Controls on the Relative Importance of Denitri Fi Cation and Dissimilatory Nitrate Reduction to Ammonium in Estuaries." Global Biogeochemical Cycles, no. 1: 1045 – 57. https://doi.org/10.1029/2018GB005908.

Knight, D., Hammer, A. and Robert, L. 1994. "Designing Constructed Wetlands for Nitrogen Removal." Wat. Sci. Tech. 29 (4): 15 – 27. https://doi.org/https://doi.org/10.2166/wst.1994.0148.

Laanbroek, H.J. 1990. "Bacterial Cycling of Minerals That Affect Plant Growth in Waterlogged Soils: A Review." Aquatic Botany 38: 109 – 25.

Laceby, J P, Kerr, J. G., Zhu, D., Chung, C., Situ, Q., Abbasi, S., and Orwin, J. F. 2019. "Chloride Inputs to the North Saskatchewan River Watershed: The Role of Road Salts as a Potential Driver of Salinization Downstream of North America' s Northern Most Major City (Edmonton, Canada)." Science of the Total Environment 688: 1056 – 68. https://doi.org/10.1016/j.scitotenv.2019.06.208.

Land, M., Granéli, W., Grimvall, A., Hoffmann, C. C., Mitsch, W. J., Tonderski, K. S., and Verhoeven, J. T. 2016. "How Effective Are Created or Restored Freshwater Wetlands for Nitrogen and Phosphorus Removal? A Systematic Review." Environmental Evidence 5 (1): 1 – 26. https://doi.org/10.1186/s13750-016-0060-0.

Langergraber, G. 2005. "The Role of Plant Uptake on the Removal of Organic Matter and Nutrients in Subsurface Flow Constructed Wetlands: A Simulation Study." Water Science & Technology 51 (9): 213 – 23.

Lee, C. G., Fletcher, T. D., and Sun, G. Z. 2009. "Nitrogen Removal in Constructed Wetland Systems." Engineering in Life Sciences 9 (1): 11 – 22. https://doi.org/10.1002/elsc.200800049.

Lee, D. Y., De-Meo, O. A., Thomas, R. B., Tillett, A. L., and Neubauer, S. C. 2016. "Design and Construction of an Automated Irrigation System for Simulating Saltwater Intrusion in a Tidal Freshwater Wetland." Wetlands 36 (5): 889 – 98. https://doi.org/10.1007/s13157-016-0801-4.

Leverenz, H. L., Haunschild, K., Hopes, G., Tchobanoglous, G., and Darby, J. L. 2010. "Anoxic Treatment Wetlands for Denitrification." Ecological Engineering 36 (11): 1544 – 51. https://doi.org/10.1016/j.ecoleng.2010.03.014.

Li, Y. C., Zhang, D. Z., and Wang, M. 2017. "Performance Evaluation of a Full-Scale Constructed Wetland for Treating Stormwater Runoff." Clean - Soil, Air, Water 45 (11). https://doi.org/10.1002/clen.201600740.

Li, Y. C., and Migliaccio, K. 2010. Water Quality Sampling, and Concepts, Analyses. CRC Press.

Lin, Y. F., Jing, S. R., Lee, D. Y., and Wang, T. W. 2002. "Nutrient Removal from Aquaculture Wastewater Using a Constructed Wetlands System." Aquaculture 209 (1 – 4): 169–84. https://doi.org/10.1016/S0044-8486(01)00801-8.

Lindell, J. E., Moore, W. P., and King, H. K. 2017. Handbook of Hydraulics. Eighth Edition.

Liolios, K. A, Konstantinos, M., and Vassilios, T. 2014. "Comparative Modeling of HSF Constructed Wetland Performance with and without Evapotranspiration and Rainfall." Environmental Processes, no. 1: 171 – 86. https://doi.org/10.1007/s40710-014-0019-5.

Luo, X., and Li, X. Y. 2018. "Using the EFDC Model to Evaluate the Risks of Eutrophication in an Urban Constructed Pond from Different Water Supply Strategies." Ecological Modelling 372 (January): 1 – 11. https://doi.org/10.1016/j.ecolmodel.2018.01.020.

Lv, J., Wu, H. J., and Chen, M. Q. 2011. "Effects of Nitrogen and Phosphorus on Phytoplankton Composition and Biomass in 15 Subtropical, Urban Shallow Lakes in Wuhan, China." Limnologica 41 (1): 48 – 56. https://doi.org/10.1016/j.limno.2010.03.003.

Maltais-landry, G., Chazarenc, F., Comeau, Y., Troesch, S., and Brisson, J. 2007. "Effects of Artificial Aeration, Macrophyte Species, and Loading Rate on Removal Efficiency in

Constructed Wetland Mesocosms Treating Fish Farm Wastewater." J. Environ. Eng. Sci. 6 (November): 409 – 14. https://doi.org/10.1139/S06-069.

Maltais-Landry, G., Maranger, R., Brisson, J., and Chazarenc, F. 2009. "Nitrogen Transformations and Retention in Planted and Artificially Aerated Constructed Wetlands." Water Research 43 (2): 535 – 45. https://doi.org/10.1016/j.watres.2008.10.040.

Mangangka, I. R., Liu, A., Egodawatta, P., and Goonetilleke, A. 2015. "Sectional Analysis of Stormwater Treatment Performance of a Constructed Wetland." Ecological Engineering 77: 172 – 79.

Marshall, C., Richardson, J., and Paul, E. 1986. "Processes Controlling Movement, Storage, and Export of Phosphorus in a Fen Peatland." Ecological Monographs 56 (4): 279 – 302. https://doi.org/https://doi.org/10.2307/1942548.

Martínez, J., Reca, J., Morillas, M. T., and López, J. G. 2005. "Design and Calibration of a Compound Sharp-Crested Weir." Journal of Hydraulic Engineering 131 (2): 112 – 16. https://doi.org/10.1061/(ASCE)0733-9429(2005)131:2(112).

Masi, F. 2008. Enhanced Denitrification by a Hybrid HF-FWS Constructed Wetland in a Large-Scale Wastewater Treatment Plant. In book Wastewater Treatment, Plant Dynamics and Management in Constructed and Natural Wetlands, pp 267–275.

Masi, F., and Martinuzzi, N. 2007. "Constructed Wetlands for the Mediterranean Countries: Hybrid Systems for Water Reuse and Sustainable Sanitation Related Papers Constructed Wetlands for the Mediterranean Countries:" Desalination 215 (1 – 3): 44 – 45. https://doi.org/10.1016/j.desal.0000.00.000.

McConnaughey, T. A., LaBaugh, J. W., Rosenberry, D. O., Striegl, R. G., Reddy, M. M., Schuster, P. F., and Carter, V. 1994. "Carbon Budget for a Groundwater-Fed Lake: Calcification Supports Summer Photosynthesis." Limnol. Oceanogr 39 (6): 1319 – 32. https://doi.org/https://doi.org/10.4319/lo.1994.39.6.1319.

Meers, E., Tack, F. M., Tolpe, I., and Michels, E. 2008. "Application of a Full-Scale Constructed Wetland for Tertiary Treatment of Piggery Manure: Monitoring Results." Water Air Soil Pollut 193 (3): 15 – 24. https://doi.org/10.1007/s11270-008-9664-5.

Metcalf & Eddy, Inc. 1991. Wastewater Engineering: Treatment, Disposal and Reuse. 3rd ed.

Mierau, R., and Trimble, P. 1988. “Hydrologic characteristic of the Kissimmee River floodplain boney marsh experimental area.” Resource Planning Department South Florida Water Management District. URL

Mitsch, W. J., and Gossilink, J. G. 1986. Wetlands. Van Nostrand Reinhold. New York. https://doi.org/10.1016/S0921-8009(00)00165-8.

Mitsch, W. J, Horne, A. J., and Nairn, R. W. 2000. “Nitrogen and Phosphorus Retention in Wetlands-Ecological Approaches to Solving Excess Nutrient Problems.” Ecological Engineering. Vol. 14. www.elsevier.com/locate/ecoleng.

Morales-marín, L. A., Chun, K. P., Wheater, H. S., and Lindenschmidt, K. 2017. “Trend Analysis of Nutrient Loadings in a Large Prairie Catchment.” Hydrological Sciences Journal 62 (4): 657 – 79. https://doi.org/10.1080/02626667.2016.1255747.

Nairn, R. W., and Mitsch, W. J. 2000. “Phosphorus Removal in Created Wetland Ponds Receiving River Overflow.” Ecological Engineering 14 (1 – 2): 107 – 26. https://doi.org/10.1016/S0925-8574(99)00023-3.

Nayeb, Y., Scott, M. D., Sample, D. J., and Wang, X. X. 2021. “Efficacy of a Retention Pond in Treating Stormwater Nutrients and Sediment.” Journal of Cleaner Production 290: 125787. https://doi.org/10.1016/j.jclepro.2021.125787.

Neufeld, S. 2010. “North Saskatchewan River Water Quality.” EPCOR Water Services. URL.

Nguyen-quang, T., Hushchyna, K., McLellan, K., and Sabir, Q. 2018. “Modified Redfield Ratio Combined with Artificial Neural Network Simulation to Estimate the Algal Bloom Pattern.” ENVIRONMENTAL PROBLEMS 3 (1).

Olguín, E. J., Sánchez-Galván, G., Melo, F. J., Hernández, V. J., and González-Portela, R. E. 2017. “Long-Term Assessment at Field Scale of Floating Treatment Wetlands for Improvement of Water Quality and Provision of Ecosystem Services in a Eutrophic Urban Pond.” Science of the Total Environment 584 – 585: 561 – 71. https://doi.org/10.1016/j.scitotenv.2017.01.072.

Ouellet-plamondon, C., Chazarenc, F., Comeau, Y., and Brisson, J. 2006. “Artificial Aeration to Increase Pollutant Removal Efficiency of Constructed Wetlands in Cold Climate.” Ecological Engineering 27: 258 – 64. https://doi.org/10.1016/j.ecoleng.2006.03.006.

Pant, H.K., and Reddy, K. R. 2001. “Hydrologic Influence on Stability of Organic Phosphorus in Wetland Detritus.” Journal of Environmental Quality 30 (2): 668 – 74. https://doi.org/10.2134/jeq2001.302668x.

Patricia Mitchell Environmental Consulting. 2006. Guidelines for Quality Assurance and Quality Control in Surface Water Quality Programs in Alberta. Alberta Environment. URL.

Patrick, W H, and Khalid, R A. 1974. “Phosphate Release and Sorption by Soils and Sediments: Effect of Aerobic and Anaerobic Conditions.” Advancement Of Science 186 (4158): 53 – 55.

Patrick, W.H., Wyatt, R. 1964. “Soil Nitrogen Loss as a Result of Alternate Submergence and Drying.” SOIL SCIENCE SOCIETY PROCEEDINGS, 647 – 53. https://doi.org/10.2136/sssaj1964.03615995002800050021x.

Patrick, W. H., Gotoh, J. S., and Williams, B. G. 1973. “Strengite Dissolution in Flooded Soils and Sediments.” Science 179 (4073): 564 – 65. https://www.jstor.org/stable/1735435.

Pavlineri, N., Skoulikidis, N. T., and Tsihrintzis, V. A. 2017. “Constructed Floating Wetlands: A Review of Research, Design, Operation and Management Aspects, and Data Meta-Analysis.” Chemical Engineering Journal 308: 1120 – 32. https://doi.org/10.1016/j.cej.2016.09.140.

Platzer, C., and Netter, R. 1994. “Factors Affecting Nitrogen Removal in Horizontal Flow Reed Beds.” Wat. Sci. Tech 29 (4): 319 – 24.

Rahman, M. E., Halmi, M. I., Samad, M. Y., Uddin, M. K., Mahmud, K., Shukor, M. Y., Abdullah, R. S., and Shamsuzzaman, S. M. 2020. “Design, Operation and Optimization of Constructed Wetland for Removal of Pollutant.” International Journal of Environmental Research and Public Health. MDPI AG. https://doi.org/10.3390/ijerph17228339.

Ramirez, E. R., Bonilla, P., Sainz, G., Lopez, M., Cerda, J. M., and Warren, A. 2005. "Occurrence of Pathogenic Free-Living Amoebae and Bacterial Indicators in a Constructed Wetland Treating Domestic Wastewater from a Single Household." Eng. Life Sci 5 (3): 1 – 6. https://doi.org/10.1002/elsc.200420071.

Reddy, K. R. and D'Angelo, E. M. 1994. "Soil Processes Regulating Water Quality in Wetlands." Global Wetlands: Old World and New 23 (5): 309 – 24.

Reddy, K. R., and D'Angelo, E. M. 1997. "Biogeochemical Indicators to Evaluate Pollutant Removal Efficiency in Constructed Wetlands." Water Science and Technology. https://doi.org/10.1016/S0273-1223(97)00046-2.

Reddy, K. R, and Patrick, W. H. 1984. "Nitrogen Transformations and Loss in Flooded Soils and Sediments." CRC Critical Reviews in Environmental Control 13 (4): 273 – 309. https://doi.org/10.1080/10643388409381709.

Reddy, K. R., Tucker, J. C., and DeBusk, W. F. 1987. "The Role of Egeria in Removing Nitrogen and Phosphorus from Nutrient Enriched Waters." Journal of Aquatic Plant Manage, no. 25: 14–19.

Rhue, R. D., and Harris, W. G. 1999. "Phosphorus Sorption/Desorption Reactions in Soils and Sediments-Phosphorus Biogeochemistry in Subtropical Ecosystems." In edited by Schelske CL Reddy KR, O'Connor GA, 187 – 206. Boca Raton, Florida. https://doi.org/10.4319/lo.1992.37.3.0577.

Richardson, C. J. 1985. "Mechanisms Controlling Phosphorus Retention Capacity in Freshwater Wetlands." Science, 228 (4706): 1424 – 27.

Richardson, C. J., Qian, S., Craft, C. B., & Quails, R. G. (1997). Predictive models for phosphorus retention in wetlands. Wetlands Ecology and Management, 4(3), 159–175. https://doi.org/10.1007/bf01879235

Rousseau, D. P. L., Lesage, E., Story, A., Vanrolleghem, P. A., and Pauw, N. D. 2008. "Constructed Wetlands for Water Reclamation." Desalination 218 (February 2006): 181–89. https://doi.org/10.1016/j.desal.2006.09.034.

Ruan, X., Xue, Y., Wu, J., Ni, L., Sun, M., and Zhang, X. 2006. "Treatment of Polluted River Water Using Pilot-Scale Constructed Wetlands." Bull. Environ. Contam. Toxicol. 76 (October 2005): 90 – 97. https://doi.org/10.1007/s00128-005-0893-7.

Saeed, T., and Sun, G. Z. 2012. "A Review on Nitrogen and Organics Removal Mechanisms in Subsurface Flow Constructed Wetlands: Dependency on Environmental Parameters, Operating Conditions and Supporting Media." Journal of Environmental Management 112: 429 – 48. https://doi.org/10.1016/j.jenvman.2012.08.011.

Schober, P. and Schwarte, L. A. 2018. "Correlation Coefficients: Appropriate Use and Interpretation." Anesthesia and Analgesia 126 (5): 1763 – 68. https://doi.org/10.1213/ANE.0000000000002864.

Selbig, W. R. 2016. "Evaluation of Leaf Removal as a Means to Reduce Nutrient Concentrations and Loads in Urban Stormwater." Science of the Total Environment 571: 124 – 33. https://doi.org/10.1016/j.scitotenv.2016.07.003.

Song, K., Xenopoulos, M. A., Marsalek, J., and Frost, P. C. 2015. "The Fingerprints of Urban Nutrients: Dynamics of Phosphorus Speciation in Water Flowing through Developed Landscapes." Biogeochemistry 125 (1): 1 – 10. https://doi.org/10.1007/s10533-015-0114-3.

Sosiak, A, and Dixon, J. 2006. "Impacts on Water Quality in the Upper Elbow River" 7 (1993): 309 – 16. https://doi.org/10.2166/wst.2006.326.

Stein, O. R., and Hook, P. B. 2005. "Temperature, Plants, and Oxygen: How Does Season Affect Constructed Wetland Performance?" Journal of Environmental Science and Health - Part A Toxic/Hazardous Substances and Environmental Engineering 40 (6–7): 1331 – 42. https://doi.org/10.1081/ESE-200055840.

Sultana, M. Y., Mourti, C., Tatoulis, T., Akratos, C. S., Tekerlekopoulou, A. G., and Vayenas, D. V. 2016. "Effect of Hydraulic Retention Time, Temperature, and Organic Load on a Horizontal Subsurface Flow Constructed Wetland Treating Cheese Whey Wastewater." Journal of Chemical Technology and Biotechnology 91 (3): 726 – 32. https://doi.org/10.1002/jctb.4637.

Tchobanoglous, G and Schroeder, E. D. 1985. Water Quality: Characteristics, Modeling, Modification. Addison-Wesley, ©1985. https://doi.org/http://hdl.handle.net/1969.3/24440.

Troitsky, B., Zhu, D. Z., Loewen, M., Duin, B. V., and Mahmood, K. 2019. "Nutrient Processes and Modeling in Urban Stormwater Ponds and Constructed Wetlands." Canadian Water Resources Journal 44 (3): 230 – 47. https://doi.org/10.1080/07011784.2019.1594390.

U.S. Environmental Protection Agency, EPA. 1975. Process Design Manual for Nitrogen Control. EPA. Washington, DC: Office of Technology Transfer.

USDA-Soil Conservation Service. 1989. "Hydrology Training Series. Module 111-Reservoir Flood Routing." Washington, DC, USA. NRCS-NEDC-000105.

Valenca, R., Le, H., Zu, Y. Y., Dittrich, T. M., Tsang, D. C. W., Datta, R., Sarkar, D., and Mohanty, S. K. 2021. "Nitrate Removal Uncertainty in Stormwater Control Measures: Is the Design or Climate a Culprit?" Water Research 190: 1167 – 81. https://doi.org/10.1016/j.watres.2020.116781.

Verhoeven, J. T.A. 1986. "Nutrient Dynamics in Minerotrophic Peat Mires." Aquatic Botany 25 (C): 117 – 37. https://doi.org/10.1016/0304-3770(86)90049-5.

Vogel, J. R., and Moore, T. L. 2016. "Urban Stormwater Characterization, Control, and Treatment." Water Environment Research 88 (10): 1918 – 50. https://doi.org/10.2175/106143016x14696400495938.

Vymazal, J. 1995. Algae and Element Cycling in Wetlands. Chelsea, Michigan: Lewis Publishers. https://doi.org/10.2307/1467440.

Vymazal, J. 2005. "Horizontal Sub-Surface Flow and Hybrid Constructed Wetlands Systems for Wastewater Treatment." Ecological Engineering 25 (5): 478 – 90. https://doi.org/10.1016/j.ecoleng.2005.07.010.

Vymazal, J. 2007. "Removal of Nutrients in Various Types of Constructed Wetlands." Science of the Total Environment 380 (1 – 3): 48 – 65. https://doi.org/10.1016/j.scitotenv.2006.09.014.

Vymazal, J. 2011. "Long-Term Performance of Constructed Wetlands with Horizontal Sub-Surface Flow: Ten Case Studies from the Czech Republic." Ecological Engineering 37 (1): 54 – 63. https://doi.org/10.1016/j.ecoleng.2009.11.028.

Wang, C. Y, and Sample, D. J. 2014. "Assessment of the Nutrient Removal Effectiveness of Floating Treatment Wetlands Applied to Urban Retention Ponds." Journal of Environmental Management 137: 23 – 35. https://doi.org/10.1016/j.jenvman.2014.02.008.

Wang, R. Y., Baldy, V., Périssol, C., and Korboulewsky, N. 2012. "Influence of Plants on Microbial Activity in a Vertical-down Fl Ow Wetland System Treating Waste Activated Sludge with High Organic Matter Concentrations." Journal of Environmental Management 95: S158–64. https://doi.org/10.1016/j.jenvman.2011.03.021.

Wang, X. H. 2006. "Section Two-Physical Processes and Influencing Factors on Water Surface Evaporation." In Hydrology, 31 – 34. Huazhong University of Science and Technology Press. textbooks.

Water Environment Research Foundation, WERF. 2005. Critical Assessment of Stormwater Treatment and Control Selection Issues. https://doi.org/10.13140/RG.2.1.2231.7921.

Werker, A. G., Dougherty, J. M., Mchenry, J. L., and Van, L. W. A. 2002. "Treatment Variability for Wetland Wastewater Treatment Design in Cold Climates." Ecological Engineering 19: 1 – 11. https://doi.org/https://doi.org/10.1016/S0925-8574(02)00016-2.

Winston, R. J., Hunt, W. F., Kennedy, S. G., Merriman, L. S., Chandler, J., and Brown, D. 2013. "Evaluation of Floating Treatment Wetlands as Retrofits to Existing Stormwater Retention Ponds." Ecological Engineering 54: 254 – 65. https://doi.org/10.1016/j.ecoleng.2013.01.023.

Winter, T. C. 1981. "Uncertainties in Estimating the Water Balance of Lakes." Water Resources Bulletin (American Water Resources Association) 17 (1): 82 – 115.

Wong, T. H. F., Breen, P. F., and Somes, N. L. G. 1999. "Ponds vs Wetlands - Performance Consideration in Stormwater Quality Management." Proceedings of the 1st South Pacific Conference on Comprehensive Stormwater and Aquatic Ecosystem Management 2: 223 – 31.

Wood, J. D, Gordon, R., Madani, A., and Stratton, G. W. 2008. “A Long-Term Assessment of Phosphorus Treatment by a Constructed Wetland Receiving Dairy Wastewater.” WETLANDS 28 (3): 715 – 23.

Wu, G. Z., and Xu, Z. X. 2011. “Prediction of Algal Blooming Using EFDC Model: Case Study in the Daoxiang Lake.” Ecological Modelling 222 (6): 1245 – 52. https://doi.org/10.1016/j.ecolmodel.2010.12.021.

Xie, L. Q., Xie, P., Li, S. X., Tang, H. J., and Liu, H. 2003. “The Low TN:TP Ratio, a Cause or a Result of Microcystis Blooms?” Water Research 37 (9): 2073 – 80. https://doi.org/10.1016/S0043-1354(02)00532-8.

Xu, Y. H., Peng, H., Yang, Y. Q., Zhang, W. S., and Wang, S. L. 2014. “A Cumulative Eutrophication Risk Evaluation Method Based on a Bioaccumulation Model.” Ecological Modelling 289: 77 – 85. https://doi.org/10.1016/j.ecolmodel.2014.07.006.

Zhang, C. B., Liu, W. L., Wang, J., Ge, Y., Gu, B. H., and Chang, J. 2012a. “Effects of Plant Diversity and Hydraulic Retention Time on Pollutant Removals in Vertical Flow Constructed Wetland Mesocosms.” Ecological Engineering 49 (December): 244 – 48. https://doi.org/10.1016/j.ecoleng.2012.08.010.

Zhang, D. Q., Tan, S. K., Gersberg, R. M., Zhu, J. F., Sadreddini, S., and Li, Y. F. 2012b. “Nutrient Removal in Tropical Subsurface Flow Constructed Wetlands under Batch and Continuous Flow Conditions.” Journal of Environmental Management 96 (1): 1 – 6. https://doi.org/10.1016/j.jenvman.2011.10.009.

Zhang, D. Q., Jinadasa, K. B., Gersberg, R. M., Liu, Y., Ng, W. J., and Tan, S. K. 2014. “Application of Constructed Wetlands for Wastewater Treatment in Developing Countries - A Review of Recent Developments (2000-2013).” Journal of Environmental Management 141: 116 – 31. https://doi.org/10.1016/j.jenvman.2014.03.015.

Zhang, D. Q., Gersberg, R. M., and Keat, T. S. 2009. “Constructed Wetlands in China.” Ecological Engineering 35 (10): 1367 – 78. https://doi.org/10.1016/j.ecoleng.2009.07.007.

Zhang, L. Y., Xia, X. F., Zhao, Y., Xi, B. D., Yan, Y. N., Guo, X., and Xiong, Y. 2011. “The Ammonium Nitrogen Oxidation Process in Horizontal Subsurface Flow Constructed

Wetlands." Ecological Engineering 37 (11): 1614 – 19. https://doi.org/10.1016/j.ecoleng.2011.06.020.

Zhang, L. Y., Zhang, L., Liu, Y. D., Shen, Y. W., Liu, H., and Xiong, Y. 2010. "Effect of Limited Artificial Aeration on Constructed Wetland Treatment of Domestic Wastewater." Desalination 250 (3): 915 – 20. https://doi.org/10.1016/j.desal.2008.04.062.

Zhao, Y. J., Zhang, H., Xu, C., Er, N., Hua, J. L., Jian, H., and Zheng, Z. 2011. "Efficiency of Two-Stage Combinations of Subsurface Vertical Down-Flow and up-Flow Constructed Wetland Systems for Treating Variation in Influent C/N Ratios of Domestic Wastewater." Ecological Engineering 37 (10): 1546 – 54. https://doi.org/10.1016/j.ecoleng.2011.06.005.

Zhao, Y. J., Liu, B., Zhang, W. G., Ouyang, Y., and An, S. Q. 2010. "Performance of Pilot-Scale Vertical-Flow Constructed Wetlands in Responding to Variation in Influent C/N Ratios of Simulated Urban Sewage." Bioresource Technology 101 (6): 1693 – 1700. https://doi.org/10.1016/j.biortech.2009.10.002.